Impacts of Mixtures of Copper and 1,2-dihydroxyanthraquinone on Physiology and Gene Expression in *Lemna gibba* L.G-3.

by

Anabel Ueckermann

A thesis
presented to the University of Waterloo
in fulfillment of the
thesis requirement for the degree of
Master of Science
in
Biology

Waterloo, Ontario, Canada, 2008

AUTHOR'S DECLARATION

I hereby declare that I am the sole author of this thesis. This is a true copy of the thesis, including any required final revisions, as accepted by my examiners.

I understand that my thesis may be made electronically available to the public.

Abstract

Polycyclic aromatic hydrocarbons (PAHs) and metals are co-contaminants of aquatic environments near industrial and urbanized areas. Mixtures could result in synergistic toxicity impairing macrophyte growth and potentially causing bioaccumulation and biomagnification throughout the ecosystem. In this study, combinations of 1,2-dihydroxyanthraquinone (1,2-dhATQ) and copper (Cu) at low concentrations synergistically inhibited *Lemna gibba* (duckweed) growth. Further analysis using fluorescence techniques showed an increase in reactive oxygen species (ROS) levels upon Cu exposures possibly through redox cycling in the chloroplasts. Pulse amplitude modulated (PAM) and fast repetition rate fluorometry (FRRF) indicated that plants exposed to 1,2-dhATQ had impaired photosynthetic electron transport that manifested as a decrease in the yield of photosynthesis and change in the redox status of the plastoquinone (PQ) pool. At the gene expression level acetyl coA carboxylase (ACC), a key enzyme in membrane repair, and serine decarboxylase (SDC), another enzyme needed for membrane repair were up-regulated in response to copper and 1,2-dhATQ, respectively. The mechanism for mixtures toxicity is thought to involve the reduced PQ pool which could serve as a source of electrons for copper redox cycling thereby increasing ROS production and causing synergistic growth inhibition. When the antioxidant glutathione (GSH) was added, copper toxicity was ameliorated but 1,2-dhATQ toxicity increased possibly through formation of reactive conjugates or suppression of the native antioxidant system. This study emphasizes that mixtures of

toxicants at low concentrations can cause more biological damage than individual toxicants via alterations of the redox status and increases in ROS production.

Acknowledgements

I would like to thank my committee members Dr. B. McConkey and Dr. S. Chuong and my co-supervisors Dr. B. Greenberg and Dr. R. Smith for editing and support. I would like to thank Ontario Graduate Scholarships and the University of Waterloo for financial support.

I would also like to thank the following people whom have contributed to my project: Daryl Enstone for the confocal microscopy, Greg Silsbe for help with the FRR Fluorometry set-up and analysis, Julie Nykamp with the cloning, molecular work, and excellent editing, Jola Gurska for help with PAM, molecular protocols, editing and everything in between, Yuxuan (Ariel) Guo for doing PAM measurements, and Neel (Aluru Neelakanteswar) and Jenn Czarny with QPCR. Thanks to the rest of the Greenberg lab members past and present especially: Pearl Chang, Xiao-Dong Huang, Dave Isherwood, Mark Lampi, Lizzy Wang, Wenxi Wang, and Shan-Shan Wu.

Thanks to the Strydoms, the Ueckermanns, Ma (with editing), Pa and my brother Mp and my friends: Jenn Cardiff, Brian Ellis, Jess Fortin (with editing), Heather MacDonald, Krissy MacDonald, Anita Pol, Andrea Pol, and Gah-Ning Tang.

Table of Contents

List of Figures ix
List of Tables xi
Glossary xii
Chapter 1 Introduction 1
1.1 Metals 2
1.2 Polycyclic Aromatic Hydrocarbons (PAHs) 6
1.3 Mixtures of polycyclic aromatic hydrocarbons and metals in the natural environment 10
1.4 Molecular Ecotoxicology 11
1.5 Toxic effects of PAHs and metals on *L. gibba* 13
1.6 Study Goals 19
Chapter 2 Materials and Methods 21
2.1 Plant Growth Conditions 21
2.2 Experimental Treatments 21
2.3 Assessment of plant growth in presence of chemicals 22
2.4 Measurement of ROS production 23
2.5 Measurement of photosynthetic activity 27
2.6 Gene expression determination with Quantitative Polymerase Chain Reaction (QPCR) 29
2.6.1 RNA Extraction 30
2.6.2 DNase treatment of RNA 32
2.6.3 RNA Quality assessment 32
2.6.4 Reverse Transcription of RNA 33
2.6.5 Polymerase Chain Reaction using specific primers 33
2.6.6 Resolution of PCR products 34
2.6.7 Extraction of PCR products 35
2.6.8 Cloning of PCR products 36
2.6.9 Isolating of plasmid DNA 36

2.6.10 Restriction digestion of purified plasmids..... 38
2.6.11 Sequencing of PCR products 38
2.6.12 Construction of Relative Standard Curves for QPCR..... 39
2.6.13 Quantification of samples using QPCR 40
2.7 Statistical Analysis..... 41
Chapter 3 Results 42
3.1 Growth of *L. gibba* exposed to copper and 1,2-dhATQ..... 42
3.2 Growth of *L. gibba* exposed to ROS scavengers under PAR..... 47
3.3 Growth of *L. gibba* exposed to combinations of 1,2-dhATQ and Cu, with and without GSH under PAR and SSR 51
3.4 The production of ROS in *L. gibba* exposed to copper, 1,2-dhATQ and their combinations..... 54
3.5 The study of photosynthetic electron transport of *L. gibba* exposed to copper and 1,2-dhATQ and their mixtures 61
3.6 Changes in the expression of two genes involved in fatty acid synthesis of *L. gibba* exposed to 1,2-dhATQ, Cu and their combination..... 77
Chapter 4 Discussion 86
4.1 Growth Analysis of *L. gibba* exposed to Cu, 1,2-dhATQ and their combination..... 86
4.1.1 Growth of *L. gibba* exposed to copper under PAR and SSR 86
4.1.2 Growth of *L. gibba* exposed to 1,2-dhATQ under PAR and SSR..... 87
4.1.3 Growth of *L. gibba* exposed to 1,2-dhATQ and Cu combinations under PAR and SSR 88
4.2 ROS production in *L. gibba* when exposed to Cu, 1,2-dhATQ and their combination. 89
4.2.1 ROS production after 24 hour exposures to 1,2-dhATQ, Cu and their combination 89
4.2.2 ROS production after a 4 day exposure to 1,2-dhATQ, Cu and their combination... 90
4.3 Effects of 1,2-dhATQ, Cu and their combination on photosynthetic electron transport 91
4.3.1 The effects of 1,2-dhATQ, Cu and their combination on F_v / F_m and qN obtained with PAM fluorometry 91

4.3.2 The effects of 1,2-dhATQ, Cu and their combination on F_s obtained with PAM fluorometry 92
4.3.3 The effects of 1,2-dhATQ, Cu and their combination on yield of photosynthesis and photochemistry obtained with PAM fluorometry 93
4.3.4 The effects of 1,2-dhATQ, Cu and their combination on F_v / F_m measured using FRRF 94
4.3.5 The effects of 1,2-dhATQ, Cu and their combination on the cross-sectional absorption coefficient 95
4.3.6 The effects of 1,2-dhATQ, Cu and their combination on the time constant 95
4.3.7 Proposed Mechanism of 1,2-dhATQ and Cu Mixture Toxicity 96
4.4 Effects of 1,2-dhATQ and Cu on genes involved in fatty acid synthesis 97
4.4.1 Effects of 1,2-dhATQ, Cu and their combination on the expression of serine decarboxylase 98
4.4.2 Effects of 1,2-dhATQ, Cu and their combination on the expression of acetyl CoA carboxylase 99
4.5 Study Conclusions 100
4.6 Future work 102
References 103

List of Figures

Figure 1.1 Possible routes of entry of copper and 1,2-dhATQ into plant cells. 5
Figure 1.2 Jablonski Diagram for excitation of a polycyclic aromatic hydrocarbon that could lead to photosensitization and photomodified reactions. 8
Figure 1.3 Measurement of chlorophyll fluorescence using pulse amplitude modulated (PAM) fluorometry. 16
Figure 1.4 Measurement of chlorophyll fluorescence using fast repetition rate fluorometry (FRRF). 17
Figure 2.1 Images of a *Lemna* frond and the mesophyll cells at higher magnification. 26
Figure 2.2 Overview of operations performed with v6 software. 29
Figure 2.3 Steps in the QPCR protocol described briefly. 30
Figure 3.1 *L. gibba* growth inhibition exposed to $CuSO_4$ under PAR and SSR. 44
Figure 3.2 *L. gibba* growth inhibition exposed to 1,2-dhATQ under PAR and SSR. 46
Figure 3.3 *L. gibba* growth exposed to DMTU, AA and GSH with and without 8 µM Copper under PAR. 48
Figure 3.4 *L. gibba* growth inhibition exposed to 0–0.35 mM GSH with 3 µM 1,2-dhATQ under PAR. 50
Figure 3.5 *L. gibba* growth inhibition exposed to 1,2-dhATQ, copper and their combinations under PAR and SSR with and without GSH. 52
Figure 3.6 *L. gibba* DCF fluorescence exposed to 1,2dhATQ, copper and their combination for 24 hours under PAR. 56
Figure 3.7 *L. gibba* DCF fluorescence exposed to 1,2-dhATQ, Cu and their mixtures for 24 hours and 4 days under PAR. 57
Figure 3.8 DCF fluorescence in *L. gibba* mesophyll cells visualized with CLSM. 60
Figure 3.9 The effects of 1,2-dhATQ and copper after 4 hour, 24 hour and 4 day exposures on the maximum quantum yield of PSII. 66
Figure 3.10 The effects of 1,2-dhATQ and copper after 4 hour, 24 hour and 4 day exposures on the steady state fluorescence. 67

Figure 3.11 The effects of 1,2-dhATQ and copper after 4 hour, 24 hour and 4 day exposures on the yield of photosynthesis. 68
Figure 3.12 The effects of 1,2-dhATQ and copper after 4 hour, 24 hour and 4 day exposures on the photochemical quenching. 69
Figure 3.13 PAM fluorometry traces of an untreated plant (A), and plants exposed to 4 µM copper (B), 3 µM 1,2-dhATQ (C) and their combination (D) for 24 hours. 72
Figure 3.14 The effects of 1,2-dhATQ and copper on σ_{PSII} (A) and τ (B) after a 4 hour exposure. 76
Figure 3.15 RNA from treated and untreated plants on a denaturing gradient gel (A) and bands (B) of 26S RNA, actin, acetyl coA carboxylase and serine decarboxylase with negative controls on a TAE gel. 78
Figure 3.16A Nucleotide sequence alignment of actin from *L. gibba* using blastn. 80
Figure 3.16B Predicted amino acid alignment of actin from *L. gibba* using BLASTX. 80
Figure 3.17A Nucleotide sequence alignment of serine decarboxylase. 81
Figure 3.17B Nucleotide sequence alignment of acetyl coA carboxylase. 81
Figure 3.18 ACTquantification graph (A), ACT melt curve (B), SDC quantification graph (C), SDC melt curve (D) and ACC quantification graph (E) and ACC melt curve (F) obtained using QPCR. 83
Figure 3.19 Expression of serine decarboxylase (A) and acetyl coA carboxylase (B) normalized to actin. 85
Figure 4.1 Effects of 1,2-dhATQ, Cu and their combination on ROS production, photosynthesis and gene expression. 97

List of Tables

Table 2.1 Sequences of gene specific primers for SDC, ACC 26S and ACT used in QPCR 34
Table 3.1 Ratios of inhibition of *L.gibba* exposed to GSH and 3 µM 1,2-dhATQ 49
Table 3.2 Ratio of inhibition to determine synergistic growth inhibition of *L. gibba* exposed to mixtures of 1,2-dhATQ and copper 53
Table 3.3 F_o, F_m, F'_m and qN obtained using PAM fluorometry of *L. gibba* exposed to 1,2-dhATQ, Cu and their mixtures with and without GSH under PAR for 4 hours. 62
Table 3.4 F_o, F_m, F'_m and qN obtained using PAM fluorometry of *L. gibba* exposed to 1,2-dhATQ, Cu and their mixtures with and without GSH under PAR for 24 hours. 63
Table 3.5 F_o, F_m, F'_m and qN obtained using PAM fluorometry of *L. gibba* exposed to 1,2-dhATQ, Cu and their mixtures with and without GSH under PAR for 4 days..... 64
Table 3.6 F_o, F_m and F_v / F_m obtained using FRRF fluorometry of *L. gibba* exposed to 1,2-dhATQ, Cu and their mixtures with and without GSH under PAR for 4 hours. 74

Glossary

AA	Ascorbic Acid
ACC	Acetyl coA carboxylase
ANT	Anthracene
CLSM	Confocal Laser Scanning Microscopy
Cu	Copper
DCF	Dichlorofluorescein
H_2DCFDA	2', 7'-dichlorodihydrofluorescein diacetate
1,2-dhATQ	1,2-dihydroxyanthraquinone
DMTU	Dimethyl thiourea
F'_m	Maximum fluorescence in actinic light
F_m	Maximum fluorescence in the dark
F_o	Minimum fluorescence in the dark
FRRF	Fast Repetition Rate Fluorometry
F_s	Steady-state fluorescence under actinic light
F_v/F_m	Maximum quantum yield of PSII
GSH	Glutathione (reduced)
MT	Multiple Turnover
PAH	Polycyclic Aromatic Hydrocarbon
PAM	Pulse Amplitude Modulated
PAR	Photosynthetically Active Radiation
PQ	Plastoquinone

PSII	Photosystem II
qN	Non-photochemical quenching of fluorescence
qP	Photochemical quenching of fluorescence
QPCR	Quantitative Polymerase Chain Reaction
RO	Reverse Osmosis
ROS	Reactive Oxygen Species
σ_{PSII}	Functional absorption cross-section
SDC	Serine decarboxylase
SH	Sulfhydryl
SSR	Simulated Solar Radiation
ST	Single Turnover
τ	Time constant of electron transport from PSII to PSI
Y	Yield of photosynthesis
Zn	Zinc

Chapter 1
Introduction

The field of ecotoxicology evolved rapidly due to increased awareness of the state of environmental contamination as a result of human activities. One focus of ecotoxicological research is the influx of anthropogenic contaminants to pristine environments especially aquatic environments. Water pollution can negatively impact aquatic ecosystems as well as cause serious human health risks, if contaminated water is used for agricultural or recreational purposes and/or as a source of drinking water (Sherry 2003; Ohe et al. 2004; Calace et al. 2006). Aquatic environments are directly vulnerable to complex mixtures of agricultural and industrial origin or indirectly through atmospheric deposition (Sherry 2003; Ohe et al. 2004; Calace et al. 2006). According to the Canadian Environmental Protection Agency (CEPA) 2000 tonnes of polycyclic aromatic hydrocarbons (PAHs) and 123 tonnes of metals are released annually into the Canadian environment (CEPA 1994; CEPA 1999; Ohe et al. 2004). Hydrophobic compounds such as PAHs accumulate in the sediments while metals are found in the water column as free ions or complexed with organic or inorganic substances in sediments (Ohe et al. 2004; Calace et al. 2006). The anthropogenic emission of polycyclic aromatic hydrocarbons and metals are increasing; and to better understand and prevent damage to the aquatic environment more research is needed (Ohe et al. 2004).

To protect aquatic ecosystems, regulations are often based on arbitrary toxicity tests (Sherry 2003). There is a need for comprehensive studies that can be used to predict potential adverse effects to ensure that environmental regulations are in fact protective

(Sherry 2003). Conducting single-compound experiments and then estimating additive toxicity using models could potentially underestimate mixture effects (McConkey et al. 2000). Since macrophytes are a large part of the biomass in aquatic environments, their use in toxicity testing has been well developed (Greenberg et al. 1992; Mkandawire and Dudel 2005). The macrophyte, *Lemna gibba* (*L. gibba*), can be used to evaluate contaminants effects on ecosystem health (Mkandawire and Dudel 2005). The focus of this thesis is on the toxicity of the co-contaminants, PAHs and metals, which could be present in urban and industrial areas. More studies are needed to understand the mechanisms of toxicity, especially in mixtures to be able to better predict toxic effects, and to ensure environmental limits are protective (Ohe et al. 2004).

1.1 Metals

Metal contamination of water and soil is largely due to urban, industrial, and agricultural activities (Briat and Lebrun 1999; Prasad et al. 2001; Ohe et al. 2004). Certain metals such as aluminum, cadmium, and nickel are directly toxic to plants while others such as iron and copper are able to cause formation of hydroxyl radicals during cellular oxidation (Briat and Lebrun 1999). Because plants are directly exposed to metals, it is important to understand the mechanism of plant resistance to metal toxicity (Briat and Lebrun 1999). The CEPA lists copper as a priority substance (CEPA 1999). Copper smelters and refineries are responsible for the discharge of copper in the processing and cooling effluents and as particulates into the air (CEPA 1999). Aquatic organisms can be exposed to high concentrations of metals as far as 14 km from these facilities nationally (CEPA 1999). Annual atmospheric and wastewater releases have been reported as high as

123 and 23.9 tonnes, respectively (CEPA 1999). The concentration of copper in the undiluted effluents can range from 3.8 to 31 µg/L, which is higher that the critical toxicity value set at 2.6 µg/L as determined using algal toxicity studies (CEPA 1999). Another source of copper in the environment is its application as a fungicide to control mildew and fungus on fruits and vegetables (Dewez et al. 2002; Frankart et al. 2002). It is thus important to study the effects of copper on aquatic organisms as it could have immediate and long-term effects on the environment and its biodiversity.

Copper is an essential micronutrient with many functions in plant cells (Zenk 1996; Raven et al. 2003). Most vascular plants need 6 mg/kg or 0.0006% copper concentration in dry tissues (Raven et al. 2003). Specifically, copper is involved in electron transfer reactions in respiration (cytochrome *c* oxidase, alternate oxidase) and photosynthesis (plastocyanin) (Fox and Guerinot 1998). Other important processes that involve copper include ethylene perception, the lignification of cell walls (laccase) and detoxification of superoxide radicals (Cu-Zn superoxide dismutase) (Fox and Guerinot 1998; Puig et al. 2007). Copper deficiency in young leaves can cause twisted and misshapen leaves, with the presence of necrotic spots (Raven et al. 2003). On a molecular level, copper deficiency causes up-regulation of the *COPT1* gene in *Arabidopsis* that encodes a putative copper transporter (Fox and Guerinot 1998).

It is important to maintain copper ion homeostasis by balancing its uptake, storage and efflux (Andrés-Colas et al. 2006). Copper is taken up at the root surface by high-affinity Cu^{+} uptake transporters or specifically in *Arabidopsis* coppers transporters (COPT) from the conserve copper transporter (CTR) family (Figure 1.1) (Puig et al. 2007; Andrés-Colas

et al. 2006). These transporters import metals through the plasma membrane into the cytosol where it is transported through the xylem chelated by organic acids (Andrés-Colas et al. 2006; Puig et al. 2007). To limit the solubility and reactivity inside the cell, soluble Cu-binding chaperones complex and direct copper to where it is needed such as cytosolic Cu-Zn superoxide dismutase, mitochondrial cytochrome *c* oxidase, chloroplastic plastocyanin and P-type ATPases (Andrés-Colas et al. 2006; Puig et al. 2007).

The same redox properties that make copper an essential micronutrient cause copper toxicity, when it is present at elevated levels. In high concentrations, the tolerance mechanisms in the root zone are overloaded allowing excess copper to be translocated via the xylem and phloem to the leaves (Pätsikkä et al. 1998). Excess copper can catalyze the formation of reactive oxygen species (ROS), which damage membranes, proteins and nucleic acids (Pätsikkä et al. 1998; Ahktar et al. 2005; Puig et al. 2007). Also, excess copper can replace other metals in metalloproteins, interact with sulfhydryl (SH) groups of proteins, and cause ROS formation (Pätsikkä et al. 1998; Teisseire and Guy 2000).

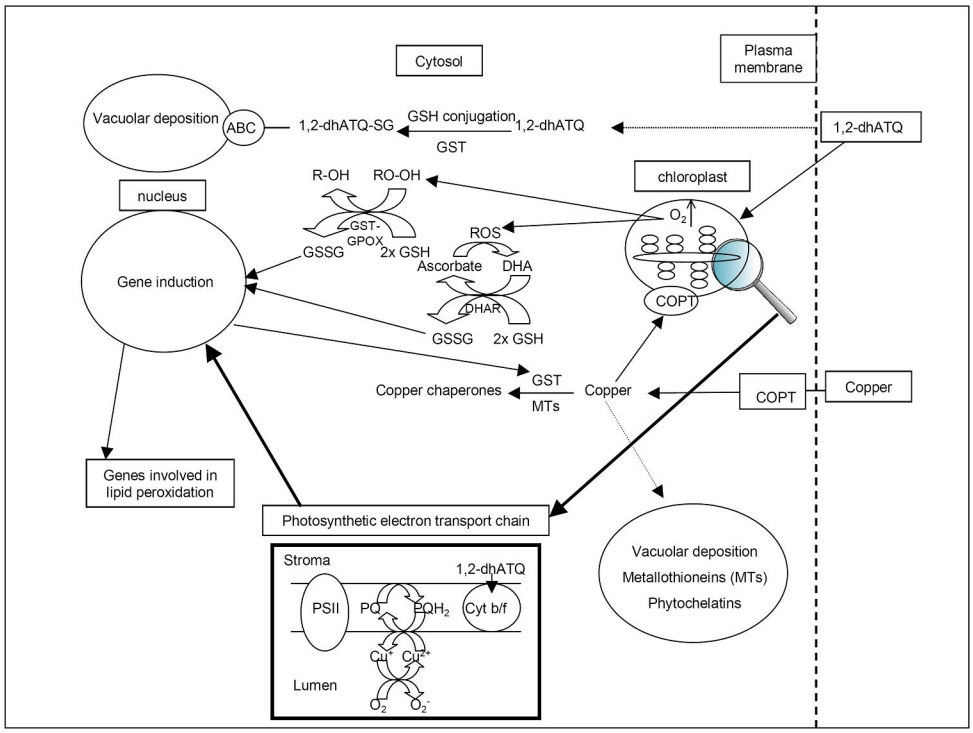

Figure 1.1 Possible routes of entry of copper and 1,2-dhATQ into plant cells.

COPT transporters take up copper into the cytosol where it is complexed with chaperones. If copper is taken up into the chloroplast it can lead to ROS formation. 1,2-dhATQ can pass through membranes and once in the cytosol can form conjugates with GSH catalyzed by glutathione transferases (GSTs) or it can interrupt photosynthetic electron transport if it accumulates in the chloroplasts. Gene induction is triggered by changes in the redox potential of the cell due to GSSG (glutathione oxidized) and GSH (glutathione reduced) cycling, oxidative stress and changes in redox potential in the photosynthetic electron transport chain such as that of plastoquinone (PQ) (Adapted from Sandermann (2004)).

Copper-catalyzed Fenton-type reactions that form ROS take place mainly in the chloroplasts (Pätsikkä et al. 1998; Akhtar et al. 2005). High concentrations of copper in the divalent state, Cu^{+2}, can cause the formation of the hydroxyl radical (•OH) from oxygen and hydrogen peroxide (H_2O_2) (Pätsikkä et al. 1998). Hydroxyl radical is very reactive and causes the oxidation of unsaturated membrane lipids and chlorophyll, thus

inhibiting photosynthetic electron transport (Pätsikkä et al. 1998; Teisseire and Guy 2000). Lipoperoxidation can lead to a loss of cellular membrane integrity (Zenk 1996). Copper toxicity manifests as inhibition of root growth, chlorosis (loss of chlorophyll), defects in flowers and decreases in plant size, numbers and size of leaves, and germination (Puig et al. 2007).

Copper overloading leads to activation of antioxidant defense systems in plants (Briat and Lebrun 1998). Enzymes such as glutathione reductase (GR), glutathione S-transferase (GST), ascorbate peroxidase, and Cu-Zn superoxide dismutase are up regulated to scavenge ROS (Briat and Lebrun 1998; Teisseire and Guy 2000). Glutathione is a tripeptide consisting of γ-L-glutamyl-L-cysteinyl-glycine used in both enzymatic and non-enzymatic reactions as an antioxidant (Mullineaux and Rausch 2005). Glutathione depletion is also seen when plants are exposed to metals since it is used in the production of phytochelatins (Schützendübel and Polle 2002). Phytochelatins sequester metals, lowering their toxicity (Schützendübel and Polle 2002). Glutathione is also involved in the redox balance of the cell, regulation of the cell cycle, detoxification of oxidants and transporting reduced forms of sulphur (Schützendübel and Polle 2002). Therefore its depletion leads to an accumulation of ROS when high levels of copper are present (Schützendübel and Polle 2002).

1.2 Polycyclic Aromatic Hydrocarbons (PAHs)

Polycyclic aromatic hydrocarbons (PAHs) are listed by the CEPA as priority substances (CEPA 1994). Both naturally and anthropogenically occurring PAHs are formed during

incomplete combustion of organic materials. The majority of PAHs are of anthropogenic origin (CEPA 1994; Arfsten et al. 1996; Ohe et al. 2004). The largest anthropogenic source according to the CEPA is aluminum smelters, which are estimated to release 925 tonnes of PAHs per year into the atmosphere (CEPA 1994). Creosote-treated products (200 tonnes per year), petroleum spills (76 tonnes per year), products from metallurgical and coking plants (4 tonnes per year), and atmospheric deposition of unknown amounts contaminate both aquatic and soil environments (CEPA 1994; Arfsten et al. 1996). A specific PAH of interest is anthracene (ANT) of which 0.1-1 tonne per year is produced and 1-10 tonnes per year imported (CEPA 1994). ANT has been found in water at concentrations ranging from 0.13 to 81 µg/L and in sediment ranging from 0.01 to 10.9 µg/g dry weight (CEPA 1994).

Generally PAHs have low volatility and due to their hydrophobicity are associated with particulate matter in aquatic environments (CEPA 1994; Ramesh et al. 2004). Sediments are the major sinks for PAHs, and because degradation commonly occurs slowly it could adversely affect aquatic organisms especially benthic organisms (CEPA 1994; Ramesh et al. 2004). PAHs can be re-released from sediments if sediments are disturbed (CEPA 1994; Ramesh et al. 2004). Besides negatively impacting natural environments, these contaminants could bioaccumulate in humans and other animals where they could have carcinogenic, reproductive, developmental, hemato-, cardio-, and immunotoxicities (Ramesh et al. 2004). PAHs constitute a large class of over a 100 individual compounds and because only a few have been extensively studied, more research is needed. Studies

involving plants and other organisms are necessary as most PAH research has focused on human health (CEPA 1994).

An interesting PAH that has been studied using *Lemna gibba* is 1,2-dihydroxyanthraquinone (1,2-dhATQ) (Babu et al. 2005). This oxygenated PAH (oxyPAH) is derived from anthracene (ANT) when it is exposed to solar radiation (Huang et al. 1997; Mallakin et al. 2000; Mallakin et al. 2002). When the conjugated π-orbital systems of the PAH absorb visible (400-700 nm) and ultraviolet (280-400 nm) radiation, photosensitization and photomodification reactions of the PAHs occur (Figure 1.2) (Arfsten et al. 1996; Sternberg and Dolphin 1998; Mallakin et al. 2000).

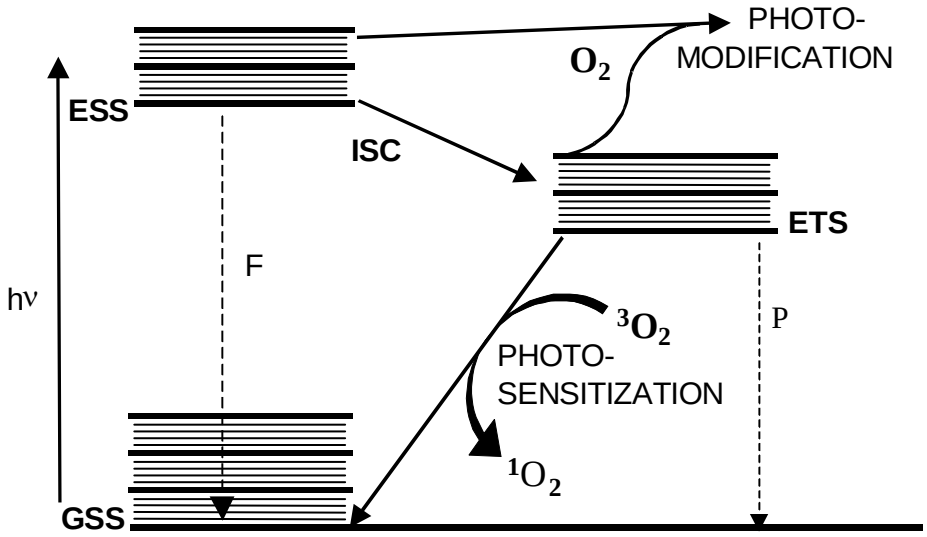

Figure 1.2 Jablonski Diagram for excitation of a polycyclic aromatic hydrocarbon that could lead to photosensitization and photomodified reactions.

In photosensitization reactions, a photon (h*v*) is absorbed and an electron from the ground singlet state (GSS) is promoted to the excited singlet state (ESS) (Sternberg and Dolphin 1998). From the ESS, the excited molecule can fluoresce (F) back to the GSS or undergo intersystem crossing (ISC) to the excited triplet state (ETS) (Sternberg and Dolphin 1998). From the ETS electrons can return to the GSS by phosphorescence (P) or

through a photosensitization reaction whereby triplet state oxygen ($^3O_2$) is excited to singlet oxygen ($^1O_2$) and the ETS PAH is returned to the ground state (Sternberg and Dolphin 1998). Both ESS and ETS molecules can undergo photochemical modification with oxygen creating photomodified products such as 1,2-dihydroxyanthraquinone from the parent PAH, ANT (Sternberg and Dolphin 1998; Mallakin et al. 2000). The photomodified products are often more toxic than the parent PAH as their hydrophobicity generally decreases resulting in higher concentrations in the surrounding aqueous environment (Xie et al. 2006). They are also often more reactive that the parent PAHs (Huang et al. 1997; Mallakin et al. 2000; Mallakin et al 2002).

Nutrient and water absorption of *L. gibba* occurs through the lower surfaces of the fronds (Figure 1.1) (Tront 2004). PAH absorption is a passive process across plant membranes driven by a concentration gradient between the aqueous phase contaminant concentration and the internal unaltered contaminant concentration of the plant cell (Korte et al. 2000; Dietz and Schnoor 2001; Suresh and Ravishankar 2004; Tront 2004). Very hydrophobic PAHs accumulate in the membrane bilayers of *L. gibba* but oxyPAHs are hydrophilic enough to travel through the membrane where they could interact with proteins, DNA and RNA (Duxbury et al. 1997; Suresh and Ravishankar 2004). ANT and its photoproducts in *L. gibba* were found to be concentrated in the thylakoid membranes and to a lesser extent membranes of microsomes (Duxbury et al. 1997).

Previous research has shown 1,2-dhATQ obstructs photosynthetic electron transport at the Cytochrome b_6/f complex (Babu et al. 2005). This leads to over reduction of the plastoquinone (PQ) pool that serves as a pool of accessible electrons for copper that could lead to the generation of ROS (Babu et al. 2005). 1,2-dhATQ functions in similar ways to 2,5-dibromo-6-isopropyl-3-methyl-1,4-benzoquinone (DBMIB), which blocks electron transport at the Cytochrome b_6/f complex (Babu et al. 2001).

Plants are well adapted to metabolize xenobiotics (Suresh and Ravishankar 2004). Several phases of transformation could occur: Phase I is conversion; Phase II is conjugation; and Phase III is compartmentalization (Dietz and Schnoor 2001). Xenobiotic enzymes such as Cytochrome P_{450}, glutathione S-transferase, carboxyesterases, O-glucosyl transferases and other transferases are effective in transforming PAHs (Suresh and Ravishankar 2004). Glutathione-S-transferases (GSTs) are important not only in xenobiotic metabolism but also in antioxidant protection (Suresh and Ravishankar 2004). Soluble GSTs form dimers that bind glutathione and the xenobiotics, allowing them to be translocated across the cytoplasmic membrane for degradation using ABC transporters (Suresh and Ravishankar 2004).

1.3 Mixtures of polycyclic aromatic hydrocarbons and metals in the natural environment

In natural environments, several factors influence the toxicity of environmental contaminants. These include trophic conditions, presence of UV radiation, modification of bioavailability and interactions with other contaminants that can lead to greater toxicity (Teisseire and Guy 2000; Xie et al. 2006). Both metals and polycyclic aromatic hydrocarbons enter aquatic environments as a result of human activities and would most likely be found in mixtures. PAHs and metals must be studied in mixtures to determine whether their combined toxicity increases. Previous work has found that mixtures of copper and 1,2-dhATQ caused increased toxicity through a burst of ROS (Figure 1.1) (Babu et al. 2001; Babu et al. 2005; Xie et al. 2006). The observed toxicity was greater than

the additive effects of each contaminant and, thus, can be described as synergistic (Frankart et al. 2002).

Plants are continually exposed to UV radiation in the natural environment. Moreover, it is known that UV radiation increases the toxicity of copper and PAHs individually (Huang et al. 1993; Babu et al. 2003; Akhtar et al. 2005). Therefore, it is important to include UV radiation effects on PAHs and metals especially as destruction of ozone in the stratosphere increased amounts of UV radiation reaching the Earth's surface (Farooq et al. 2000). Toxic effects of UV radiation in plants include inhibition of photosynthesis, destruction of pigments, decreases in biomass and protein content, alterations in metabolic processes, and are dependent on the intensity and length of exposure (Farooq et al. 2000). In order to alleviate stress, ROS are detoxified using peroxidases (Farooq et al. 2000). UV radiation, metals and PAH toxicities have been attributed to ROS formation therefore addition of ROS scavengers such as ascorbic acid and glutathione could potential relieve some of the toxicity (Xie et al. 2006).

1.4 Molecular Ecotoxicology

A broad definition of toxicology is the qualitative and quantitative study of adverse effects of chemicals on living organisms (Shank 2004). Whereas, ecotoxicology or environmental toxicology is the science of the occurrence, transformation, bioavailability or exposure and the mode of action of physical, chemical and biological environmental agents on living organisms (Sandermann 2004; Boudou and Ribeyre 1997). Impacts of environmental stressors can be measured at several levels of biological organization

namely whole-organism, organelle, cellular and molecular (Sandermann 2004). The field of molecular ecotoxicology developed through advances in toxicology and molecular biology fueled by the need to address the complex issue of environmental pollution. Molecular ecotoxicology is used to investigate, at the gene level, the mechanisms that regulate and limit the responses of an organism to environmental contaminants (Shugart and Theodorakis 1998). Changes in gene expression can indicate exposure to toxicants directly or indirectly, a disease state, and changes in cellular metabolism (Snape et al. 2004; Lettieri 2006). Because transcriptional changes occur rapidly, these results can be used to predict consequences at higher levels of biological organization (Waring et al. 2004; Shugart and Theodorakis 1998; Kim et al. 2007). Since, some molecular ecotoxicology techniques are sensitive and specific, they are able to characterize how cells and organisms adapt to external changes, thus providing a solid scientific basis for ecological risk assessment (Shugart and Theodorakis 1998; Lettieri 2006).

The main methods used to assess genetic patterns are allozyme electrophoresis and molecular genetic techniques often referred to as "omics" (Belfiore and Anderson 2001; Brønsted et al. 2006; Overemm et al. 2005). The allozyme method is limited by the availability of tissues and only represents a small finite portion of genetic variability (Belfiore and Anderson 2001). Most molecular techniques use PCR to examine neutral markers or patterns at coding loci (Belfiore and Anderson 2001). "Omics" technologies can be used to monitor complete classes of cellular molecules in a single analysis enabling researchers to look at cascades of gene interactions (Brønsted et al. 2006). Discrimination among potential sources of genetic change is the largest disadvantage of

DNA methods (Belfiore and Anderson 2001). It is also known that organ and gender specific expression could skew results (Brønsted et al. 2006). Reproducibility, accuracy, sensitivity and robustness of "omic" information must be verified and standardized before use in risk and safety assessment (Brønsted et al. 2006). Ideally, characterization of gene or protein signatures for a limited range of aquatic organisms would be useful in identifying mechanism of action of a single chemical or complex mixture rapidly (Lettieri 2006). Bradley et al. (2002) effectively used protein expression signatures to investigate endocrine disruptors in rainbow trout due to sewage effluent exposure. Alkio et al. (2005) screened potential phytoremediation genes in *Arabidopsis* by exposing plants to phenanthrene then measuring gene expression using quantitative PCR (QPCR). Ultimately, to fully address environmental contamination, a multi-disciplinary approach is required where molecular and biochemical responses to contaminants would be used together to evaluate the fitness of individual, populations and ecosystems as unique information is gained from both approaches (Anderson et al. 1994).

1.5 Toxic effects of PAHs and metals on *L. gibba*

Photosynthetic organisms like macrophytes contribute a large fraction of aquatic biomass (Greenberg et al. 1992). Macrophyte bioassays can be used in aquatic environmental risk assessment to ensure levels of PAHs and metals are not negatively impacting organisms (Fairchild et al. 1997; Ferrat et al. 2003). Macrophytes, such as duckweed, are at the base of most aquatic food webs world-wide (Greenberg et al. 1992). It is important to study organisms at the base of the food web as chemical assimilation could cause bioaccumulation and biomagnification, thus damaging the entire food web

(Greenberg et al. 1992). *Lemna gibba* and *Lemna minor* have both been successfully used in bioassays and as bio-indicator species to study aquatic ecosystem integrity (OECD 2002; Ferrat et al. 2003; Mkandawire and Dudel 2005). *Lemna* serves as an important food source for aquatic herbivores, a dietary supplement and nutrient source for humans, livestock and fish, and is used as a fertilizer supplement (Farooq et al. 2000). Advantages to using *Lemna* in bioassays are: ease of culture, small size and fast growth rate (Fairchild et al. 1997). *Lemna* is capable of assimilating numerous toxicants making its use in environmental risk and phytotoxicity assessment ideal (Greenberg et al. 1992; Mkandawire and Dudel 2005). It is comparatively sensitive to several classes of herbicides especially those that affect photosynthesis however it is not universally sensitive to all contaminants (Fairchild et al. 1997).

Investigation of PAHs and metal toxicity mechanisms requires several techniques that could include: growth assays, ROS production, photosynthetic activity, and gene expression (Greenberg et al. 1992). Static renewal growth assays are used to find the growth rates from which the effective concentration (EC50) can be calculated (Mallakin et al. 1999). ROS production of the whole plant has been successfully measured using the dye, 2',7'-dichlorodihydrofluorescein diacetate (H_2DCFDA), which fluoresces when it is oxidized to dichlorofluorescein (DCF) by ROS (Babu et al. 2003). ROS production in the mesophyll cells of a frond can be assessed using the dye and confocal laser scanning microscopy (CLSM) (Mullineaux and Rausch 2005). CLSM allows collection of high quality images of different optical sections from a living sample by excluding out-of-focus emissions with a pinhole (Paddock 1999).

Photosynthesis has been measured by observing carbon fixation and electron transport (Huang et al. 1997). Pulse amplitude modulated (PAM) fluorometry has been used extensively to study photosynthesis and the effects of toxicants on photosynthetic electron transport (Juneau et al. 1999; Babu et al. 2001; Juneau et al. 2002). PAM fluorometry is a multiple turnover method where charge separations of Q_A, Q_B and plastoquinone (PQ) are induced (Suggett et al. 2003). This technique gives information on the status of Photosystem II (PSII) such as the flow of electrons and the rate of photosynthesis (Maxwell and Johnson 2000). Data obtained can be used to infer if damage has occurred to PSII (Figure 1.3) (Maxwell and Johnson 2000). An indicator of plant health is the maximum quantum yield of PSII ($F_v/F_m = (F_m-F_o)/F_m$), which measures the maximum potential quantum efficiency if all PSII centres were open (Babu et al. 2001; Lees 2005; Maxwell and Johnson 2000). Photochemical quenching $qP = (F'_m-F_s)/(F'_m- F_o)$ indicates the proportion of open PSII reaction centers and redox status of the plastoquinone pool (Babu et al. 2001; Maxwell and Johnson 2000). Non-photochemical quenching $qN = (1-(F'_m- F_o)/(F_m- F_o))$ is related mostly to heat dissipation relative to the dark-adapted state indicating if damage has occurred to the photosynthetic apparatus (Babu et al. 2001; Maxwell and Johnson 2000). Yield of steady-state photosynthesis is measured as the quantum yield of PSII $Y = (F'_m-F_s)/F'_m$ which, is the proportion of light absorbed by chlorophyll associated with PSII used in photochemistry (Lees 2005; Maxwell and Johnson 2000). Together, F_v/F_m, qP, qN and Y can be used to study the effects of toxicants on photosynthetic electron transport.

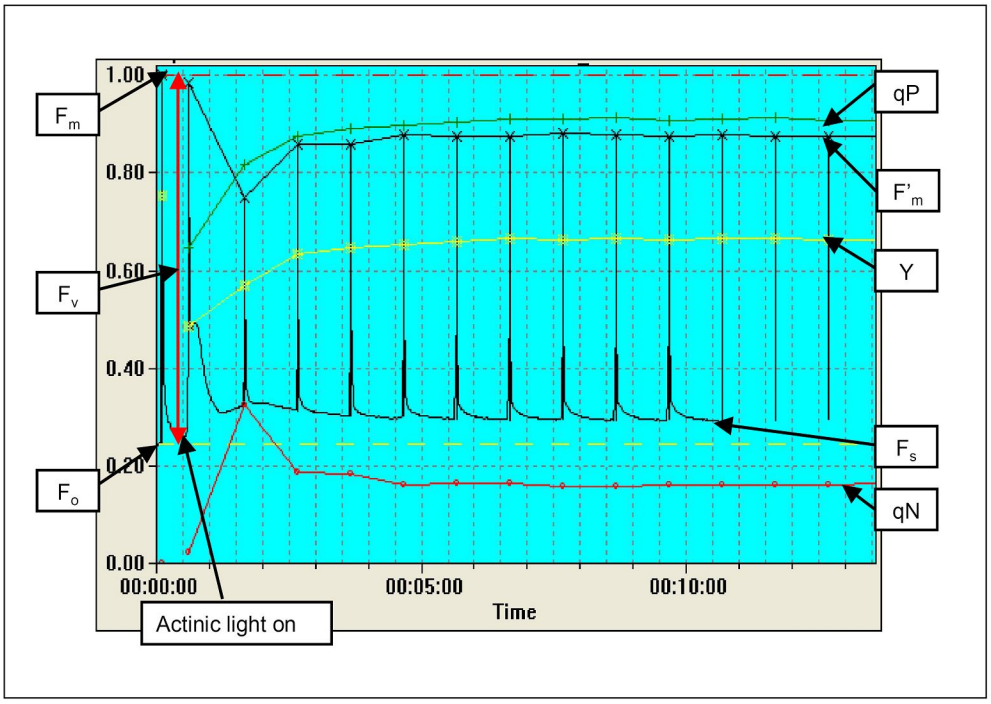

Figure 1.3 Measurement of chlorophyll fluorescence using pulse amplitude modulated (PAM) fluorometry.

F_o is measured with a weak modulated light and is the lowest level of fluorescence in the dark-adapted state when all PSII reaction centers are open. F_m is measured using high intensity short duration pulses of saturating light and is the highest level of fluorescence in the dark-adapted state. F_s and F'_m are obtained when the actinic light is turned on and are the steady state of fluorescence during photosynthesis and the maximum level of fluorescence respectively. Quenching of chlorophyll fluorescence by photochemical (qP) and non-photochemical processes (qN) and the yield (Y) of photosynthesis are also calculated from the fluorescence.

Another fluorescence method, fast repetition rate fluorometry (FRRF), is used extensively to assess the response of marine phytoplankton to nutrients, examine general photosynthetic behaviour, and study spatial-temporal distribution (Laney 2003). It can also give information on the robustness of phytoplankton communities (Lombardi et al. 2000). Short 150-400 μs intense light pulses greater than 20 000 μmol photons m^{-2} s^{-1} are

used in FRFF where only the primary electron acceptor Q_A is fully reduced making this a single turnover technique (Figure 1.4) (Suggett et al. 2003). FRRF allows for the acquisition of the functional absorption cross section, σ_{PSII}. This is the effective size of the light-absorbing target and indicates how efficiently energy transfer occurs from the light-harvesting antenna to the reaction center (Pemberton et al. 2007). Another parameter of FRRF is the time constant, τ that is the electron transport from PSII to PSI in microseconds (Suggett et al. 2003). Two fluorescent techniques can be used to investigate the effects of toxicants on photosynthetic electron transport by measuring different parameters.

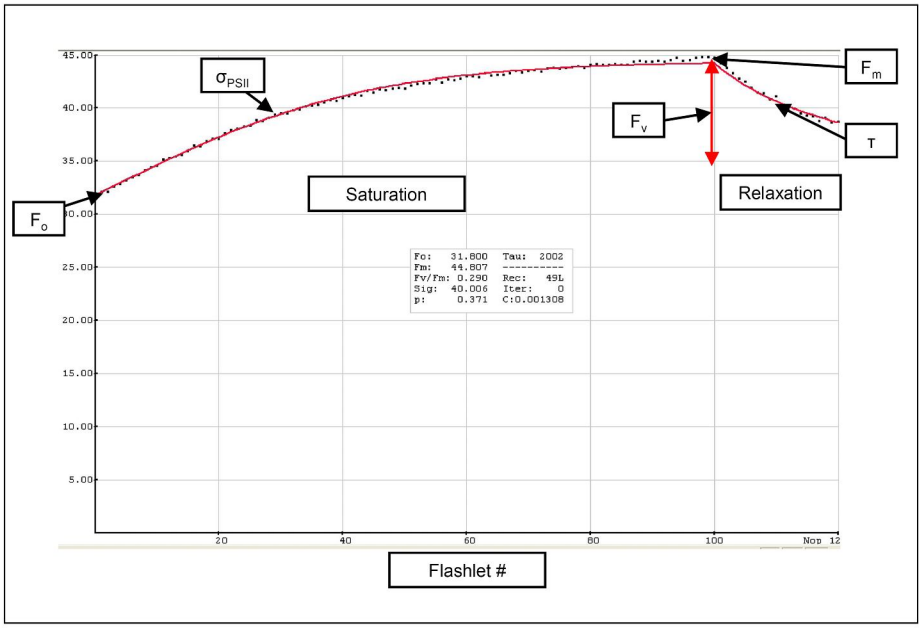

Figure 1.4 Measurement of chlorophyll fluorescence using fast repetition rate fluorometry (FRRF).

F_o is the lowest level of fluorescence and F_m is the highest level of fluorescence. During the saturation phase, σ_{PSII} the effective size of the light-absorbing target is obtained. τ the time constant is measured during the relaxation phase.

To maximize understanding of mechanisms of contaminants, traditional ecotoxicology could be linked with genomic studies. Environmental contaminants could alter gene expression directly or indirectly, which could be measured with mRNA or protein expression (Snape et al. 2004; Lettieri 2006). QPCR is a rapid, specific, and sensitive detection system, which quantify RNA or DNA (Gachon et al. 2004). A fluorescent signal emitted from double-stranded PCR products generated is measured during the exponential phase to allow accurate quantification of the starting template (Gachon et al. 2004). The threshold cycle (Ct) value is the cycle at which a significant increase in the magnitude of the PCR signal is detected and this is used to find the level of expression of the gene of interest (Gachon et al. 2004).

Some research on the genetic basis of metal tolerance in plants has been performed, however research of phytotoxicity of organic contaminants at the genetic level is lacking (Snape et al. 2004). From previous work it is plausible that PAHs and metals would affect gene expression of enzymes involved in fatty acid metabolism because they cause the formation of ROS, which could lead to destruction of membranes and proteins (Akhtar et al. 2005; Lees 2006). Two important enzymes in fatty acid metabolism are acetyl CoA carboxylase (ACC) and serine decarboxylase (SDC). Plants use ACC to catalyze the first committed step, namely carboxylation of acetyl CoA to malonyl CoA in fatty acid synthesis (Sasaki and Nagano 2004). Two soluble forms of ACC are present namely the homomeric form in the cytosol and the heterometric form in the chloroplast (Sasaki and Nagano 2004). SDC is a soluble, pyridoxal 5'-phosphate-dependent enzyme that catalyzes decarboxylation of serine to form ethanolamine necessary for the synthesis of

phophatidylethanolamine, phosphatidylcholine and glycine betaine (Fujimore and Ohta 2003; Rontein et al. 2003; Akhtar et al. 2005). Together physiological and molecular methods can be used to explore mechanisms of the toxicity of PAHs and metals especially in mixtures.

1.6 Study Goals

Anthracene toxicity has been studied using *L. gibba* leading to the identification of several photomodified compounds namely anthraquinones (Huang et al. 1997; Mallakin et al. 1999). Of the photooxidation products of anthracene, the compound 1,2-dhATQ, proved to be very interesting (Mallakin et al. 2002). 1.2-dihydroxyanthraquinone was studied in mixtures with copper and found that at certain concentrations the mixture toxicity was synergistic (Babu et al. 2001; Babu et al. 2005). This thesis further probes the effects of 1,2-dhATQ and copper on *L. gibba*. The overall goals are to:

1. Study effects on *L. gibba* growth when exposed to copper, 1,2-dhATQ and their combinations, with and without a ROS scavenger under photosynthetic active radiation (PAR) and simulated solar radiation (SSR). The ROS scavenger, glutathione (GSH) is expected to ameliorate the copper and 1,2-dhATQ toxicities by decreasing ROS production and by forming conjugates with 1,2-dhATQ. It is expected that the toxicities of the toxicants will increase under SSR compared to PAR.
2. Quantify ROS production in whole plants, and locate ROS production within mesophyll cells. It is known that copper directly causes ROS production and is suspected that 1,2-dhATQ does so indirectly. Therefore, the ROS levels measured with a plate reader

fluorometer are expected to increase when plants are exposed to copper, 1,2-dhATQ and their combination. Using confocal laser scanning microscopy (CLSM), it is expected that the location of ROS production in mesophyll cells will be the chloroplasts.

3. Measure photosynthetic electron transport and determine the plastoquinone (PQ) redox status. PAHs and metals affect photosynthesis, which can be studied using two different fluorometry techniques, namely the multiple turnover method [pulse amplitude modulated (PAM) fluorometry] and the single turnover technique [fast repetition rate fluorometry (FRRF)].

4. Investigate gene expression of two genes involved in fatty acid synthesis in *L. gibba* exposed to 1,2-dhATQ, Cu and their combination. Early defenses can be investigated using molecular techniques such as quantitative PCR (QPCR). Previous studies performed with copper and mixtures of cadmium and 1,2-dhATQ identified certain genes that were up regulated (Akhtar et al. 2005; Lees 2006). Of those genes serine decarboxylase (SDC) and acetyl CoA carboxylase (ACC) with actin (ACT) as the housekeeping gene were selected to study their expression as it is suspected that their expressions will be up regulated. It is also of interest to study the expression of these genes when they are exposed to combinations of 1,2-dhATQ and Cu as very few studies exist that have done so.

Chapter 2
Materials and Methods

2.1 Plant Growth Conditions

Lemna gibba L. G-3 cultures were aseptically maintained in 250 mL Erlenmeyer flasks on 50% Hutner's media (3 mM KNO_3, 3 mM $Ca(NO_3)_2 \cdot 4H_2O$, 3 mM KH_2PO_4, 3 mM $MgSO_4 \cdot 7H_2O$, 3.5 µM $ZnSO_4 \cdot 7H_2O$, 0.6 µM $MnSO_4 \cdot H_2O$, 0.12 µM $CuSO_4 \cdot 5H_2O$, 0.413 µM $Na_2MoO_4 \cdot 2H_2O$, 3 µM $FeC_6H_5O_7$, 8 µM EDTA Na_2, 16 µM H_3BO_3 (pH 4.7), supplemented with 1% [w/v] sucrose) (Hutner 1953). They were maintained at 20°C in a growth chamber under 75 $\mu mol \cdot m^{-2} \cdot s^{-1}$ continuous photosynthetically active radiation (PAR) generated by cool-white fluorescent lamps and halogen bulbs (F48T12-CW, National Biological Co., Twinsberg, OH, USA).

2.2 Experimental Treatments

Before experiments, plants were acclimated for a month on 30 mL inorganic 50% Hutner's medium in sterile plastic petri dishes. The growth medium was replaced every 3 days during acclimation and experimental periods. The acclimated plants were used in all subsequent experiments after transferring plants to small plastic petri dishes filled with 10 ml medium containing chemicals unless stated otherwise.

Plants were grown for 24 hours under 75 $\mu mol \cdot m^{-2} \cdot s^{-1}$ PAR and/or 16 hours simulated solar radiation (SSR) (75 $\mu mol \cdot m^{-2} \cdot s^{-1}$ PAR, 10 $\mu mol \cdot m^{-2} \cdot s^{-1}$ UV-A [320-400] and 0.75 $\mu mol \cdot m^{-2} \cdot s^{-1}$ UV-B [290-320]) light regimes supplied by fluorescent and UV lamps

(Akhtar et al. 2005). The fluence rates and ratios of SSR were measured with a calibrated spectroradiometer (Oriel, Inc., Stratford, CT, USA). SSR has a PAR:UV-A:UV-B ratio equivalent to natural sunlight, however it only has 5% of total solar PAR and UV radiation.

Toxicant treatments included: copper (Cu) (Sigma Chemical Company, St. Louis, MO, USA), 1,2-dihydroxyanthraquinone (1,2-dhATQ) (Alfa Aesar Lancaster, Pelham, NH, USA), glutathione (GSH) (Sigma Chemical Company, St. Louis, MO, USA), ascorbic acid (AA) (Sigma Chemical Company, St. Louis, MO, USA), and dimethylthiourea (DMTU) (Sigma Chemical Company, St. Louis, MO, USA). Copper was diluted to 2-10 µM from stocks solutions of 2, 4, 6, 8, and 10 mM in reverse osmosis (RO) water (Babu et al. 2003). Copper bioavailability could be decreased due to the presence of EDTA in the Hutner's media (Babu et al. 2001). 1,2-dhATQ was diluted to final concentrations of 1-5, 10 µM from 1-5, 10 mM 1,2-dhATQ stocks in dimethylsulfoxide (DMSO) (Caledon Laboratory Chemicals, Georgetown, ON, Canada). Controls contained 0.1% DMSO as this concentration did not adversely affect plant growth (Huang et al. 2003). GSH, AA and DMTU were diluted to final concentrations of 0.25 mM, 0.5 mM, and 2.5 mM from stocks solutions of 100 mM, 0.5 M and 1M prepared in RO water respectively.

2.3 Assessment of plant growth in presence of chemicals

To assess the effects of chemicals on growth, whole organism growth assays were performed in triplicate in three independent trials. Growth assays of mixture treatments were done with and without 0.25 mM GSH. Assays were conducted for eight days with

static medium replacement every second day growth. The fronds were counted at the beginning and end of the experiment. Growth rates, growth inhibition and EC50's were determined using SYSTAT 10® (Systat Software, Point Richmond, CA, USA). The possible interactions between 1,2-dhATQ and copper were estimated using Abott's formula where the expected inhibition is expressed as a percentage (Frankart et al. 2002). According to the model, synergistic toxicity of the mixture was defined as toxicity greater than the expected additive inhibition (C_{exp}) = A + B – (A x B/100) where A and B are the inhibition levels of individual chemicals (Frankart et al. 2002). A ratio of inhibition can be calculated as RI = Observed inhibition/C_{exp} where RI<1 is antagonistic, RI >1 is synergistic and R=1 is additive between the two chemicals (Frankart et al. 2002). Chemical treatments under PAR included 2-10 µM Cu, 1-5, 10 µM 1,2-dhATQ and combinations of 3, 4, and 5 µM 1,2-dhATQ with 4 or 6 µM Cu. Chemical treatments under SSR included 2-10 µM Cu, 1-10 µM 1,2-dhATQ and combinations of 2 µM 1,2-dhATQ with 4 µM Cu and 2 µM 1,2-dhATQ with 4 µM Cu. ROS scavengers at 2.5 mM DMTU, 0.5 mM AA and 0.25 mM GSH were tested for their effects on *L. gibba* growth and their abilities to ameliorate copper toxicity.

2.4 Measurement of ROS production

Production of reactive oxygen species (ROS) was measured with the dye 2',7'-dichlorodihydrofluorescein diacetate (H_2DCFDA) (Molecular Probes, Invitrogen, Burlington, Ontario, Canada). (Babu et al. 2001; Akhtar et al. 2005). Chemical exposures were done for 24 hours and 4 days after which the ROS levels were measured with a fluorescence plate reader (Cytofluor 2350, Millipore, Mississauga, ON, Canada). Plants

were washed three times with 50% Hutner's medium and placed in 5 µM H_2DCFDA at room temperature for 30 minutes. H_2DCFDA was taken up and, once inside the cell, was cleaved by esterases allowing oxidation of the dye by ROS to the fluorescent compound 2',7'-dichlorofluorescein (DCF). DCF was excited by 485 nm light and the emissions were collected at 530 nm using the fluorescence plate reader. The DCF fluorescence was measured on intact plants and normalized to plant fresh weights (Akhtar et al. 2005). The fluorescence measured at time zero was subtracted from the measurements taken after 30 minutes. Individual toxicant exposures included 3, 4 and 5 µM 1,2-dhATQ and 4 and 6 µM Cu with and without 0.25 mM GSH under PAR. Mixture concentrations tested were 3 µM 1,2-dhATQ and 4 µM Cu and 5 µM 1,2-dhATQ and 6 µM Cu with and without 0.25 mM GSH.

To observe the site of ROS production in mesophyll cell, confocal laser scanning microscopy was used. Plants under PAR were exposed to 3 µM 1,2-dhATQ, 6 µM Cu and their combination for 24 hours. All experiments were done on three plants per treatment and 2-3 fronds per plant. Before imaging, the plants were exposed to 5 µM H_2DCFDA for 2 hours. The mesophyll cells were imaged with the Carl Zeiss LSM 510 confocal microscope (version 3.2 SP2, Carl Zeiss Canada, Mississauga, Ontario, Canada) with the C-apochromat objective 40x/1.2W using the Argon/2 laser (6.9% of 25% total output, tube current 4.7 A) with an excitation wavelength of 488 nm. The fluorescence emission was collected simultaneously on the Meta channel at 507.6-571.8 nm for DCF and 657.4-700.2 nm for chlorophyll autofluorescence. To minimize light exposure the pinhole was set at 72 nm (0.99 Airy units), and the scanned frame size at 512 x 512 (pixel dwell time

1.6 μs). Images were taken 38 μm into the frond (Figure 2.1). Emissions were collect simultaneously of chlorophyll and DCF fluorescence and DCF fluorescence alone. This was done to allow assessment of DCF fluorescence alone to that of chlorophyll autofluorescence and DCF fluorescence. Images from plants exposed to Cu, 1,2-dhATQ and their combination were compared to plants treated with 5 μM H_2DCFDA only and untreated plants.

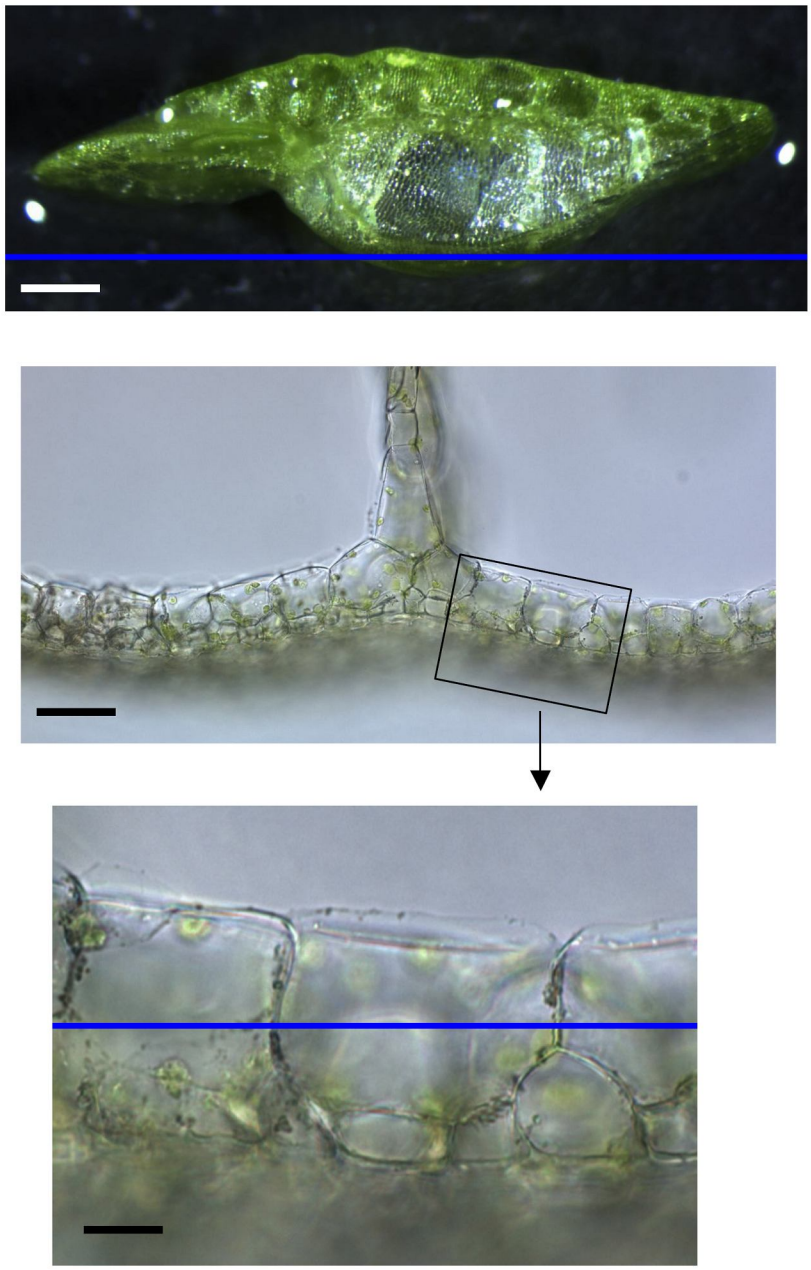

Figure 2.1 Images of a *Lemna* frond and the mesophyll cells at higher magnification.

A *Lemna gibba* frond was scanned from the bottom with an Ar laser. DCF and chlorophyll fluorescence from mesophyll cells were collected in the mid-region of the cell as indicated by the middle blue line (Scale bars = 50 mm, 100 µm and 25 µm from top to bottom) (Pictures provided by Daryl Enstone)..

2.5 Measurement of photosynthetic activity

A Pulse Amplitude Modulated (PAM) fluorometer was used to measure photosynthetic electron transport (Portable Chlorophyll Fluorometer PAM-2000, Heinz Walz GmbH, Effeltrich, Germany) (Babu et al. 2001). PAM fluorometry is a multiple turnover (MT) technique that fully reduces Q_A, Q_B, and plastoquinone (PQ). To ensure all PSII reaction centers were open, treated plants were dark-adapted for 30 minutes (Maxwell and Johnson 2000; Babu et al. 2001; Lees 2005). After dark-adaptation plants were transferred to a small petri dish with 50% Hunter's medium under a weak modulated light (<1 $\mu mol \cdot m^{-2} \cdot s^{-1}$ at 650nm). The initial fluorescence, F_o, was adjusted to 0.200 by changing the gain (Babu et al. 2001; Lees 2005). The maximum fluorescence, F_m, was measured in the dark by a single non-modulated saturating 0.6 s light pulse (2000 $\mu mol \cdot m^{-2} \cdot s^{-1}$ of PAR). After 30 seconds, the steady-state fluorescence, F_s, was measured using the non-modulated 640-700 nm actinic radiation (70 $\mu mol \cdot m^{-2} \cdot s^{-1}$) for 14 minutes (Babu et al. 2001; Lees 2005). Single non-modulated saturating 0.6 s light pulses were triggered every minute to measure the maximum fluorescence, F'_m in the presence of actinic light (Babu et al. 2001; Lees 2005). The maximum potential quantum efficiency ($F_v/F_m = (F_m-F_o)/F_m$) was derived first (Maxwell and Johnson 2000; Babu et al. 2001; Lees 2005). Photochemical quenching ($qP = (F'_m-F_s)/(F'_m- F_o)$), non-photochemical quenching ($qN = (1-(F'_m- F_o)/(F_m-F_o)$), and the yield of steady-state photosynthesis ($Y = (F'_m-F_s)/F'_m$) were all calculated using PAMwin software (PC software PAMWin V2.00f, Heinz Walz GmbH, Germany). Treatments included 3 and 5 µM 1,2-dhATQ and 4 µM and 6 µM Cu with and without 0.25 mM GSH under PAR. Combinations tested were 3 µM 1,2-dhATQ and 4 µM Cu and

5 µM 1,2-dhATQ and 6 µM Cu with and without 0.25 mM GSH under PAR. More concentrations were used however treatments with 4 µM 1,2-dhATQ gave very similar results to that of 3 µM 1,2-dhATQ (data not shown). Plants were exposed to the same treatments for four hours, 24 hours and 4 days to study the effects over time.

The single turnover technique Fast Repetition Rate Fluorometry (FRRF) was used to further study photosynthetic electron transport with the FAST^{tracka} FRR Fluorometer (Chelsea Technologies Group, United Kingdom) (Suggett et al. 2000; Pemberton 2007). This technique only reduced Q_A (Suggett et al. 2000). Before measurements plants were dark-adapted for 30 minutes after which they were transferred to a platform in front of the dark chamber excitation window. The excitation window was covered with 3 layers of a neutral density filter to decrease intensity of flashes. F_o and F_m were obtained in the dark from 470 nm acquisitions flashes (~32 500 µmol$\cdot m^{-2}\cdot s^{-1}$) measured with the LiCor-1000 data logger (LI-COR BioSciences, Lincoln, NE). Acquisitions were 100 saturation flashes and 20 relaxation flashes followed by a 30 second sleep time between the acquisitions (Suggett et al. 2003). The flash duration was set to 100 and the gain was set to 1. The functional absorption cross-section, σ_{PSII} (A^2(quanta)$^{-1}$) and the time constant, τ (µs) were obtained (Suggett et al. 2003). After the "real-time" data was collected, post-processing software was used to reject "bad" data (Figure 2.2) (Laney and Letelier 2008). Data was rejected when F_o was greater than F_m, F_o=0 and F_t was very low. Plants were exposed to 3 and 5 µM 1,2-dhATQ and 4 and 6 µM Cu and combinations of 3 µM 1,2-dhATQ and 4 µM Cu and 5 µM 1,2-dhATQ and 6 µM Cu with and without 0.25 mM GSH under PAR for four hours.

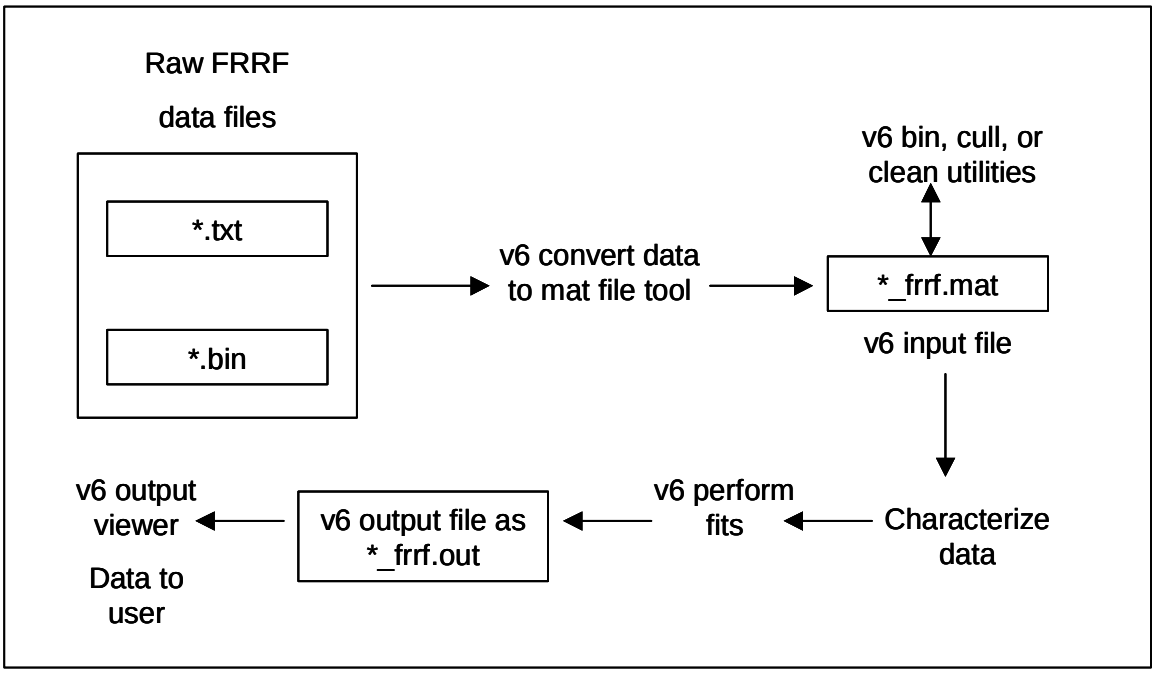

Figure 2.2 Overview of operations performed with v6 software.

Raw FRRF files are converted to Matlab *_frrf.mat files from ASCII format (*.txt) or binary format (*bin.txt). In the *_frrf.mat format files are then used to perform fits and data is given in *_frrf.out format.

2.6 Gene expression determination with Quantitative Polymerase Chain Reaction (QPCR)

The gene expression of serine decarboxylase (SDC), acetyl coA carboxylase (ACC) and actin (ACT) were studied with QPCR. Plants were treated with 5 µM 1,2-dhATQ and 6 µM Cu and their combination for fours hours under PAR after which the RNA was extracted, cDNA was made and QPCR was performed (Figure 2.3).

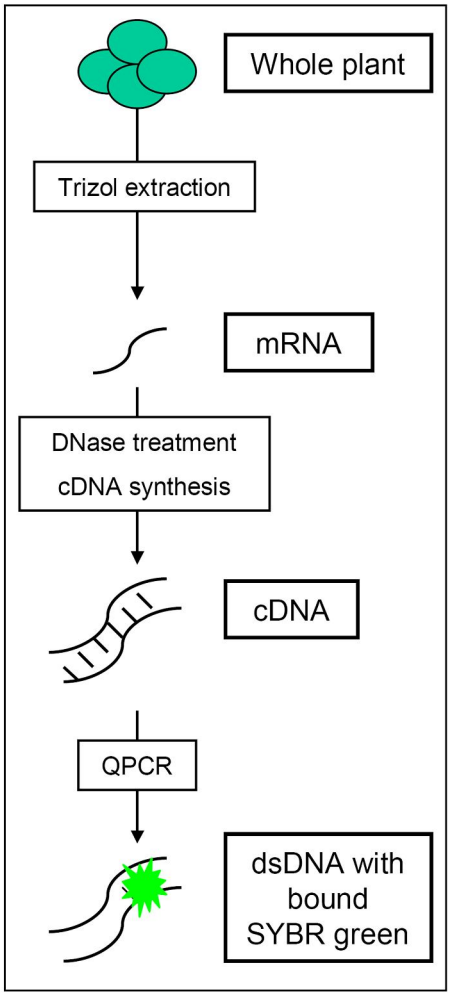

Figure 2.3 Steps in the QPCR protocol described briefly.

Using Trizol total RNA was extracted from plants exposed to 1,2-dhATQ, Cu and their combination and untreated plants. The RNA was treated with DNase I to remove residual DNA after which cDNA was made using oligo(dT)$_{18}$ primers. The cDNA was used with specific primers for SDC, ACC and ACT to perform QPCR. SYBR green fluorescence was used to detect the presence of the specific products for SDC, ACC and ACT.

2.6.1 RNA Extraction

All reagents used for RNA extractions were made RNase-free with 0.1% diethylpyrocarbonate (DEPC) (Bioshop, Burlington, ON, Canada). All glassware was

baked at 280 ºC overnight prior to use or treated with RNase Away (Molecular Bioproducts, San Diego, CA, USA). Total RNA was extracted from six whole plants per dish for treated and untreated plants using the protocol as described by Akhtar et al. (2005) and Lees (2005). Plants were homogenized in 1 mL Trizol (Sigma Chemical Company, St. Louis, MO, USA) using a motorized mortar and pestle for 20 seconds. The homogenate was transferred to a 1.5 mL RNase-free microcentrifuge tube (Ultident, Mississauga, ON, Canada) and centrifuged in a bench top microcentrifuge (Model 541C, Eppendorf-Brinkmann, Mississauga, ON, Canada) at 4 ºC at 12 000xg for 10 minutes. The supernatant was transferred to a new 1.5 mL microfuge tube and incubated at room temperature for 3 minutes to complete dissociation of nucleoprotein complexes. 200 µL chloroform (Sigma Chemical Company, St. Louis, MO, USA) was added and the tube was vortexed for 15 seconds. Phase separation was allowed to occur at room temperature for 15 minutes and then the tube was centrifuged at 4 ºC at 12 000xg for 15 minutes. The upper aqueous phase was carefully transferred to a new 1.5 mL RNase-free microfuge tube. RNA was precipitated with 500 µL of isopropanol at room temperature for 10 minutes (Sigma Chemical Company, St. Louis, MO, USA). RNA was pelleted by centrifugation at 4 ºC at 12 000xg for 10 minutes and the supernatant was discarded. The pellet was washed in 1 mL of 75% ethanol and centrifugation at 8000xg for 5 minutes. The supernatant was discarded and the pellet was air dried for 10 minutes to evaporate residual ethanol. The RNA pellet was dissolved in 50 µL of DEPC treated water at 55-60 ºC for 10 minutes. The concentration of RNA was determined spectrophotometrically using a Nanodropper (NanoDrop ND-1000 3.3, National

Instruments Corporation, USA). Average RNA concentrations were 800 ng/µl with 230/260 ratios of 1.7 and 260/280 ratios of 2.0. The purified RNA samples were stored at –80 ºC.

2.6.2 DNase treatment of RNA

The RNA was treated with the DNA-free RNA kit according to the manufacturer instructions to remove DNA (Zymo Research, California, U.S.A.). Briefly, 5 µg of RNA was diluted with 70 µL DEPC water. After addition of 10 µL 10X DNase I buffer and 5 µL RNase-free DNase I the RNA was incubated at 25 ºC for 10 minutes. Four volumes of RNA binding buffer was added and the reaction was transferred to a Zymo-Spin™ collection tube and centrifuged at 10 000 rpm for 30 seconds. The flow-through was discarded and 200 µL of RNA Wash buffer was added. The sample was centrifuged twice at 10 000 rpm for 30 seconds. 10 µL of DNase/RNase-free water was added to the column, placed in a new RNase-free 1.5 ml tube, and centrifuged at 10 000 rpm for 60 seconds. The eluted RNA concentration was re-measured before further processing.

2.6.3 RNA Quality assessment

RNA integrity was verified by denaturing gel electrophoresis as described by Lees (2005). 2 µg total RNA was resuspended in 7 µL of loading buffer (50% formamide [v/v], 17% formaldehyde [v/v], 0.02 M morpholinepropanesulfonic acid (MOPS) buffer, 5 mM sodium acetate, 1 mM EDTA, 10% glycerol [v/v], 0.05% bromophenol blue [w/v] and 0.7 $mg \cdot mL^{-1}$ ethidium bromide) then heated for 10 minutes at 65 ºC . Samples were cooled on ice for 5 minutes and loaded onto a 1.2% agarose gel [w/v] containing 18%

formaldehyde [v/v] and 0.02M MOPS buffer [v/v]. A RiboRuler™ RNA Ladder was added to the gel for size comparison (MBI Fermentas, Burlington, Ontario). RNA was separated for 2 hours at 80 volts using 0.02 M MOPS as a running buffer and then visualized under UV light with a Fluorochem imaging system (Bio-Imaging system, Biotech Inc, Montreal, Canada).

2.6.4 Reverse Transcription of RNA

After verification of RNA integrity, double-stranded complementary DNA (cDNA) was synthesized from 3 μg of DNase treated RNA using the First Strand cDNA synthesis kit (MBI Fermentas, Burlington, ON). RNA was diluted with 11 μL of DEPC water. 1 μL of 3' and 5' 0.5 μg oligo $(dT)_{18}$ primers were added. To denature the RNA, samples were heated to 70 ºC for 10 minutes. Samples were cooled on ice and briefly centrifuged. 4 μL of the 5X reaction buffer, 2 μL 10 mM dNTP mix and 1 μL 20U ribonuclease inhibitor were added and the samples were incubated at 37 ºC for 5 minutes and then centrifuged. 2 μL of 20 U Moloney Murine Virus (M-MuLV) reverse transcriptase was added to the samples and incubated at 37 ºC for 1 h. The reaction was terminated by heating to 70 ºC for 10 minutes prior to storage at –20 ºC.

2.6.5 Polymerase Chain Reaction using specific primers

Ready-To-Go PCR Beads (Amersham Pharmacia Biotech Inc., Baie d'Urfe, QU) in 0.5 mL microcentrifuge tubes were used in 25 μL PCR reactions (200 μM dNTP, 10 mM Tris-HCl pH 9.0, 50 mM KCl, 1.5 mM $MgCl_2$, and 2.5 units of PuReTaq™ DNA polymerase). 5 μL of 1:10 diluted cDNA from untreated and treated samples, 1 μL of the 10 mM stocks

for the 3' and 5' specific primers for LgSDC, LgACC, Lg26s and LgACT were diluted into 18 µL of sterile water in a PCR tube as described by Akhtar et al. (2005) and Lees (2005) (Table 2.1). Included in each set of reactions was a negative control that contained all reaction components except cDNA. The cycling conditions for the reactions were as follows: 94 ºC for 1 minute, 35 ºC for 5 minutes, 72 ºC for 5 minutes followed by 39 cycles of 94 ºC for 2 minutes, 50 ºC for 2 minutes, and 70 ºC for 2 minutes. All PCR reactions were performed in a PTC-200 thermocycler (MJ Research Products, Waltham, MA, USA). PCR products were stored at –20 ºC until further use.

Table 2.1 Sequences of gene specific primers for SDC, ACC 26S and ACT used in QPCR

Primer Name	Sequence (5'→ 3')	Tm (ºC)
5' LgSDC	AGT CTA GAG CTC CAG CAG CAC	54
3' LgSDC	CTG GAT AGA GCA ACA ATTC	54
5' LgACC	GAA TGT GCT CTC AGC GGC TG	57
3' LgACC	CCA GCC TTC TTC ATC GTC TCC	57
5' Lg26S	CGT CGC TTC GGT GAA T CA CTTG	68
3' Lg26S	ACT CCG AAT ACA GGC CGT CATC	68
5' LgACT	CAC CTT CTA CAA CGA GCT CC	61
3' LgACT	CAC CAT CAC CAG AAT CAA GC	61

2.6.6 Resolution of PCR products

The products were electrophoresed on a 1% [w/v] agarose gel with 5 mM Tris-acetate (TAE) buffer. The gel contained 0.7 mg·mL^{-1} ethidium bromide and a GeneRuler 100 base pair DNA Ladder Plus was run along-side samples for size comparison (MBI Fermentas, Burlington, ON) for 1 hour at 95 volts. 1 g agarose was added to 100 ml of 5 M TAE. 5 µl

of PCR products and 1 µl 6x loading buffer (3 mL 100% Glycerol, 3 mL 0.5 M EDTA, 3 mg Bromophenol Blue, 3 mg Xylene Cyanol, 4 mL Sterile Water) were loaded onto the gel. The predominant bands at the specifically desired molecular weight were visualized under UV light with a Fluorochem imaging system (Bio-Imaging system, Biotech Inc, Montreal, Canada).

2.6.7 Extraction of PCR products

Bands were cut from the gel with a flame-sterilized razor blade. Gel slices were transferred to 1.5 mL microfuge tubes and DNA was extracted using the EZ-10 Spin Column Gel Extraction kit for agarose gels according to the manufacturer's instructions (BioBasics, Markham, Ontario) (Lees 2005). Briefly, four volumes of Binding Buffer II were added to each tube and incubated at 55 ºC for 10 minutes with periodic shaking. The mixture was added to a spin column and left at room temperature for 2 minutes. The spin column was centrifuged at 5000 rpm for 1 minute and the flow-through discarded. 500 µL of the wash solution was added and the tube was centrifuged at 8000 rpm for 1 minute. The wash step was repeated and then a final spin was done at 10 000 rpm for 1 minute. The column was placed in a new 1.5 ml centrifuge tube and 40 µL of elution buffer was added to the centre. After incubating for 2 minutes, the tube was spun at 10 000 rpm for 1 minute. The eluted DNA was diluted in 20 µL of sterile water and the concentration was determined spectrophotometrically by reading absorbance at 260 nm and 280 nm using a Nanodropper (NanoDrop ND-1000 3.3, National Instruments Corporation, USA). Typical yields were between 10-50 $\mu g \cdot mL^{-1}$. The isolated DNA was stored at –20 ºC until further use.

2.6.8 Cloning of PCR products

3.5 µL of the recovered PCR band was ligated into the pGEM T-easy vector (Promega, Madison, WI, USA) in a 10.5 µL reaction containing 5 µL of 2X ligation buffer (100 mM Tris-HCl pH 7.5, 20 mM MgCl2, 20 mM DTT), 1 µL of vector (50 ng·µL^{-1}), and 1 µL of T4 DNA ligase (2 Weiss units µL^{-1}). Ligations were performed at 4 ºC for 24 hours. Two µL of the ligation reaction was transferred to a 1 mL microfuge tube and allowed to incubate with 50 µL of *E. coli* JM109 competent cells (Promega, Madison, WI, USA) for 20 minutes on ice followed by heat shock at 42 ºC for 30 seconds. Tubes were immediately placed on ice for 3 minutes and then 500 µL of LB broth (1% [w/v] tryptone, 0.5% [w/v] yeast extract, 0.5% [w/v] NaCl) was added and the tubes were agitated at 150 rpm at 37 ºC for 1.5 hours. Following the incubation, 100 µL of the transformed bacteria was spread on LB agar plates containing 100 µg·ml^{-1} ampicillin (MBI Fermentas, Burlington, ON), 0.5 mM IPTG, and 80 µg·ml^{-1} X-Gal (Promega, Madison, WI, USA). The transformed bacteria were allowed to adsorb to the agar at room temperature for 20 minutes and were then incubated at 37 ºC for 16 hours (Diener 2004; Akhtar 2005).

2.6.9 Isolating of plasmid DNA

Plasmid DNA was isolated from white colonies with the pGEM T-easy vector insert using the modified alkaline lysis method (Lees 2005). Two colonies from each plate were inoculate into 5 mL of LB broth supplemented with 100 µg·ml^{-1} ampicillin (Diener 2004; Akhtar 2005). Culture tubes were agitated at 200 rpm and incubated at 37 ºC for 16 hours. 1.5 mL of the culture was transferred to a fresh 1.5 mL microfuge tube. Cells were pelleted by centrifugation at 4 ºC at 13 000xg for 1 minute. The supernatant was

discarded and the remaining culture was added and centrifuged as before. The pellet was re-suspended in 200 µL of ice-cold solution I (50 mM glucose, 25 mM Tris-HCl pH 8.0, 10 mM EDTA pH 8.0) by vigorous vortexing. The re-suspended cells were lysed with 200 µL freshly prepared solution II (0.2 M NaOH, 1% SDS [w/v]). The suspension was gently mixed by inverting the tube and placed on ice for 4 minutes. The bacterial lysate was neutralized with 200 µL of solution III (3 M potassium acetate, 5 M glacial acetic acid), mixed and placed on ice for 5 minutes at which time the lysed cells were pelleted by centrifugation at 4 ºC at 13 000xg for 10 minutes. The supernatant was removed and transferred to a fresh 1.5 mL microfuge tube. RNA was removed with 10 µL of Pancreatic RNase A (10 $mg \cdot mL^{-1}$; MBI Fermentas, Burlington, ON) and incubated at 37 ºC for 25 minutes. Following RNase A digestion, 600 µL phenol:chloroform (1:1) was added to the sample and immediately vortexed for 30 seconds followed by centrifugation at 4 ºC at 13 000xg for 2 minutes. The upper aqueous phase was transferred to a fresh 1.5 mL microfuge tube and 600 µL of chloroform was added to remove residual proteins, lipids and phenol from the sample. The tube was immediately vortexed for 30 seconds and centrifuged at 13 000xg at 4 ºC for 2 minutes. The upper aqueous phase was again transferred to a fresh 1.5 mL microfuge tube to which 420 µL of ice-cold 100% isopropanol was added to precipitate the DNA. The tube was incubated for 10 minutes at room temperature followed by centrifugation at 13 000xg at 4 ºC for 10 minutes. The supernatant was removed and the pellet was resuspended in 70% ethanol by vortexing followed by centrifugation at 13 000xg and 4 ºC for 3 minutes. The supernatant was removed and the pellet was allowed to air dry for 10 minutes. The dried

pellet was dissolved in 25 µL of sterile water and stored at –20 ºC until further use (Diener 2004; Akhtar 2005).

2.6.10 Restriction digestion of purified plasmids

Purified plasmids were analyzed for inserts by restriction enzyme digests using Eco R1 (Promega, Madison, WI, USA) (Diener 2004; Akhtar 2005). To a 0.5 mL microfuge tube, 1.5 µg of plasmid was digested in a 20 µL reaction containing 2 µL of 10X Reaction Buffer H (90 mM Tris-HCl pH 7.5, 500 mM NaCl, 100 mM $MgCl_2$), 0.5 µL BSA (0.1 $mg \cdot mL^{-1}$), and 0.5 µL of Eco R1 (10 U μL^{-1}). The mixture was incubated for 2 hours at 37 ºC. Afterwards the mixtures were run on a 1% [w/v] agarose gel containing 0.7 $mg \cdot mL^{-1}$ ethidium bromide run for 1.5 hours at 70 volts. A GeneRuler 100 base pair DNA Ladder Plus (MBI Fermentas, Burlington, ON) was included to confirm and determine the presence and relative size of the inserts.

2.6.11 Sequencing of PCR products

Sequencing was done to confirm the identity of PCR products. After dilution of PCR products to 100 ng/µl in a 20 µl final volume they were sequenced in the Molecular Core Facility in the Department of Biology at the University of Waterloo with the Opengene DNA sequencer (Visible Genetics Inc.). They were sequenced with SP6 and T7 primers with sequences of ATT TAG GTG ACA CTA TAG AAT AC and TAA TAC GAC TCA CTA TAG GG respectively (Lees 2005). Sequences were compared to those of Akhtar et al. 2005 for the same genes in Genbank using the NCBI (National Centre for Biotechnology Information) network BLAST software version 1.8 (Altschul *et al*. 1997).

Nucleotide and predicted amino acid sequences were analyzed with the blastn and blastx databases respectively.

2.6.12 Construction of Relative Standard Curves for QPCR

Relative standard curves were constructed for target genes (SDC and ACC) and the house-keeping (ACT) gene using a treated sample (Lees 2005). Log concentrations from 0.01 to 100x undiluted cDNA were used to construct standard curves. iQ SYBR Green Supermix (Biorad, Mississauga, Ontario) was used in 20 μL reactions (50 mM KCl, 20 mM Tris-HCl (pH 8.4), 0.20 mM dATP, 200 μM dCTP, 200 μM dGTP, 400 μM dTTP, 3 mM $MgCl_2$, 25 units/ml iTaq DNA polymerase and 10 nM flourescein). The supermix was added to 0.2 ml low profile white tubes with flat caps (Biorad, Mississauga, Ontario). Primer pairs (10 μM) and sterile water was added to the Supermix, with the template cDNA added last. Tube strips were placed in the MiniOpticon™ Personal Thermal cycler PCR machine (Biorad, Mississauga, Ontario). PCR cycle conditions used for gene amplification were: initial denaturation at 95 ºC for 3 min, 40 cycles of: denaturation at 95 ºC for 10 sec, annealing temperature of 62 ºC for 20 sec, plate read, extension at 72 ºC for 20 sec followed by another plate read and a melt curve. By designing relatively short primers the specificity can be guaranteed and can be tested by gel electrophoreses, melting curves, and sequencing data (Gachon et al. 2004). Melt curve analysis is done after amplification by increasing the temperature in small increment and measuring the fluorescence from which the negative first derivative is plotted as a function of time to distinguish non-specific from desired products (Bio-rad 2004). The melt curve conditions were as follows: initial denaturation at 95 ºC, annealing temperature at 62 ºC measured

every 1 ºC for 2 seconds. SYBRgreen® is used often as the detection dye which intercalates into the minor groove of double-stranded DNA and determines the sensitivity of the system (Gachon et al. 2004; Deprez et al. 2002). Once it binds, the fluorescence increases 100-fold (Deprez et al. 2002). Quantification is done with calibration curves to calculate the absolute amount of the target (Gachon et al. 2004). The amplification efficiency was calculated from the slope of the standard curve using the formula: $E=10^{-1/slope}$ x 100% (Bio-Rad Laboratories 2004). Efficiencies between 90-105% indicate assay reproducibility.

2.6.13 Quantification of samples using QPCR

The reaction components were the same as previously listed. QPCR was performed for both the target and the housekeeping genes (Lees 2005) (Figure 2.3). For every 20 μL QPCR reaction in duplicate, 2 μL of undiluted cDNA was used as a template and 2 μL of 10 μM of each specific primer were added. The standard curves and samples were analyzed using two methods the $2^{-\Delta\Delta CT}$ (Livak) method and the ΔC_T method using a Reference Gene. The Livak method is widely used if the amplification efficiencies are within 5% of each other and near 100% (Bio-rad Laboratories 2004). The C_T of the target gene is normalized to that of the reference gene for both the test sample and calibrator sample: $\Delta C_{T(test)} = C_{T(target,test)} - C_{T(ref,test)}$ and $C_{T(calibrator)} = C_{T(target,calibrator)} - C_{T(ref,calibrator)}$ (Bio-rad Laboratories 2004). The ΔC_T of the test sample is normalized to that of the calibrator: $\Delta\Delta C_T = \Delta C_{T(test)} - \Delta C_{T(calibrator)}$ (Bio-rad Laboratories 2004). The expression ratio is calculated as $2^{-\Delta\Delta CT}$ (Bio-rad Laboratories 2004). The ΔC_T method using a Reference Gene was used to confirm whether the Livak method gave the correct results. The difference

in this method is that the expression of the calibrator sample is not 1.0 (Bio-rad Laboratories 2004). The ratio of the reference to the target gene is calculated as: $2^{CT(reference)- CT(target)}$ (Bio-rad Laboratories 2004).

2.7 Statistical Analysis

All statistical analysis was performed using SYSTAT 10® (Systat Software, Point Richmond, CA, USA). All experiments had an n of 9, where n is the number of samples, unless stated otherwise meaning all experiments were done in triplicate in three independent trials. To find the EC50s of the chemicals, non-linear regression analysis was done. For all other experiments, analysis of variance (ANOVA) was performed using preplanned contrast with Tukey's test of significance ($p<0.05$).

Chapter 3
Results

Two classes of ubiquitous environmental contaminants known to cause damage to aquatic organisms are polycyclic aromatic hydrocarbons (PAHs) and metals. Damage can occur when they are found alone or in mixtures (Babu et al. 2001). Previous studies have found 1,2-dihydroxyanthraquinone (1,2-dhATQ) inhibits photosynthesis and copper causes ROS formation (Babu et al 2001; Akhtar et al. 2005). However, it is not known with certainty if the site with the most ROS production in the cell is the chloroplast. Furthermore, the effects of mixtures on the expression of genes involved in fatty acid synthesis have not previously been studied in *L. gibba*.

Growth assays were performed to assess the effects of the contaminants on plant growth. ROS levels were measured using a plate reader and confocal laser scanning microscopy. To study photosynthetic electron transport two fluorescent techniques, pulse amplitude modulated (PAM) and fast repetition rate (FRR) fluorometry, were used. Lastly, changes in the expression of two genes involved in fatty acids synthesis, serine decarboxylase (SDC) and acetyl coA carboxylase (ACC) were studied using quantitative PCR (QPCR).

3.1 Growth of *L. gibba* exposed to copper and 1,2-dhATQ

To study the effects of 1,2dhATQ and Cu on plant growth eight-day growth assays were used. Copper exposures under photosynthetic active radiation (PAR) and simulated solar radiation (SSR) diminished the growth of plants compared to plants only treated with 0.1% DMSO (controls). Growth in all SSR treatments was

significantly lower than that of PAR treatments. Growth inhibition due to copper exposure was significant at concentrations equal to and greater than 6 µM under PAR and 4 µM under SSR (Figure 3.1A) ($p<0.05$). The EC50 for Cu was determined to be 7 µM under PAR and 6 µM under SSR. There were other visible signs of toxicity including a decrease in frond size due to increased sub-division, bleaching of fronds indicating necrosis and abscission of the rhizoid from the fronds (Figure 3.1B). This indicates that the actual growth inhibition could be greater than estimated using the frond count method. In addition to frond count chlorophyll concentration and biomass could be used to assess toxicity.

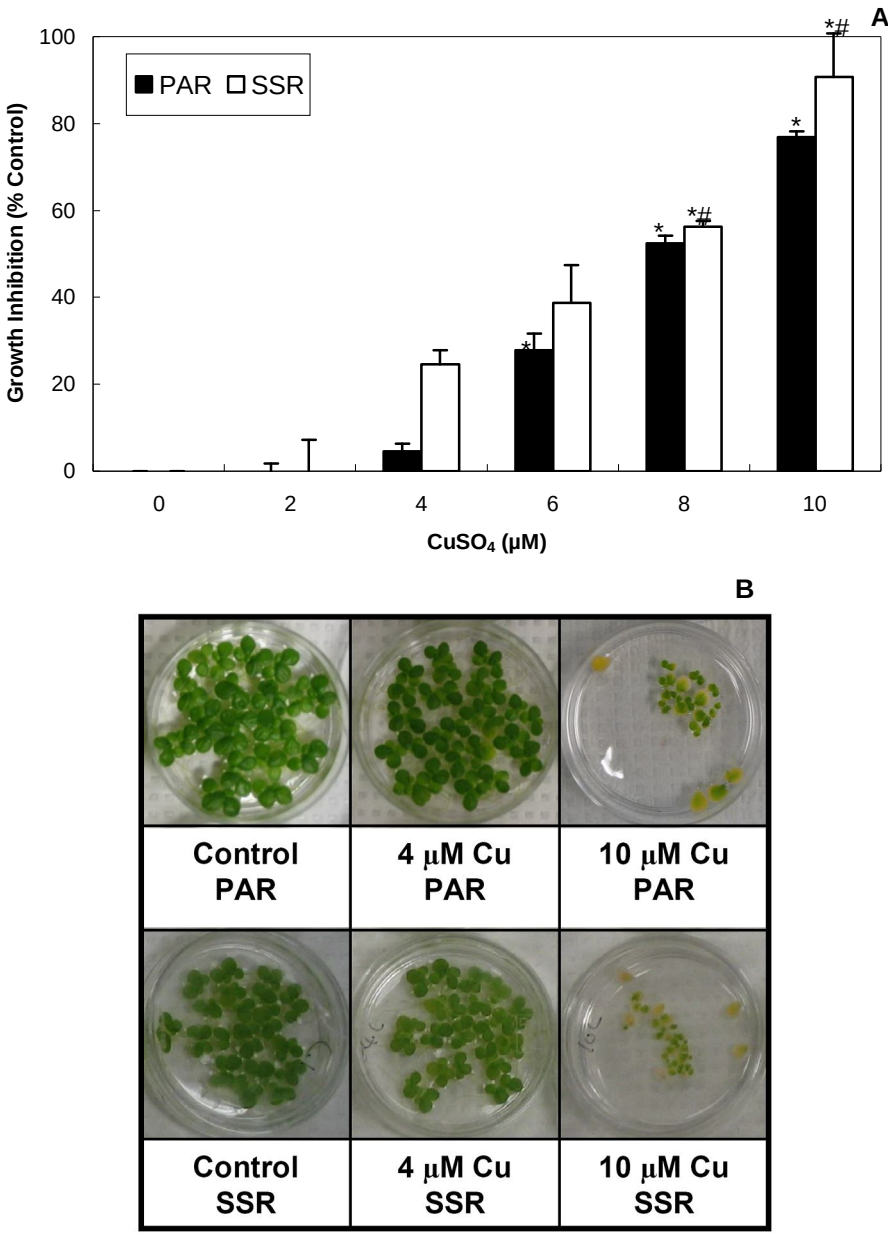

Figure 3.1 *L. gibba* growth inhibition exposed to $CuSO_4$ under PAR and SSR.

Plants were grown in Hutner's medium containing 0-10 µM $CuSO_4$ for 8 days. Fronds were counted and growth inhibition calculated. The graph (A) depicts bars of average copper growth inhibition normalized to untreated plants ± S.E. * shows significant difference when comparing all treatments to control PAR growth inhibition and # indicates significant difference when comparing all SSR treatments to control SSR growth inhibition. Representative photographs (B) were taken of *L. gibba* growth at 8 days under PAR and SSR exposed to 4 µM $CuSO_4$ and 10 µM $CuSO_4$ and their appearances were compared to that of the untreated plants.

Treatments with 1,2-dhATQ under PAR and SSR lowered plant growth even at the lowest concentrations tested. Growth inhibition was greater in SSR treatments than in PAR at higher 1,2-dhATQ concentrations (Figure 3.2A). The EC50 for 1,2-dhATQ was determined to be 5 µM under PAR and 4 µM under SSR. At higher concentrations, visible signs of toxicity included a reduction in frond size and separation of fronds from whole plants into individual fronds. Red colouration of the rhizoids and fronds was observed in *L. gibba* when concentrations of 1,2-dhATQ were greater than 5 µM (Figure 3.2B).

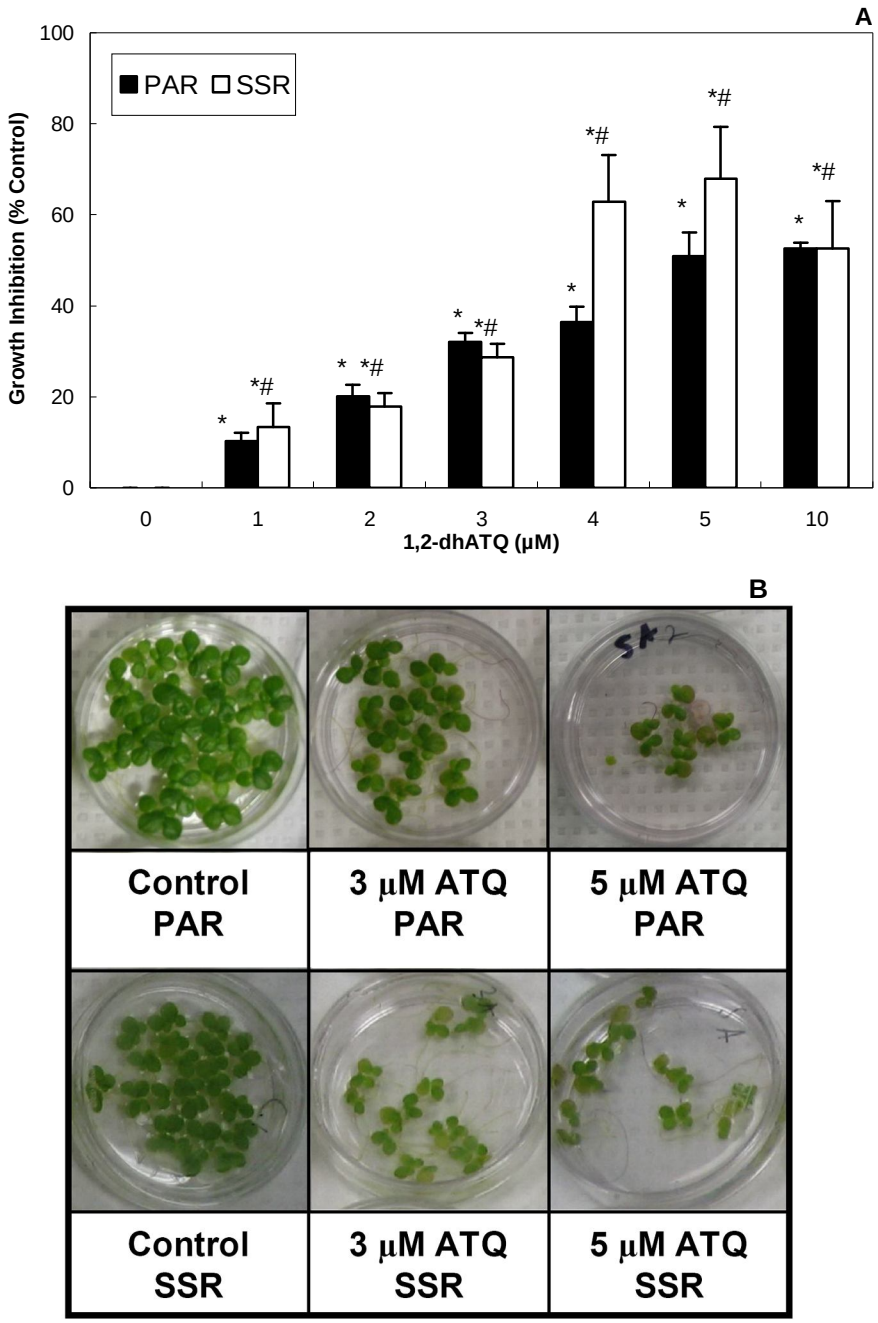

Figure 3.2 *L. gibba* growth inhibition exposed to 1,2-dhATQ under PAR and SSR.

Plants were grown in medium containing 0-10 μM 1,2-dhATQ for 8 days under PAR and SSR. Fronds were counted to assess growth inhibition. The graph (A) depicts bars of average growth inhibition of 1,2-dhATQ normalized to untreated plants ± S.E. * shows significant difference when comparing all treatments to control PAR growth inhibition and # indicates significant difference when comparing all SSR treatments to control SSR growth inhibition. Representative photographs (B) of *L. gibba* growth exposed to 3 μM 1,2-dhATQ and 5 μM 1,2-dhATQ for eight days under PAR and SSR were taken and their appearances compared to that of the untreated plants.

3.2 Growth of *L. gibba* exposed to ROS scavengers under PAR

Three ROS scavengers were tested for their abilities to ameliorate the toxicity of copper and 1,2-dhATQ. The growth inhibition of DMTU, GSH, and ascorbic acid (AA) were tested at several different concentrations to find concentrations where each had the least effect on the normal growth of *L. gibba* (Data not shown). Concentrations that had little effect on plant growth were 0.5 mM AA, 2.5 mM DMTU, and 0.25 mM GSH. When 8 µM Cu was added to 0.5 mM AA, 2.5 mM DMTU, and 0.25 mM GSH, all three of the ROS scavengers were protective against copper toxicity (Figure 3.3A and B). 0.25 mM GSH was the most protective and had the least effect on the growth of L. *gibba*. Although 0.5 mM AA was protective, it altered the morphology of the fronds reducing their sizes and causing bleaching in the untreated plants. 2.5 mM DMTU was the least protective, had the highest growth inhibition alone, and altered the morphology. Therefore GSH was selected as the ROS scavenger to further test for its ability to ameliorate 1,2-dhATQ toxicity alone and in mixtures with Cu.

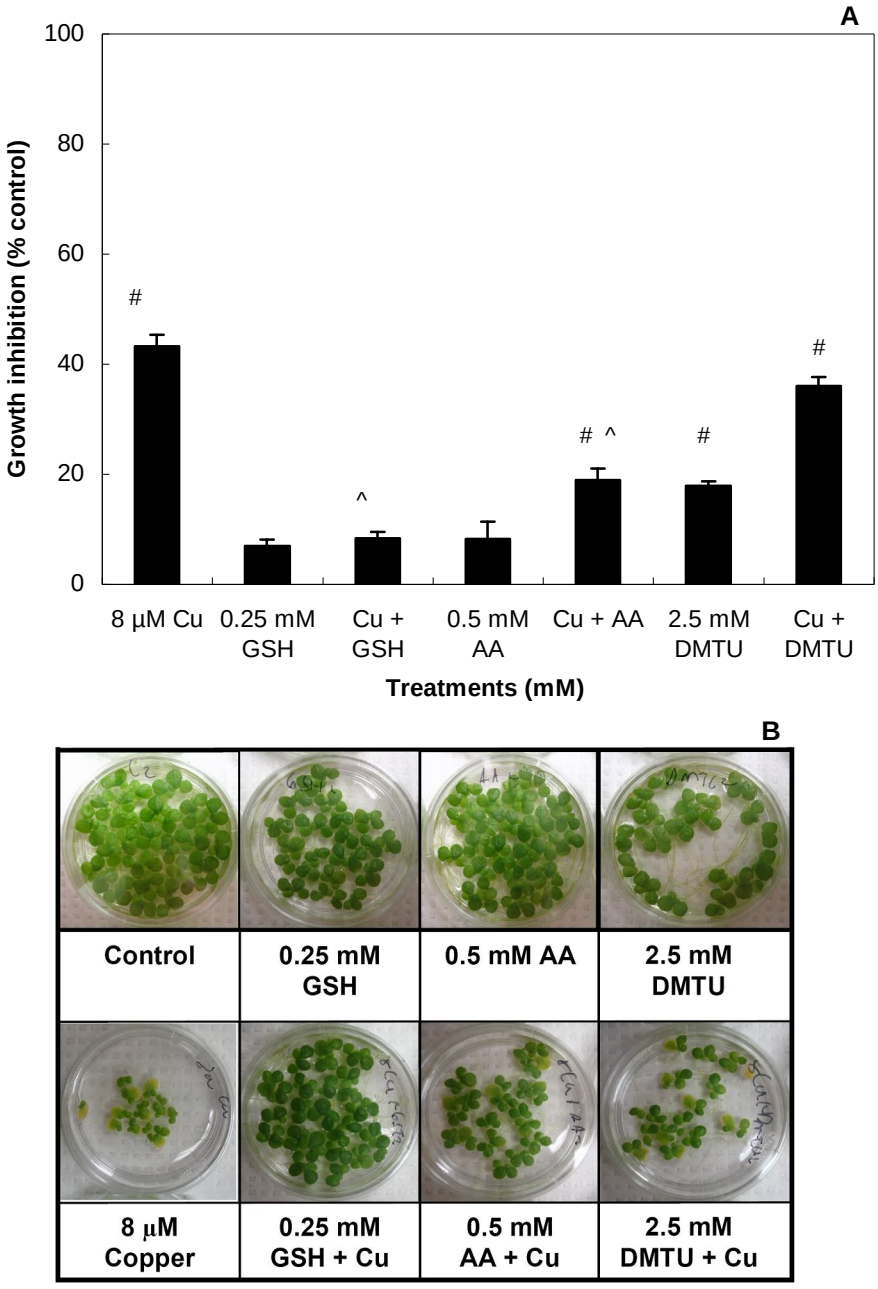

Figure 3.3 *L. gibba* growth exposed to DMTU, AA and GSH with and without 8 µM Copper under PAR.

Plants were grown in Hutner's medium containing 2.5 mM DMTU, 0.5 mM AA and 0.25 mM GSH with and without 8 µM copper to test their abilities to ameliorate copper toxicity. The graph (A) depicts bars of average growth inhibition of the treatments normalized to an untreated plant ± S.E. # indicates significant difference in growth inhibition when comparing treatments to the control and ^ indicates difference of mixture growth inhibition compared to copper alone (n=4). Representative photographs (B) of *L. gibba* growth at 8 days exposed to 2.5 mM DMTU, 0.5 mM AA and 0.25 mM GSH with and without 8 µM Copper under PAR.

To find an optimal concentration of GSH to use to ameliorate 1,2-dhATQ toxicity, a range of GSH concentrations from 0.15 to 0.35 mM was tested with 3 µM 1,2-dhATQ. 3 µM 1,2-dhATQ toxicity increased significantly with all of the GSH concentrations tested (Table 3.1 and Figure 3.4). In order to find if the effect was synergistic, the ratios of inhibition (RI) for 0.15 to 0.35 mM GSH with 3 µM 1,2-dhATQ was calculated by dividing the observed inhibition by the expected additive inhibition according to Abbot's formula. All the RI values were greater than one indicating the increase in growth inhibition is synergistic. 0.25 mM GSH had the least effect on normal growth and the increase in 1,2-dhATQ toxicity was not significantly different from any other concentration tested. Therefore, 0.25 mM GSH was further tested to see if it could decrease the toxicity of 1,2-dhATQ and Cu combinations.

Table 3.1 Ratios of inhibition of *L.gibba* exposed to GSH and 3 µM 1,2-dhATQ

Treatments (mM)	Ratio of inhibition (RI) (± S.E.)
0.15 mM GSH and 3 µM 1,2-dhATQ	1.7 ± 0.05
0.20 mM GSH and 3 µM 1,2-dhATQ	2.0 ± 0.06
0.25 mM GSH and 3 µM 1,2-dhATQ	1.8 ± 0.04
0.30mM GSH and 3 µM 1,2-dhATQ	1.8 ± 0.01
0.35 mM GSH and 3 µM 1,2-dhATQ	1.4 ± 0.01

Table 3.1 contains the ratio of inhibition for 0.15 to 0.35 mM GSH with 3 µM 1,2-dhATQ, where RI<1 is antagonistic, RI >1 is synergistic and R=1 is additive between the two chemicals ± S.E.

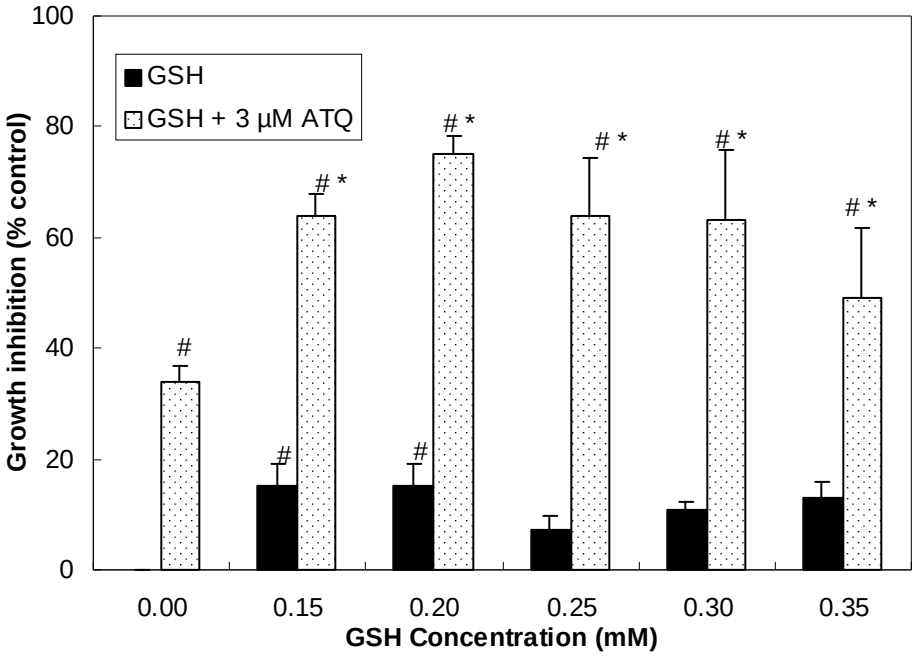

Figure 3.4 *L. gibba* growth inhibition exposed to 0–0.35 mM GSH with 3 µM 1,2-dhATQ under PAR.

Whole organism toxicity studies were conducted for 8 days. Bars represent average normalized growth inhibition of 3 µM 1,2-dhATQ with GSH ranging from 0.15 to 0.35 mM to untreated plants ± S.E. # indicates significant difference in growth inhibition when comparing treatments to the control and * indicates significant difference of mixture growth inhibition compared to 1,2-dhATQ alone (n=3).

3.3 Growth of *L. gibba* exposed to combinations of 1,2-dhATQ and Cu, with and without GSH under PAR and SSR

An important goal of this study was to evaluate the toxicity of 1,2-dhATQ and copper combinations to determine if they were more toxic together than individually. Previous research found that 3 µM 1,2-dhATQ mixed with 4 µM Cu had synergistic toxicity (Babu et al. 2005). In this study, the EC50s for the individual contaminants were used to select concentrations for the mixture treatments as well as repeat previous findings. Low concentrations used in the PAR experiments were 3 µM 1,2-dhATQ and 4 µM Cu with and without GSH, while higher concentrations used were 4 µM and 5 µM 1,2-dhATQ and 6 µM Cu with and without GSH (Figures 3.5A-C). Combinations of 1,2-dhATQ and Cu had higher growth inhibition of the contaminants alone. GSH increased the toxicity of 1,2-dhATQ, but ameliorated Cu and mixture toxicities. Combinations used for SSR experiments were selected to have similar growth inhibition than that of 3 µM and 5 µM 1,2-dhATQ and 4 µM and 6 µM Cu, therefore as both contaminants had increased toxicity under SSR the concentrations used were lower at 2 µM and 4 µM 1,2-dhATQ and 2 µM and 4 µM Cu (Figures 3.5D and E). The toxicities of the contaminants alone increased under SSR as well as the toxicity of GSH.

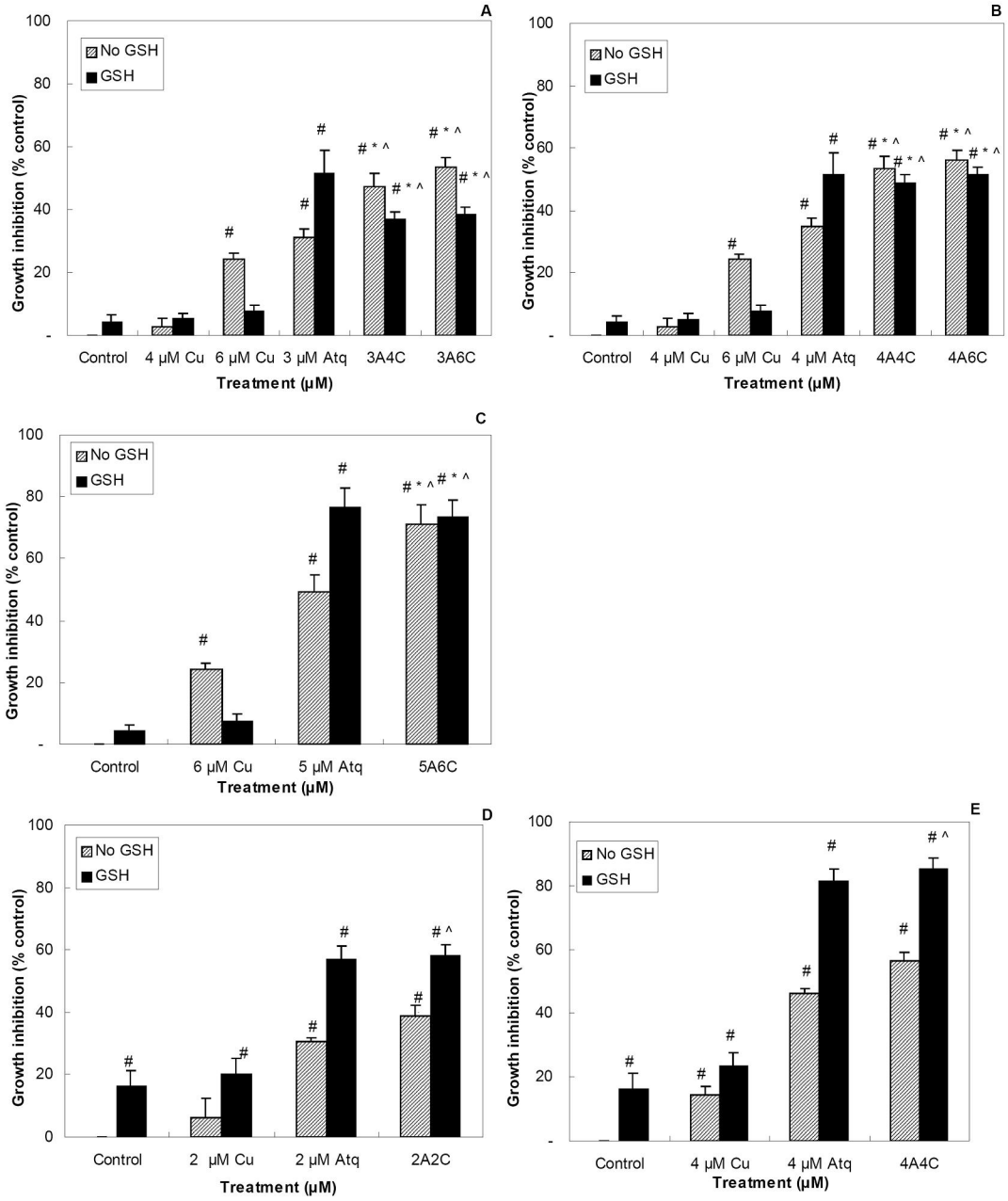

Figure 3.5 *L. gibba* growth inhibition exposed to 1,2-dhATQ, copper and their combinations under PAR and SSR with and without GSH.

Whole organism toxicity studies were conducted for 8 days. Graphs (A-C) depict bars of average growth inhibition of treatments normalized to controls under PAR and graphs (D and E) depict bars of average growth inhibition of treatments normalized to controls under SSR ± S.E. # indicates significant differences in growth inhibition when comparing treatments to the PAR control, * indicates significant differences of mixtures compared to 1,2-dhATQ alone and ^ indicates significant differences of mixtures compared to Cu alone all with and without GSH, therefore synergistic toxicity is indicated by (#^*).

In order to find combinations that were synergistic the ratio of inhibition (RI) was calculated by dividing the observed inhibition by the expected additive inhibition (Table 3.2). Synergistic growth inhibition, had RI ratios greater than 1.2, such as 3 µM 1,2-dhATQ and 4 µM copper, 4 µM 1,2-dhATQ and 4 µM copper, and 5 µM 1,2-dhATQ and 6 µM copper. Additive toxicity, having RI ratios between 1.0 and 1.1, was caused by 3 µM 1,2-dhATQ and 6 µM copper, 4 µM 1,2-dhATQ and 6 µM copper, 2 µM 1,2-dhATQ and 2 µM Cu, and 4 µM 1,2-dhATQ and 4 µM Cu. GSH ameliorated mixture toxicity and had RI ratios less than 1.

Table 3.2 Ratio of inhibition to determine synergistic growth inhibition of *L. gibba* exposed to mixtures of 1,2-dhATQ and copper

Treatments (µM)	RI (± S.E.) No GSH	RI (± S.E.) GSH
3 µM 1,2-dhATQ and 4 µM copper	1.4 ± 0.04	0.7 ± 0.07
3 µM 1,2-dhATQ and 6 µM copper	1.0 ± 0.03	0.7 ± 0.08
4 µM 1,2-dhATQ and 4 µM copper	1.5 ± 0.03	0.6 ± 0.07
4 µM 1,2-dhATQ and 6 µM copper	1.1 ± 0.02	0.6 ± 0.07
5 µM 1,2-dhATQ and 6 µM copper	1.2 ± 0.06	0.9 ± 0.07
2 µM 1,2-dhATQ and 2 µM copper	1.1 ± 0.06	0.9 ± 0.06
4 µM 1,2-dhATQ and 4 µM copper	1.1 ± 0.06	1.0 ± 0.06

Table 3.2 contains the ratio of inhibitions for combinations of 1,2-dhATQ and Cu with and without GSH under PAR and SSR.

3.4 The production of ROS in *L. gibba* exposed to copper, 1,2-dhATQ and their combinations

The contaminants individually and in combination caused growth inhibition that could be due to the production of reactive oxygen species (ROS) (Babu et al. 2001; Akhtar et al. 2005). To determine an adequate exposure time to 5 µM of the dye, 2',7'-dichlorodihydrofluorescein diacetate (H_2DCFDA), plate reader measurements were collected at 30 minutes intervals from plants treated with 3 µM 1,2-dhATQ, 6 µM Cu and their combination for 24 hours (Figure 3.6). H_2DCFDA was taken up into the fronds and cleaved by esterases to H_2DCF, which was oxidized to DCF by ROS. Over 300 minutes the DCF fluorescence of 6 µM Cu and the combination of 1,2-dhATQ and Cu increased compared to plants only treated with 5 µM H_2DCFDA whereas DCF fluorescence of 3 µM 1,2-dhATQ was similar to H_2DCFDA treated plants. The increases or decreases of DCF fluorescence at 30 minutes compared to 300 minutes for the treated plants were equivalent. To compare DCF data in this study to that of previous research, DCF measurements were taken after 30 minutes of exposure to 5 µM H_2DCFDA for all treatments (Babu et al. 2001; Akhtar et al. 2005; Lees 2005).

After 24 hours of exposure to 3 µM 1,2-dhATQ, 4 and 6 µM Cu and their combinations the ROS levels only significantly increased in the 6 µM Cu compared to untreated plants (Figure 3.7A). 3 µM 1,2-dhATQ, 4 µM Cu and combinations of 3 µM 1,2-dhATQ with 4 and 6 µM Cu had ROS levels similar to that of plants only treated with 5 µM H_2DCFDA. Glutathione lowered DCF fluorescence in all treatments. Exposure to 4 µM 1,2-dhATQ, 4 and 6 µM Cu and their mixtures with and without GSH for 24 hours gave similar results to treatments with 3 µM 1,2-dhATQ (Figure 3.7C). Treatments with 5 µM 1,2-dhATQ, 6 µM Cu and their mixture with and

without GSH after 24 hours only showed an increase in DCF in the 6 µM Cu compared to plants only treated with 5 µM H_2DCFDA whereas 5 µM 1,2-dhATQ alone and with 6 µM Cu had very low DCF levels compared to untreated plants (Figure 3.7E).

Previous research found ROS levels reached steady-state levels after 4-day exposures to 1,2-dhATQ, Cu and their mixtures (Babu et al. 2003; Akhtar et al. 2005; Lees 2005). After 4 days, the ROS levels increased in 4 and 6 µM Cu, 3 and 4 µM 1,2-dhATQ and in combinations of 3 and 4 µM 1,2-dhATQ with 4 µM Cu compared to plants only treated with 5 µM H_2DCFDA (Figure 3.7B and D). Mixtures of 3 and 4 µM 1,2-dhATQ with 6 µM Cu had DCF fluorescence levels similar to that of the untreated plants. 5 µM 1,2-dhATQ alone and with 6 µM Cu had lower ROS levels than the plants only treated with 5 µM H_2DCFDA probably due to cell death (Figure 3.7F). GSH was still able to lowered ROS levels in all treatments.

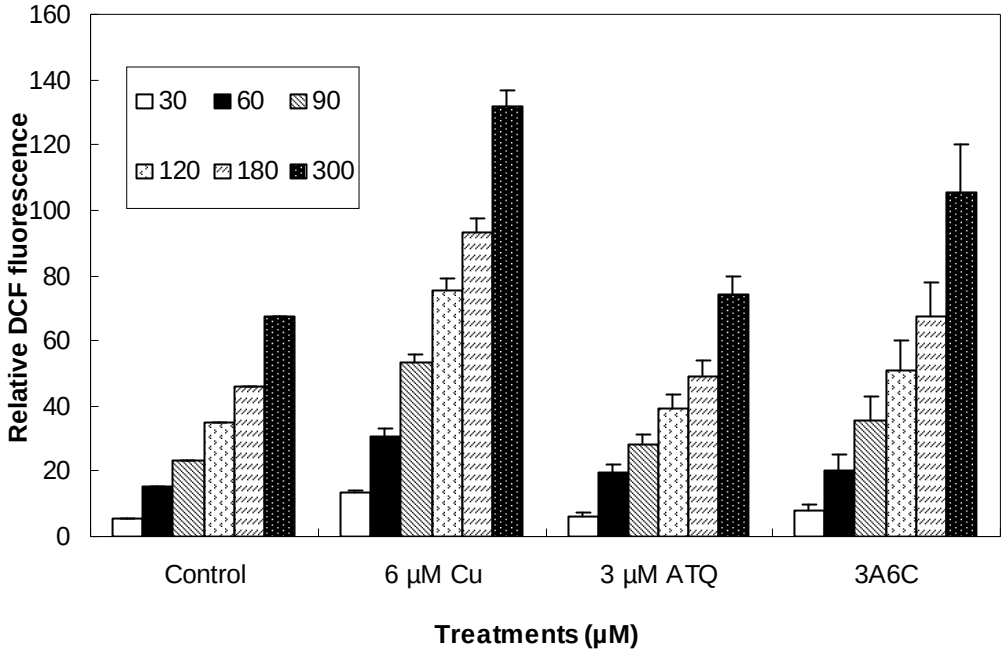

Figure 3.6 *L. gibba* DCF fluorescence exposed to 1,2dhATQ, copper and their combination for 24 hours under PAR.

Plants were exposed to 3 µM 1,2-dhATQ, 6 µM Cu and their combination for 24 hours. After 24 hours the relative DCF fluorescence was collected using excitation and emission wavelengths of 485 nm and 530 nm from the whole plants treated with 5 µM of H_2DCFDA for 30, 90, 120, 180, 240 and 300 minutes. Bars represent average relative DCF fluorescence of 1,2-dhATQ, copper and their mixtures ± S.E. (n=6).

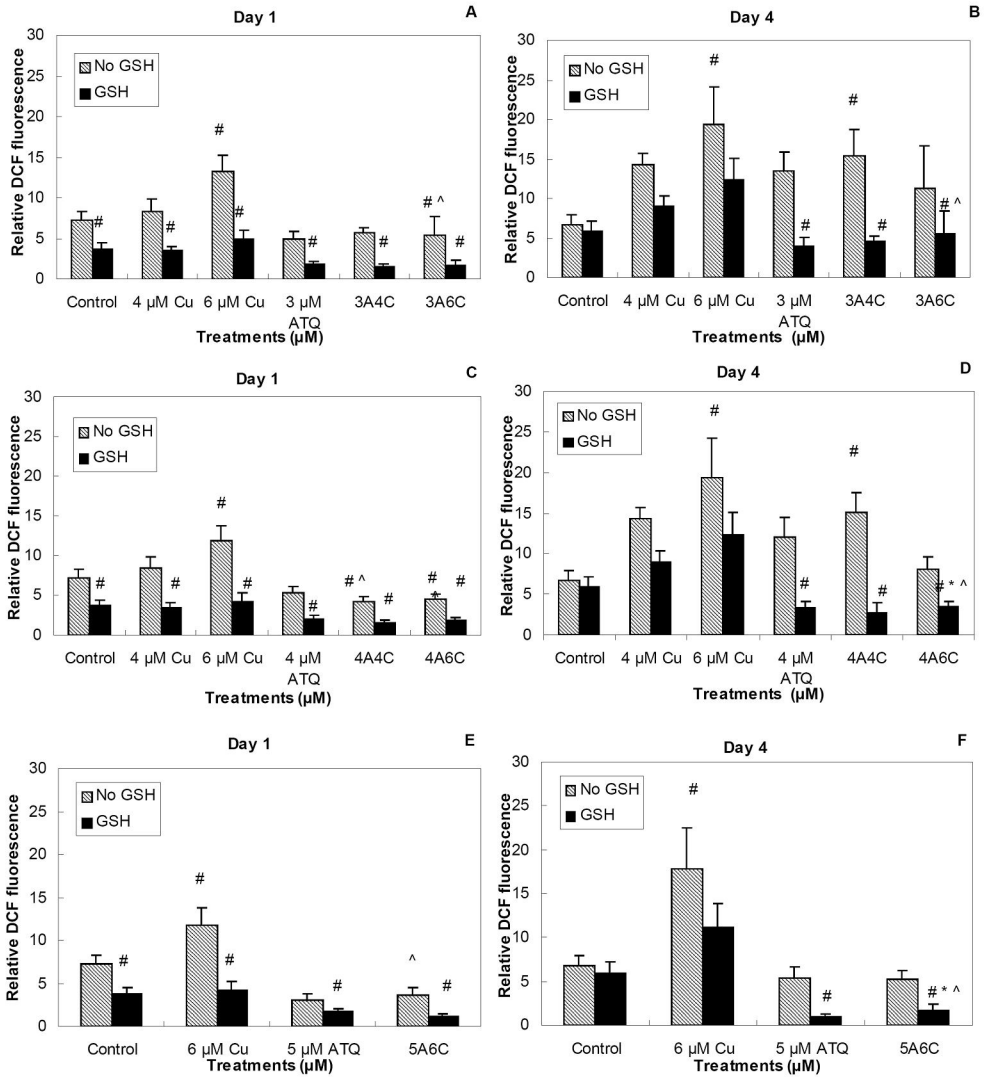

Figure 3.7 *L. gibba* DCF fluorescence exposed to 1,2-dhATQ, Cu and their mixtures for 24 hours and 4 days under PAR.

Plants were treated with 3, 4 and 5 µM 1,2-dhATQ with 4 and 6 µM Cu, with and without GSH, for 24 hours and 4 days. After 24 hours and 4 days, the relative DCF fluorescence was collected using excitation and emission wavelengths of 485 nm and 530 nm from the whole plants treated with 5 µM of H_2DCFDA for 30 minutes. Graphs (A-F) depict bars of average relative DCF fluorescence of 1,2-dhATQ, copper and their mixtures ± S.E. # indicates significant differences in DCF fluorescence when comparing treatments to plants only treated with H_2DCFDA, * indicates differences of mixtures compared to 1,2-dhATQ alone and ^ indicates differences of mixtures compared to Cu alone all with and without GSH.

To study where in the cell ROS accumulated, confocal laser scanning microscopy (CLSM) was used. Plants were treated with 3 µM 1,2-dhATQ, 6 µM Cu and their combination for 24 hours. After washing, plants were exposed to 5 µM H_2DCFDA for 2 hours. The fronds were separated and mesophyll cells were scanned. Only 24-hour exposures were used as longer exposure damaged mesophyll cells severely causing the dye to leak out of the cells (Data not shown). The excitation wavelength for DCF used was 488 nm and the emission was collected on the Meta channel at 507.6-571.8 nm. Chlorophyll autofluorescence was collected simultaneously at 657.4-700.2 nm. Simultaneous collection allowed comparison of relative fluorescence from DCF to that of chlorophyll autofluorescence. An unloaded DCF control was used to ensure there were no interfering fluorophores present. DCF fluorescence from the plants exposed to 1,2-dhATQ, Cu and their combination was compared to that of the plants only treated with H_2DCFDA.

Plants not treated with H_2DCFDA nor the contaminants strongly fluoresced at 657-700 nm and minimally at 508-572 nm. Chloroplasts were seen as flattened ovals in the cell wall within the peripheral cytoplasm with no autofluorescence in the vacuole or other cytoplasmic organelles. Plants only treated with H_2DCFDA had DCF fluorescence in the nucleus and cytoplasm but not the vacuole. Plants exposed to 6 µM Cu had increased DCF fluorescence in the chloroplast. Copper also caused damage in the epidermal and subepidermal cells, DCF-filled protrusions surrounding the chloroplasts, and a decrease in the number of total chloroplasts as well as coagulation of the cytoplasm causing a loss in DCF and chlorophyll fluorescence (Figure 3.8). 1,2-dhATQ and mixture treatments had lower DCF fluorescence

compared to plants only treated with H_2DCFDA. In some experiments, mixtures had more DCF fluorescence than 1,2-dhATQ alone. A great deal of variability was observed in the amounts of DCF fluorescence between fronds within an experiment and between experiments.

Fluorescence data collected with the plate reader and microscope had similar findings. Copper treatments increased ROS levels, after 24 hour and 4-day exposures, and were found to be associated with the chloroplasts. 24 hours of exposure to 1,2-dhATQ depressed DCF fluorescence in both techniques. Mixture treatments had similar fluorescence levels to that of 1,2-dhATQ after 24 hour exposures although confocal microscopy did show an increase in some experiments.

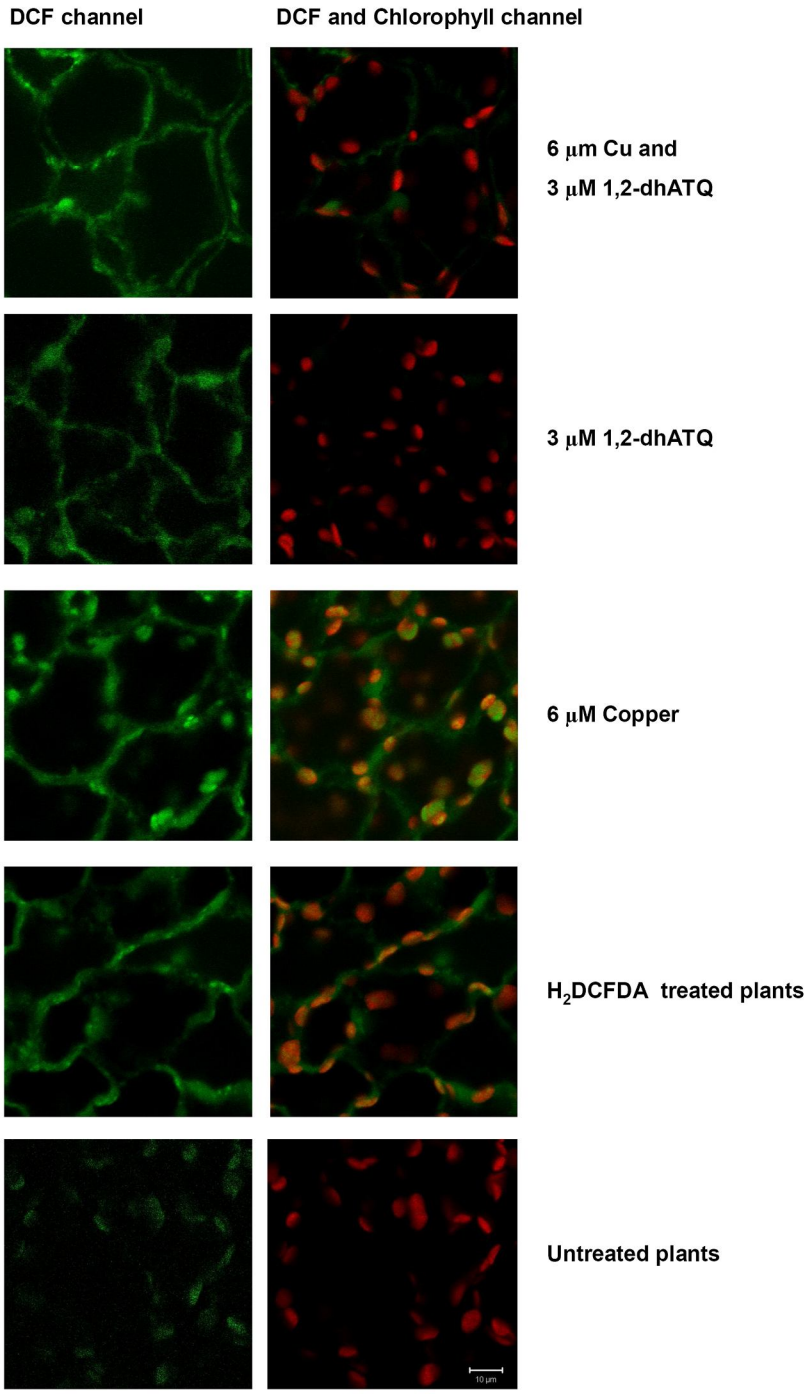

Figure 3.8 DCF fluorescence in *L. gibba* mesophyll cells visualized with CLSM.

Plants were exposed to 3 µM 1,2-dhATQ, 6 µM Cu and their combination for 24 hours and then exposed to 5 µM H_2DCFDA for 2 hours. Using CLSM DCF fluorescence and chlorophyll autofluorescence were collected simultaneously at 508-572 nm and 657-700 nm. Images of plants only treated with H_2DCFDA were used to observe increases or decreases in DCF fluorescence due to 1,2-dhATQ and Cu exposures (Scale bar – 10 µm) (Pictures provided by D. Enstone).

3.5 The study of photosynthetic electron transport of *L. gibba* exposed to copper and 1,2-dhATQ and their mixtures

To further understand the mechanisms of copper and 1,2-dhATQ toxicity, their effects on photosynthetic electron transport were studied using two fluorometric techniques namely pulse amplitude modulated (PAM) fluorometry and fast repetition rate fluorometry (FRRF). For PAM fluorometry, a multi-turnover technique, chlorophyll *a* fluorescence was measured after 4-hour, 24-hour and 4-day exposures to 1,2-dhATQ, Cu and their mixtures with and without 0.25 mM GSH. Concentrations used were 4 and 6 µM copper, 3 and 5 µM 1,2-dhATQ with and without GSH and mixtures of 3 µM 1,2-dhATQ with 4 µM copper and 5 µM 1,2-dhATQ with 6 µM Cu with and without GSH. Plants were dark-adapted for 30 minutes before PAM fluorometry measurements were taken.

Initial PAM parameters collected were F_o and F_m. F'_m and F_o did not significantly differ among any of the treatments at 4 hours, 24 hours or 4 days. After 4 hours and 4 days, F_m was slightly lower in treatments with 3 µM 1,2-dhATQ with GSH, 3 µM 1,2-dhATQ and 4 µM copper with GSH and all treatments with 5 µM 1,2-dhATQ (Tables 3.3 and 3.5). After 24 hours F_m was slightly lower in treatments of 3 µM 1,2-dhATQ with GSH, 3 µM 1,2-dhATQ and 4 µM copper with/without GSH and 5 µM 1,2-dhATQ with Cu and GSH (Table 3.4). After 4 hours non-photochemical quenching of fluorescence (qN) was lower in all treatments with 1,2-dhATQ without GSH and in 6 µM Cu treatments. After 24 hours, qN was lower in all 1,2-dhATQ treatments with and without GSH and 6 µM Cu. After 4 days, qN was lower in all treatments with 1,2-dhATQ without GSH, 6 µM Cu, and 5 µM 1,2-dhATQ and 6 µM Cu with GSH.

Table 3.3 F_o, F_m, F'_m and qN obtained using PAM fluorometry of *L. gibba* exposed to 1,2-dhATQ, Cu and their mixtures with and without GSH under PAR for 4 hours.

	F_o		F_m		F'_m		qN	
Treatments (µM)	No GSH	GSH	No GSH	GSH	No GSH	GSH	No GSH	GSH
Control	0.210 ±0.011	0.217 ±0.033	0.842 ±0.046	0.888 ±0.119	0.720 ±0.057	0.736 ±0.109	0.194 ±0.081	0.236 ±0.041
4 µM Cu	0.220 ±0.010	0.216 ±0.011	0.815± 0.202	0.876 ±0.081	0.705 ±0.109	0.703 ±0.110	0.251 ±0.099	0.262 ±0.129
3 µM ATQ	0.234 ±0.011	0.222 ±0.023	0.842 ±0.113	0.727 ±0.084 #	0.813 ±0.108	0.665 ±0.161	0.046 ±0.053#	0.146 ±0.199
3A4C	0.226 ±0.015	0.219 ±0.015	0.832 ±0.074	0.713 ±0.090 #^	0.789 ±0.067	0.679 ±0.100	0.071 ±0.037 #^	0.077 ±0.101 ^
6 µM Cu	0.216 ±0.024	0.211 ±0.012	0.806 ±0.119	0.852 ±0.093	0.605 ±0.120	0.705 ±0.086	0.359 ±0.151 #	0.221 ±0.062
5 µM ATQ	0.210 ±0.018	0.218 ±0.020	0.680 ±0.106 #	0.692 ±0.104 #	0.673 ±0.099	0.700 ±0.110	0.021 ±0.036 #	0.010 ±0.016 #
5A6C	0.217 ±0.015	0.217 ±0.016	0.712 ±0.070 #	0.680 ±0.053 #^	0.652 ±0.122	0.671 ±0.072	0.063 ±0.068 #^	0.044 ±0.047 #^

Average fluorescent values are given ± S.E. # indicates significant differences in fluorescence when comparing treatments to the untreated plants, * indicates differences of mixtures compared to 1,2-dhATQ alone and ^ indicates differences of mixtures compared to Cu alone all with and without GSH.

Table 3.4 F_o, F_m, F'_m and qN obtained using PAM fluorometry of *L. gibba* exposed to 1,2-dhATQ, Cu and their mixtures with and without GSH under PAR for 24 hours.

	F_o		F_m		F'_m		qN	
Treatments (µM)	No GSH	GSH	No GSH	GSH	No GSH	GSH	No GSH	GSH
Control	0.218 ±0.016	0.216 ±0.024	0.867 ±0.103	0.873 ±0.139	0.734 ±0.094	0.699 ±0.093	0.203 ±0.063	0.254 ±0.064
4 µM Cu	0.220 ±0.014	0.215 ±0.016	0.827 ±0.114	0.846 ±0.088	0.703 ±0.078	0.719 ±0.052	0.196 ±0.044	0.198 ±0.066
3 µM ATQ	0.232 ±0.035	0.226 ±0.020	0.748 ±0.135	0.657 ±0.157#	0.695 ±0.131	0.618 ±0.131	0.104 ±0.068 #	0.080 ±0.103 #
3A4C	0.218 ±0.030	0.230 ±0.015	0.711 ±0.083 #	0.727 ±0.160#^	0.637 ±0.102	0.693 ±0.158	0.113 ±0.067#^	0.085 ±0.112#^
6 µM Cu	0.212 ±0.020	0.214 ±0.022	0.867 ±0.103	0.838 ±0.077	0.649 ±0.136	0.710 ±0.069	0.251 ±0.128#	0.201 ±0.064
5 µM ATQ	0.225 ±0.011	0.222 ±0.041	0.728 ±0.093	0.636 ±0.196#	0.700 ±0.070	0.652 ±0.191	0.058 ±0.047#	0.086 ±0.087#
5A6C	0.218 ±0.014	0.225 ±0.024	0.726 ±0.088	0.697 ±0.151#	0.676 ±0.080	0.673 ±0.128	0.106 ±0.058#^	0.069 ±0.053#^

Average fluorescent values are given ± S.E. # indicates significant differences in fluorescence when comparing treatments to untreated plants, * indicates differences of mixtures compared to 1,2-dhATQ alone and ^ indicates differences of mixtures compared to Cu alone all with and without GSH.

Table 3.5 F_o, F_m, F'_m and qN obtained using PAM fluorometry of *L. gibba* exposed to 1,2-dhATQ, Cu and their mixtures with and without GSH under PAR for 4 days.

	F_o		F_m		F'_m		qN	
Treatments (µM)	No GSH	GSH	No GSH	GSH	No GSH	GSH	No GSH	GSH
Control	0.215 ±0.017	0.220 ±0.018	0.889 ±0.071	0.981 ±0.079	0.719 ±0.055	0.816 ±0.052	0.249 ±0.087	0.246 ±0.104
4 µM Cu	0.212 ±0.010	0.223 ±0.018	0.941 ±0.061	1.006 ±0.084	0.800 ±0.071	0.764 ±0.103	0.204 ±0.079	0.295 ±0.141
3 µM ATQ	0.209 ±0.010	0.215 ±0.013	0.806 ±0.093	0.740 ±0.096#	0.745 ±0.069	0.613 ±0.127	0.151 ±0.174#	0.219 ±0.188
3A4C	0.223 ±0.023	0.206 ±0.017	0.831 ±0.067^	0.773 ±0.111#^	0.777 ±0.071	0.691 ±0.114	0.088 ±0.066#	0.175 ±0.129
6 µM Cu	0.221 ±0.017	0.223 ±0.017	0.889 ±0.071	0.997 ±0.109	0.740 ±0.074	0.793 ±0.132	0.166 ±0.045#	0.240 ±0.117
5 µM ATQ	0.224 ±0.017	0.204 ±0.013	0.805 ±0.145	0.671 ±0.108#	0.680 ±0.148	0.585 ±0.152	0.187 ±0.163#	0.212 ±0.213
5A6C	0.212 ±0.021	0.221 ±0.013	0.779 ±0.126#^	0.758 ±0.056#^	0.744 ±0.133	0.687 ±0.111	0.082 ±0.111#	0.127 ±0.188#

Average fluorescent values are given ± S.E. # indicates significant differences in fluorescence when comparing treatments to untreated plants, * indicates differences of mixtures compared to 1,2-dhATQ alone and ^ indicates differences of mixtures compared to Cu alone all with and without GSH.

From F_o and F_m the F_v/F_m ratio was calculated (Figure 3.9A and B). F_v/F_m is the maximal chemical quantum yield of PSII with a normal value of approximately 0.750. 4 and 6 µM Cu exposures and 0.25 mM GSH did not significantly lower the ratio after 4 hours, 24 hours and 4 days. Treatments with significantly lower F_v/F_m compared to untreated plants were 3 µM 1,2-dhATQ with GSH, 3 µM 1,2-dhATQ with 4 µM Cu plus GSH, 5 µM 1,2-dhATQ with and without GSH, and 5 µM 1,2-dhATQ with 6 µM Cu with and without GSH ($p<0.05$).

The steady-state fluorescence (F_s) under actinic light for 4 and 6 µM Cu and GSH treatments were not different from the untreated control plants after 4 hour, 24 hour and 4 day exposures (Figure 3.10A and B). F_s was significantly higher in all treatments 3 and 5 µM 1,2-dhATQ with and without GSH. Mixtures of 1,2-dhATQ and Cu treatment F_s levels were lower than that of 1,2-dhATQ alone but higher than F_s levels of control plants.

The yield of photosynthesis (Y) and the photochemical quenching (qP) were not affected by 4 and 6 µM Cu nor 0.25 mM GSH after 4 hour, 24 hour and 4 day exposures (Figure 3.11A and B and Figure 3.12A and B). Exposures to 3 and 5 µM 1,2-dhATQ with and without GSH lowered Y and qP significantly compared to untreated plants. Combinations of 3 and 5 µM 1,2-dhATQ with Cu with and without GSH showed an increase in Y and qP compared to treatments with 3 and 5 µM 1,2-dhATQ alone.

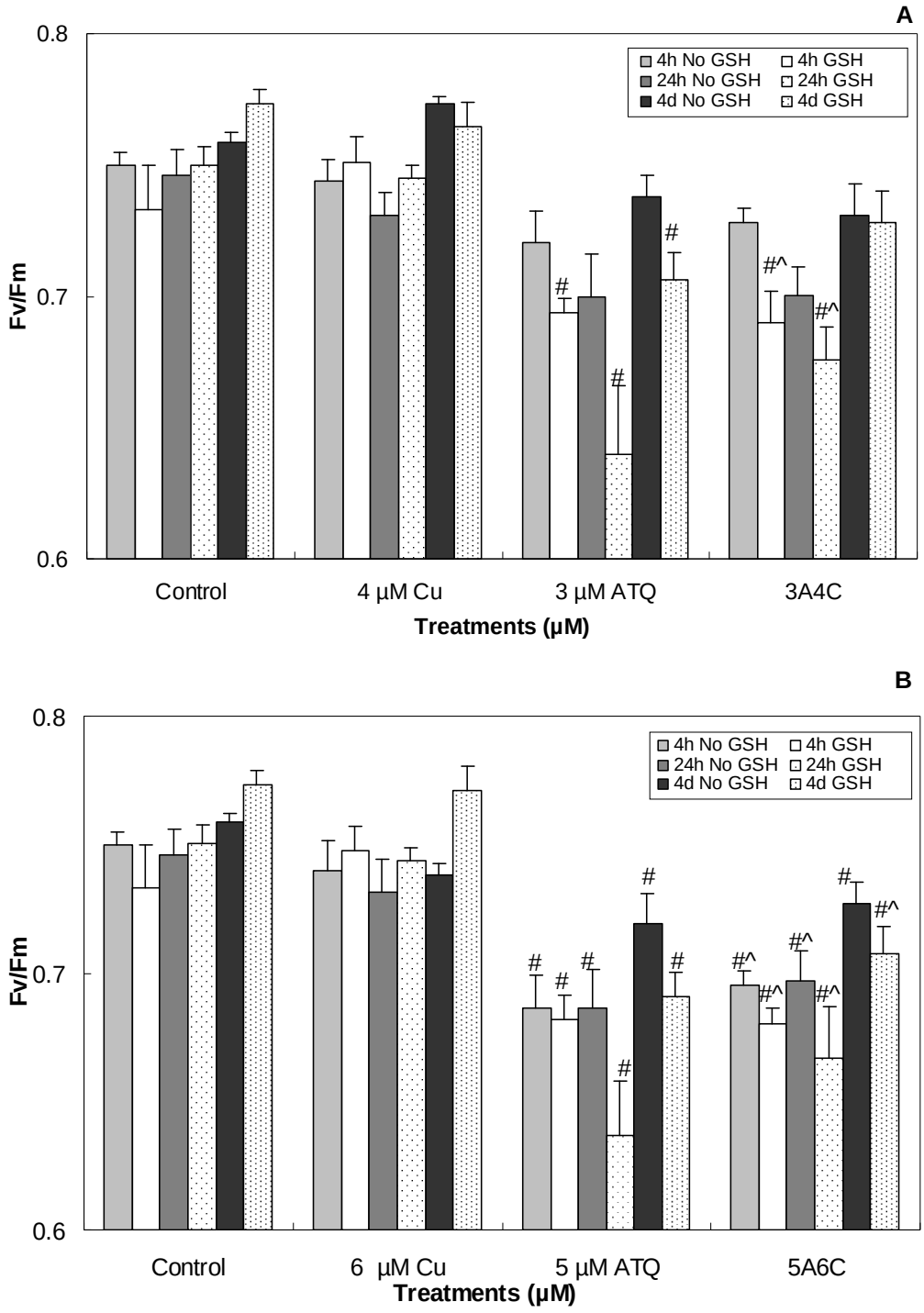

Figure 3.9 The effects of 1,2-dhATQ and copper after 4 hour, 24 hour and 4 day exposures on the maximum quantum yield of PSII.

Graphs (A and B) depict bars of average F_v/F_m values of 1,2-dhATQ, copper and their combination ± S.E. # indicates significant differences in fluorescence when comparing treatments to the control, * indicates differences of mixtures compared to 1,2-dhATQ alone and ^ indicates differences of mixtures compared to Cu alone all with and without GSH.

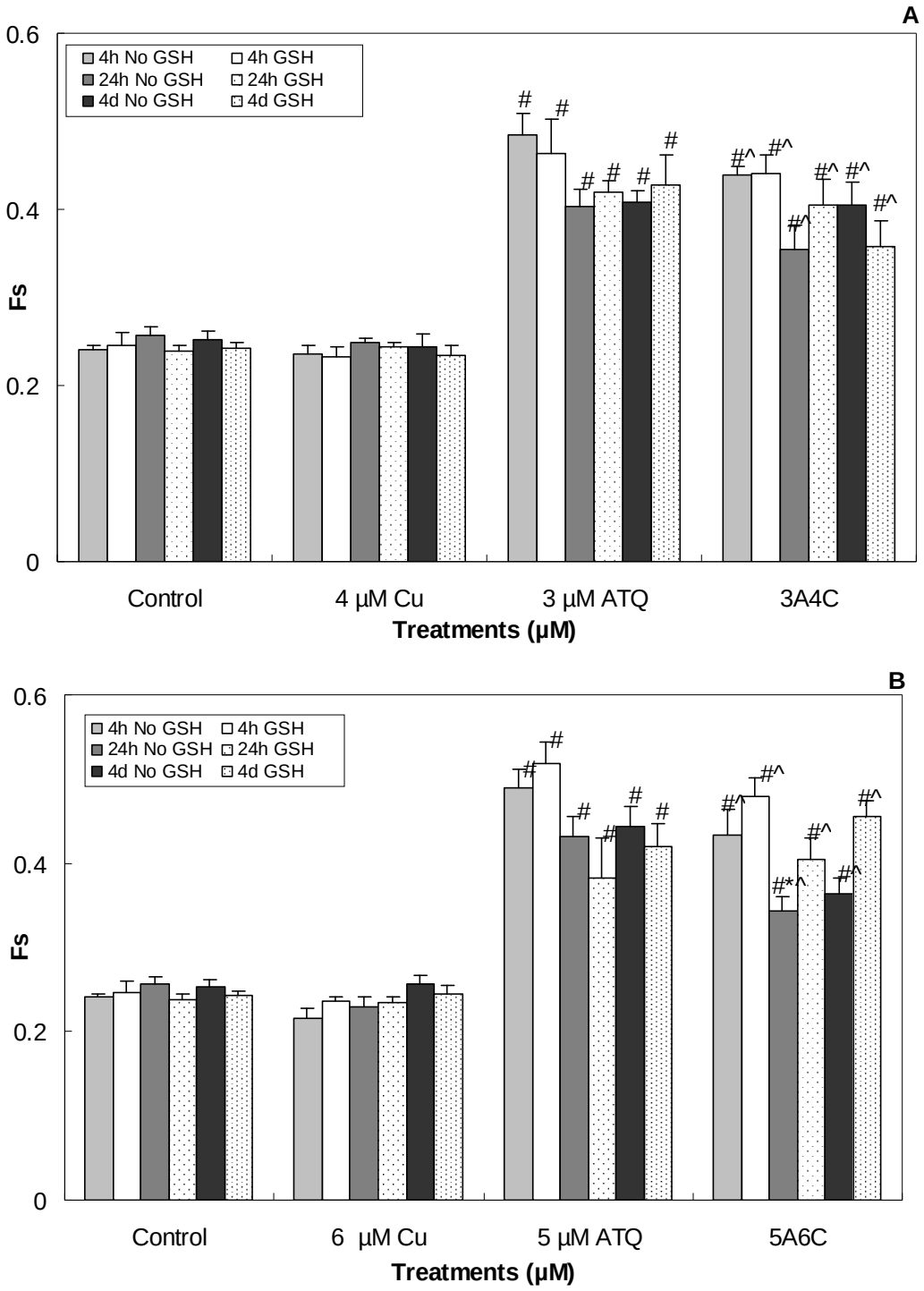

Figure 3.10 The effects of 1,2-dhATQ and copper after 4 hour, 24 hour and 4 day exposures on the steady state fluorescence.

Graphs (A and B) depict bars of average F_s values of 1,2-dhATQ, copper and their combination ± S.E. # indicates significant differences in fluorescence when comparing treatments to the untreated sample, * indicates differences of mixtures compared to 1,2-dhATQ alone and ^ indicates differences of mixtures compared to Cu alone all with and without GSH.

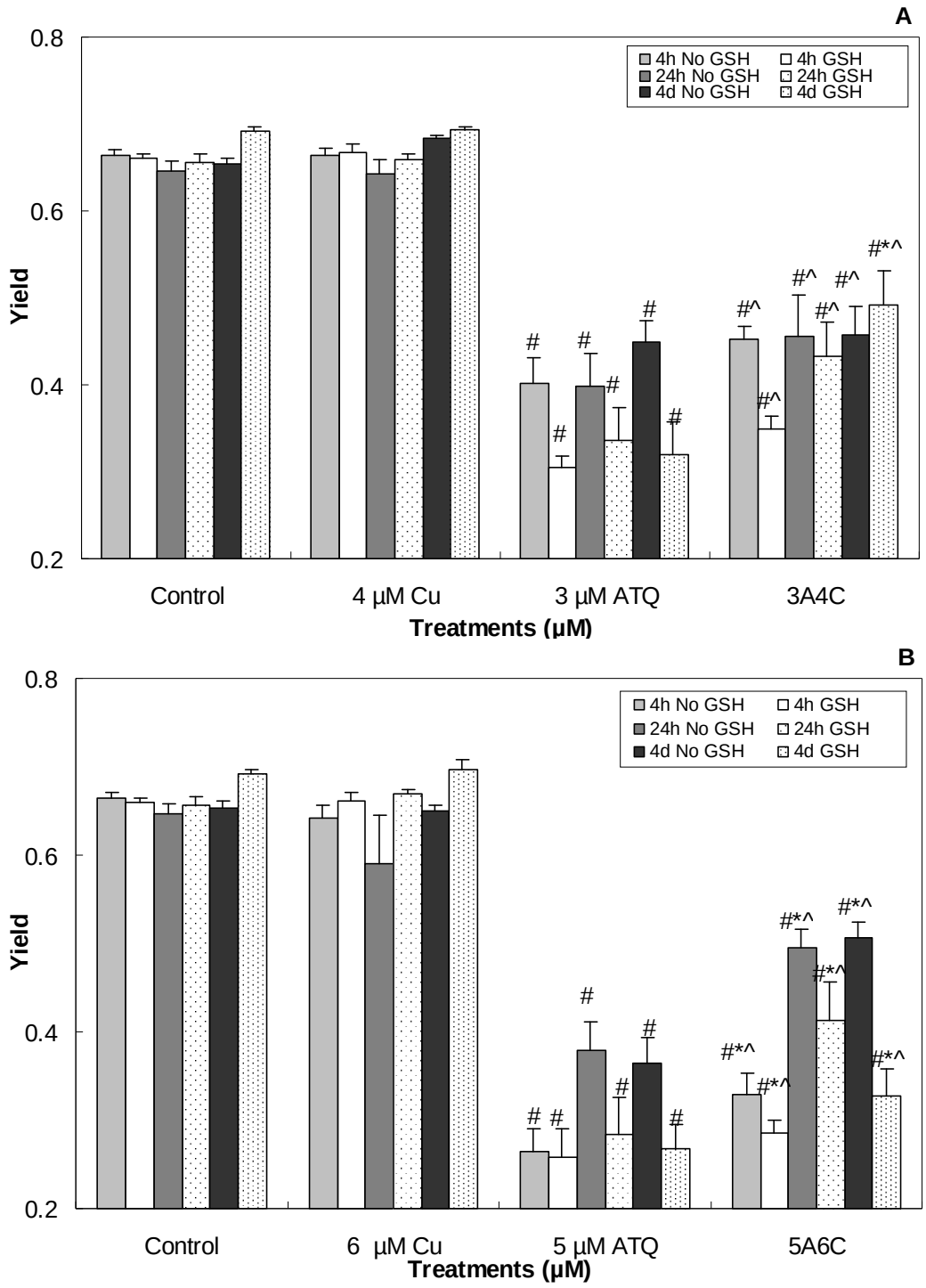

Figure 3.11 The effects of 1,2-dhATQ and copper after 4 hour, 24 hour and 4 day exposures on the yield of photosynthesis.

Graphs (A and B) depict bars of average Y values of 1,2-dhATQ, copper and their mixtures ± S.E. # indicates significant differences in yield when comparing treatments to the untreated control, * indicates differences of mixtures compared to 1,2-dhATQ alone and ^ indicates differences of mixtures compared to Cu alone all with and without GSH.

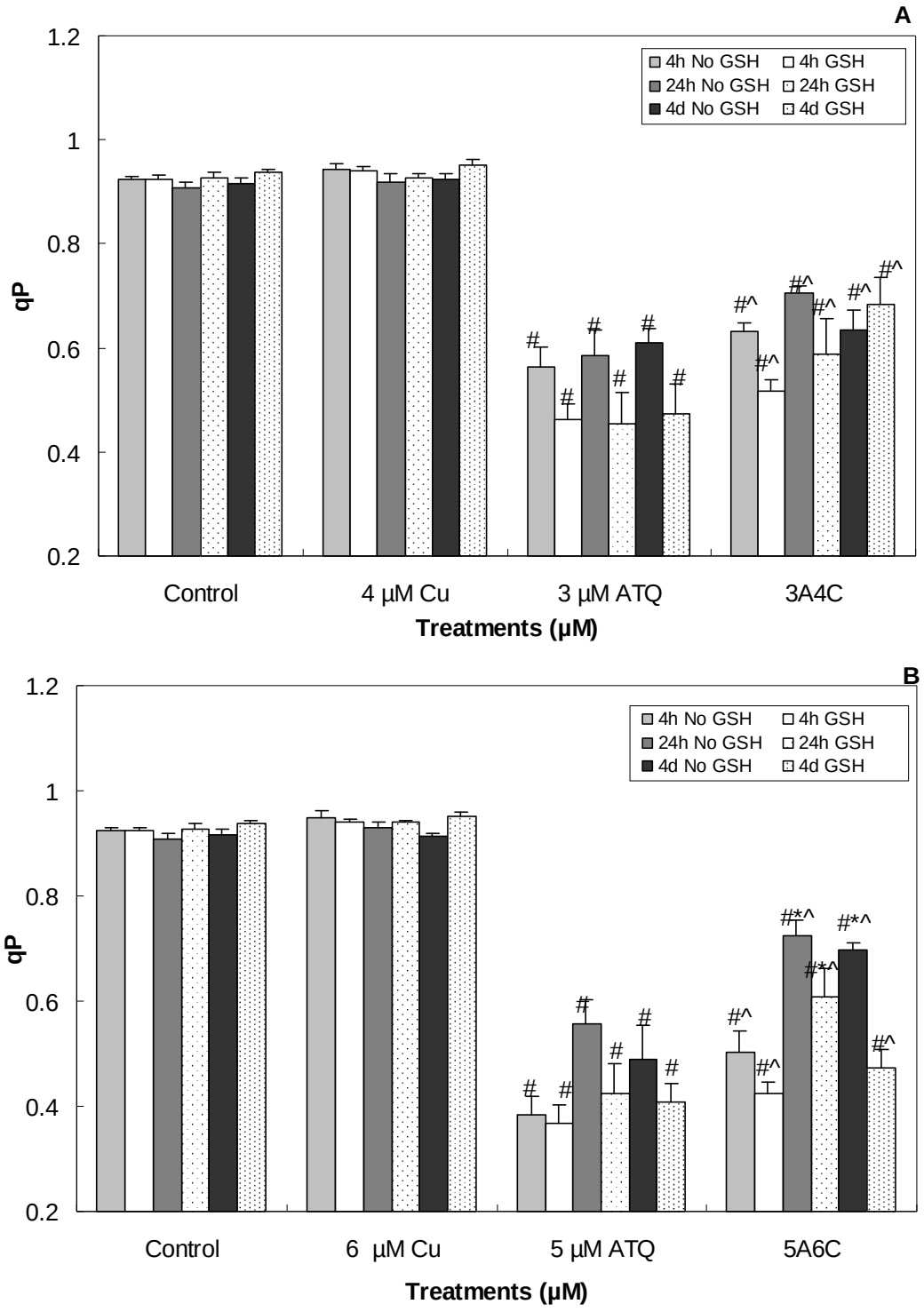

Figure 3.12 The effects of 1,2-dhATQ and copper after 4 hour, 24 hour and 4 day exposures on the photochemical quenching.

Graphs (A and B) depict bars of average qP values of 1,2-dhATQ, copper and their mixtures ± S.E. # indicates significant differences in qP when comparing treatments to the control, * indicates differences of mixtures compared to 1,2-dhATQ alone and ^ indicates differences of mixtures compared to Cu alone all with and without GSH.

Overall impacts on photosynthetic electron transport of *L. gibba* exposed to 1,2-dhATQ and combinations of 1,2-dhATQ with Cu can be illustrated with representative PAM traces (Figures 3.13A-D). In this study exposing plants to 4 and 6 µM Cu and 0.25 mM GSH for 4 hours, 24 hours and 4 days did not affect photosynthesis compared to untreated plants (Figure 3.13A and B). 3 and 5 µM 1,2-dhATQ raised the level of steady-state fluorescence by reducing plastoquinone after 4 hours up to 4 days. This led to a decrease in the yield of photosynthesis, decrease of photochemical quenching of fluorescence and lowering of the Fv/F_m (Figure 3.13C). Combining 1,2-dhATQ with Cu allowed copper to re-oxidize plastoquinone, which led to a decrease in steady-state fluorescence (Figure 3.13D). This decrease in steady-state fluorescence is responsible for the increases in the yield of photosynthesis and photochemical quenching parameters not a diminishment of 1,2-dhATQ inhibition by copper.

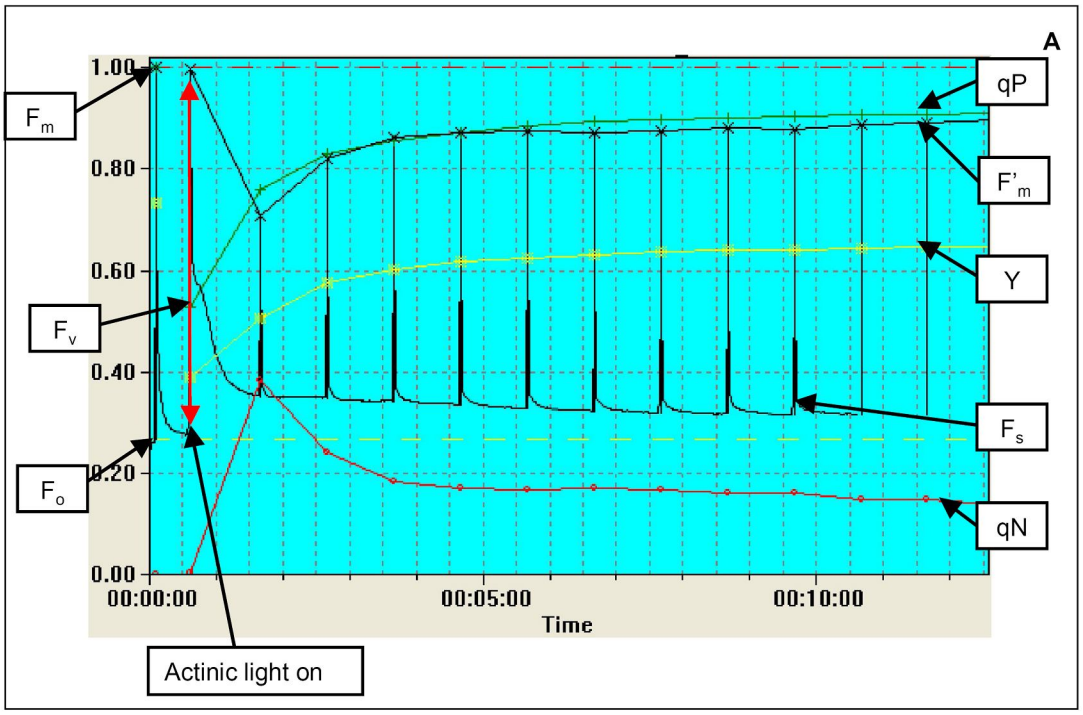
A
1.00
0.80
0.60
0.40
0.20
0.00
00:00:00
00:05:00
00:10:00
Time
Fm
Fv
Fo
qP
F'm
Y
Fs
qN
Actinic light on

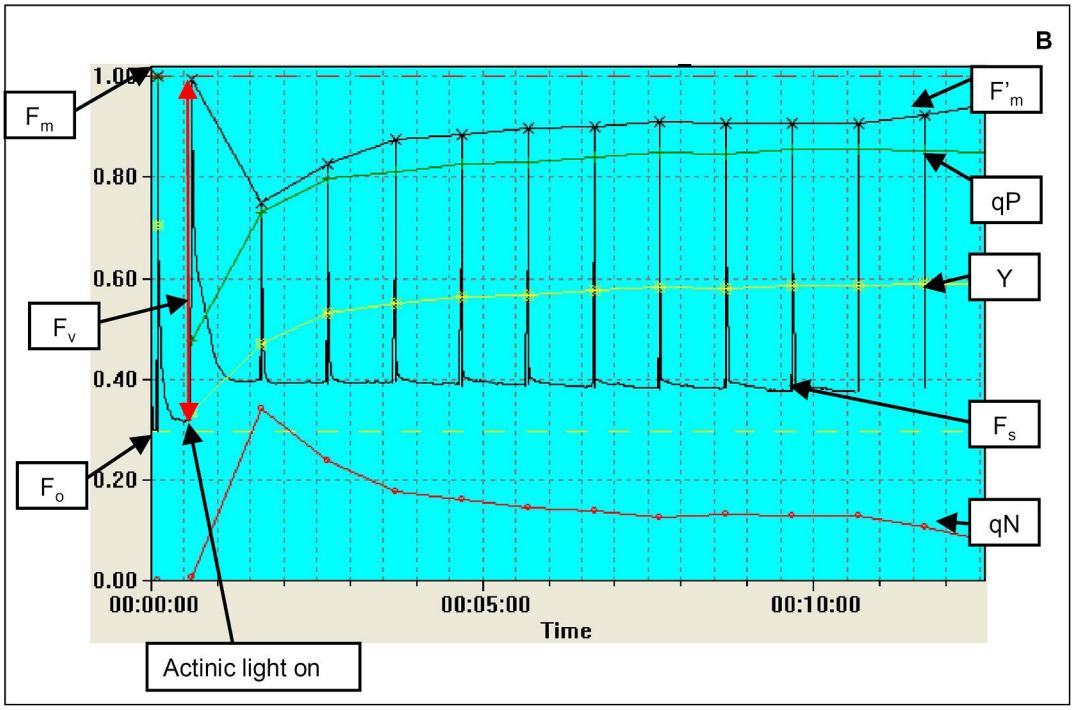
B
1.00
0.80
0.60
0.40
0.20
0.00
00:00:00
00:05:00
00:10:00
Time
Fm
Fv
Fo
F'm
qP
Y
Fs
qN
Actinic light on

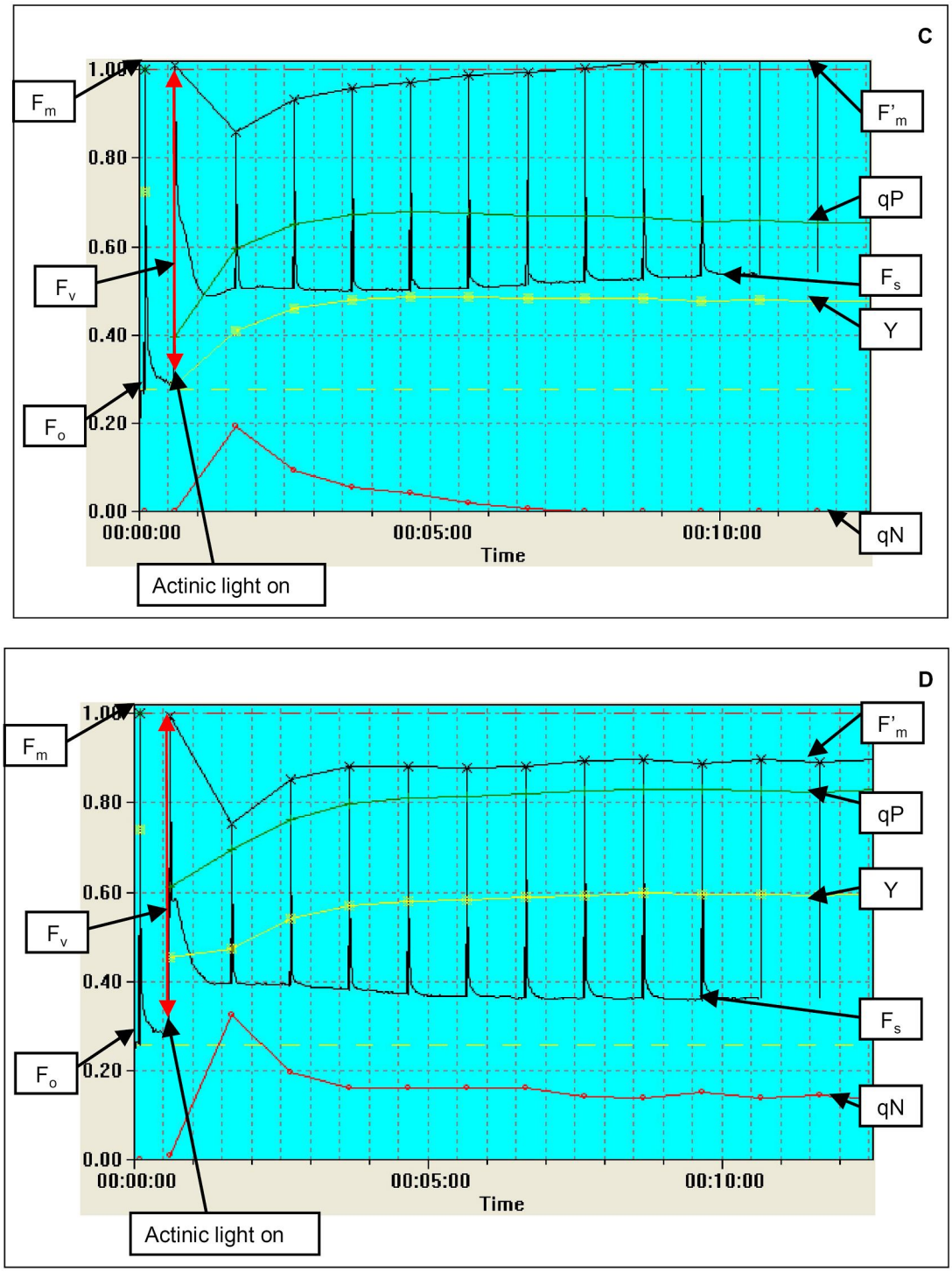

Figure 3.13 PAM fluorometry traces of an untreated plant (A), and plants exposed to 4 µM copper (B), 3 µM 1,2-dhATQ (C) and their combination (D) for 24 hours.

Representative traces showing fluorescence parameters measured using PAM fluorometry

The second fluorescence method used in this study was fast repetition rate fluorometry (FRRF). The FRR fluorometer was designed for use with algal suspensions not macrophytes. The data collected was therefore not as reproducible between replicates and experiments done on different days. To improve variability, the data was analyzed further with fluorescence analysis software that rejected data where F_o was lower than 0.3 and higher than 0.6 (vs. 6, S.R. Laney).

F_o was not significantly different when plants were exposed to 4 and 6 µM Cu and 3 and 5 µM 1,2-dhATQ with and without GSH after 4 hours (Table 3.6). F_m was significantly higher in treatments with 3 and 5 µM 1,2-dhATQ whereas 0.25 mM GSH and 4 and 6 µM Cu did not affect the value. F_v/F_m increased in 6 µM Cu, 3 and 5 µM 1,2-dhATQ exposures alone and with copper compared to the untreated control plants.

Table 3.6 F_o, F_m and F_v/F_m obtained using FRRF fluorometry of *L. gibba* exposed to 1,2-dhATQ, Cu and their mixtures with and without GSH under PAR for 4 hours.

	F_o		F_m		F_v/F_m	
Treatment (µM)	No GSH	GSH	No GSH	GSH	No GSH	GSH
Control	0.512 ±0.0.044	0.431 ±0.011	0.959 ±0.074	0.805 ±0.005	0.470 ±0.006	0.464 ±0.042
4 µM Cu	0.535 ±0.012	0.586 ±0.015	0.958 ±0.044	1.141 ±0.035#	0.436 ±0.013	0.486 ±0.003
3 µM ATQ	0.477 ±0.003	0.577 ±0.011	1.479 ±0.033#	1.590 ±0.045#	0.676 ±0.009#^	0.637 ±0.004#^
3A4C	0.427 ±0.013	0.460 ±0.013	1.151 ±0.032#	1.255 ±0.090#	0.623 ±0.012#^	0.623 ±0.017#^
6 µM Cu	0.442 ±.0.058	0.399 ±0.013	0.985 ±0.132	0.790 ±0.010	0.526 ±0.014	0.495 ±0.011
5 µM ATQ	0.463 ±0.004	0.421 ±.0.040	1.345 ±0.012#	1.100 ±0.104#	0.656 ±0.003#^	0.617 ±0.006#^
5A6C	0.433 ±0.005	0.271 ±0.019	1.145 ±0.012#	0.741 ±0.042	0.622 ±0.002#^	0.637 ±0.007#^

Average FRR fluorescent values are given ± S.E. # indicates significant differences in fluorescence when comparing treatments to the control, * indicates differences of mixtures compared to 1,2-dhATQ alone and ^ indicates differences of mixtures compared to Cu alone all with and without GSH (n=10).

The cross-sectional absorption coefficient (σ_{PSII}) indicating the size of the light absorbing target in PSII was not affected by 4 and 6 µM Cu nor 0.25 mM GSH (Figure 3.14A). Exposure to 3 and 5 µM 1,2-dhATQ decreased the size of the light-absorbing target alone and in mixtures with Cu. The addition of GSH to 3 and 5 µM 1,2-dhATQ increased σ_{PSII}. However in the mixture of 5 µM 1,2-dhATQ with 6 µM Cu the addition of GSH lowered σ_{PSII}.

The time constant (τ) measures the time required for the re-oxidation of Q_A in µs. In this study, 4 and 6 µM Cu as well as 0.25 mM GSH did not affect τ. 3 and 5 µM 1,2-dhATQ alone and in combination with Cu and GSH increased the time required for re-oxidation of Q_A (Figure 3.14B). The addition of GSH to 3 µM 1,2-dhATQ alone and in combination with Cu decreased τ.

The multiple turnover technique PAM fluorometry showed the effects of 1,2-dhATQ on photosynthetic electron transport over a steady-state period. It was seen that a reduction of plastoquinone caused an increase in the steady-state fluorescence, which led to a decrease in yield of photosynthesis. Addition of copper through re-oxidation of the plastoquinone lowered steady-state fluorescence thereby improving photosynthesis. The single turnover technique, FRRF, indicated 1,2-dhATQ decreased the size of the PSII light-absorbing target and the time needed for the re-oxidation of Q_A.

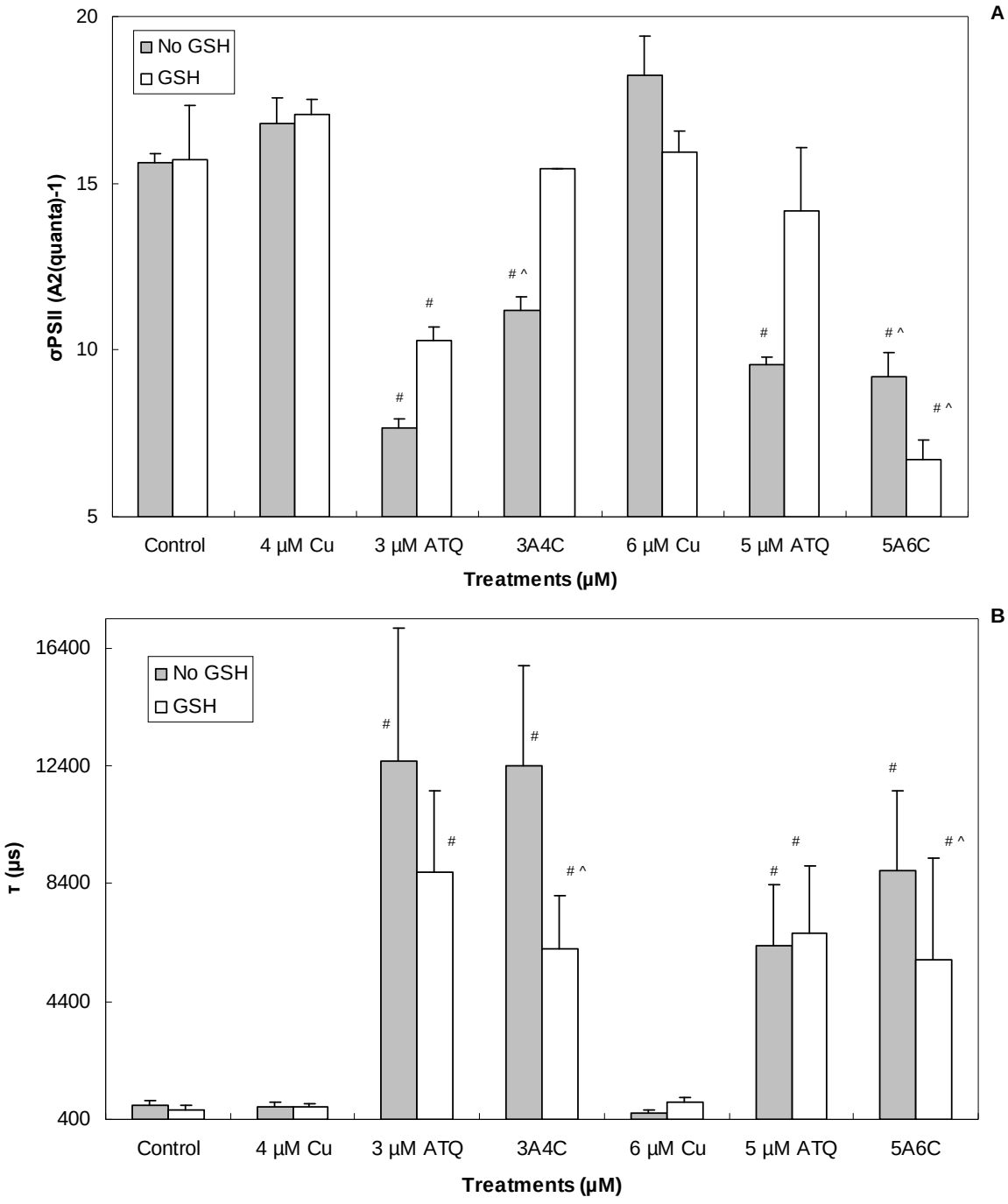

Figure 3.14 The effects of 1,2-dhATQ and copper on σ_{PSII} (A) and τ (B) after a 4 hour exposure.

Bars (A) represent average fluorescent values of σ_{PSII} and bars (B) represent average τ (time constant) in µs of electron transport at the acceptor side of PSII ± S.E. # indicates significant differences in fluorescence when comparing treatments to the control, * indicates differences of mixtures compared to 1,2-dhATQ alone and ^ indicates differences of mixtures compared to Cu alone all with and without GSH (n=10).

3.6 Changes in the expression of two genes involved in fatty acid synthesis of *L. gibba* exposed to 1,2-dhATQ, Cu and their combination

For gene studies, plants were exposed to 5 µM 1,2-dhATQ and 6 µM copper alone and their combination for four hours. A 4 hour exposure was selected for gene studies because the PAM traces indicated both 1,2-dhATQ and Cu were taken up into the plants within 4 hours. Contaminant exposed and untreated plants were homogenized and the RNA was extracted. RNA was subsequently treated with DNAse I to degrade residual DNA. Before using the RNA to synthesize complementary DNA (cDNA) the integrity was assessed with a denaturing gel (Figure 3.15A). Very bright bands appeared at the 2800 and 1800 base pair range most likely the 28S and 18S rRNA. This confirms that the RNA was intact and that there was no DNA contamination. cDNA was made and the primers for the genes of interest (SDC and ACC) and the housekeeping genes (26S and actin) were tested by performing PCR (Figure 3.15B). There were no bands in the lanes labeled (-) for ACT, ACC and SDC indicating the primers were not contaminated as these samples contained all reagents except cDNA. There were primer dimers present in the (-) lane for 26S RNA therefore it was not used as a house-keeping gene in this study. ACC, SDC and ACT all had one band that DNA was extracted from to be sequenced to confirm that these bands were ACC, SDC and ACT. In order to compare results obtained using QPCR, the PCR reactions were conducted using the same conditions, even though it was not optimal for each gene.

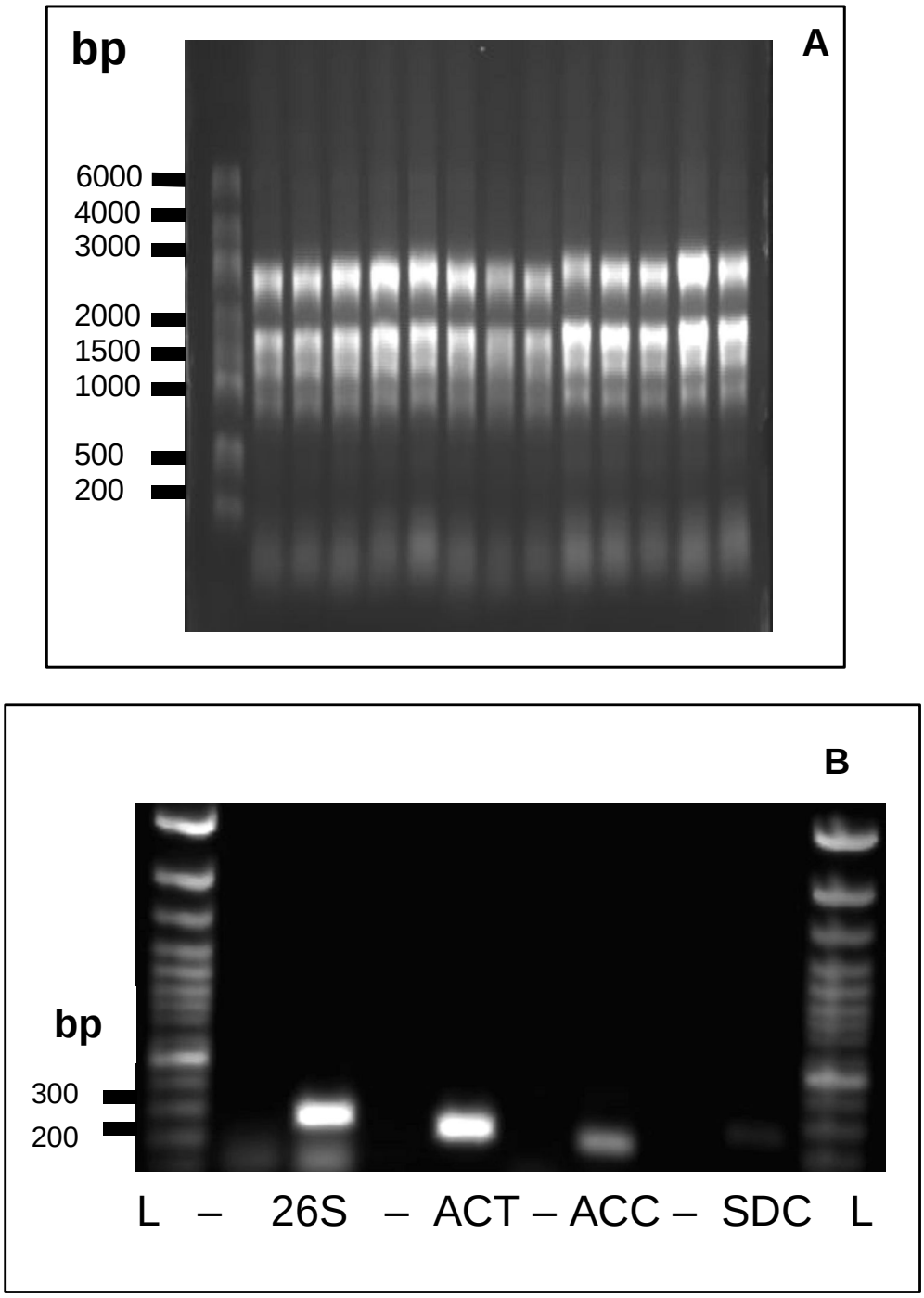

Figure 3.15 RNA from treated and untreated plants on a denaturing gradient gel (A) and bands (B) of 26S RNA, actin, acetyl coA carboxylase and serine decarboxylase with negative controls on a TAE gel.

RNA (A) was isolated using the Trizol method from control and treated plants on 13 June 2007. RNA was treated with DNase I to destroy DNA. 28S and 18S rRNA

bands are visible on the denaturing gradient gel. PCR (B) was performed with specific primers for 26S, ACC, ACT and SDC and then the products were visualized on a TAE gel. The Lg26S band was seen at 300 bp, the LgACT band was seen at 250 bp, the LgACC gene was seen at 200 bp and the LgSDC was at seen 225 bp.

In this study actin, serine decarboxylase and acetyl CoA carboxylase were identified using BLAST search algorithms through the National Center for Biotechnology Information (NCBI) database (Altschul et al. 1997). An E-value was assigned to a sequence following a BLAST search. It is the statistical confidence to the degree in which the hit and the query are similar and values closer to zero are a better match whereas values less than $1x10^{-6}$ are considered to be statistically significant. Sequenced actin, in this study, was found to be similar to actin from several species, including a freshwater algal species *Glaucocystis nostochinearum* with an expected value of 9e-24 (gb|ABJ80912.1|) (Figure 3.16A). To further support the positive identification of actin as given by the E-value, sequence alignments were also performed at the amino acid level using BLASTX. The translated actin was found to be similar to actin from many sources including *Glaucocystis nostochinearum* (gb|ABJ80912.1|) (Figure 3.16B). The sequenced serine decarboxylase gene in this study was found to be the same as Lg108 PCR cDNA Library *Lemna gibba* cDNA clone LgSDC 5' submitted by Akhtar et al. (2005) (gb|CN605603.1|) (Figure 3.17A). The sequenced acetyl coA carboxylase gene was the same as Lg102 PCR cDNA Library *Lemna gibba* cDNA clone LgACC 5' as submitted by Akhtar et al. (2005) (gb|AAF80469.1|AF163150_1) (Figure 3.17B).

```
Query 101 TCACTGAAGCCCCCTTGAACCCCAAGGCCAACAGAGAGAANANGACCCAGATCATGTTT  160
          | | | | | | | | || | || | | |  | | | | | | || | || | | | | || || ||| | ||| | | | | | | | | | ||
Sbjct 319 CTCACTGAAGCCCCCCTGAACCCCAAGGCTAACAGAGAGAAGATGACCCAGATCATGTTT  378

Query 161 GAGACCTTCAAC-TCCCCAGCTATGTATGTGGCTATCCAGGCTGTTCTTTCTCTGNATGC  219
          | | | | | | | | || | || | |  | | | | | || | || | | | | || || || ||| | ||| | | | | | | | | |
Sbjct 379 GAGACCTTCAACGTCCC-AGCCATGTATGTGGCCATCCAGGCTGTGCTGTCCCTGTACGC  437

Query 220 CAGTGGTCGCACAACAGGTATTGTGCTTGATTCTGGTGATGGTG  263
          |  |  | | | | | | | | | | |  | | |  | | | | | | |  | | | | | | | | | | | | | | | |
Sbjct 438 TTCCGGTCGTACCACCGGTATTGTGCTGGATGCTGGTGATGGTG  481
```

Figure 3.16A Nucleotide sequence alignment of actin from *L. gibba* using blastn.

Alignment of the *L. gibba* cloned nucleotide sequence to that of the match in the NCBI database with an e-value of 9e-24, identity matched 142 / 164 (86%) with 2 / 164 (1%) gaps of the plus / plus strands.

```
Query 143 TFYNELRVAPEEHPILLTEAPLNPKANREKMTQIMFETFNSPAMYV  6
          TFYNELRVAPEEHP+LLTEAPLNPKANREKMTQIMFETFNSPAMYV
Sbjct 67  TFYNELRVAPEEHPVLLTEAPLNPKANREKMTQIMFETFNSPAMYV  112
```

Figure 3.16B Predicted amino acid alignment of actin from *L. gibba* using BLASTX.

The cloned L. gibba nucleotide sequenced matched a protein in the Genbank database with an e-value of 2e-26, an identity of 45 / 46 (79%), 46 / 46 positives and 0 gaps of the –3 frame.

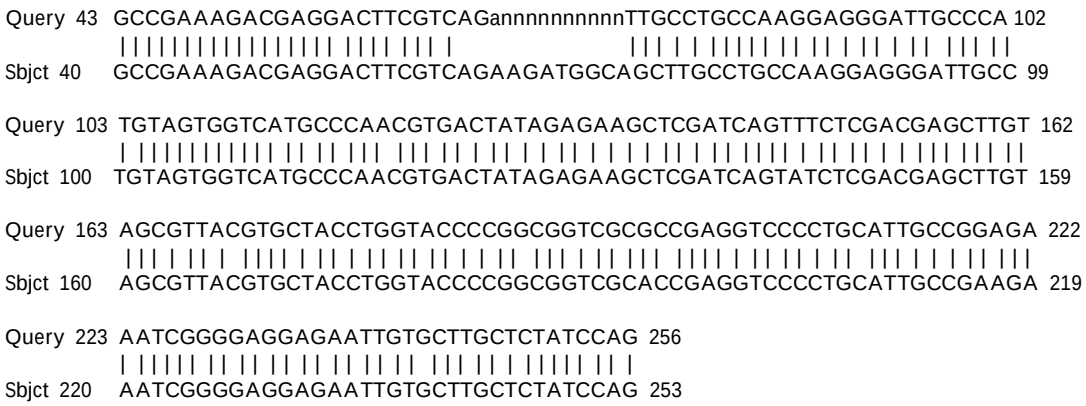

Figure 3.17A Nucleotide sequence alignment of serine decarboxylase.

Alignment of the *L. gibba* cloned SDC nucleotide sequence to LgSDC 5' with an e-value of 3e-91, an identity of 201/214 (93%) with 0/214 (0%) gaps of the plus/plus strands.

Figure 3.17B Nucleotide sequence alignment of acetyl coA carboxylase.

Alignment of the *L.gibba* cloned nucleotide sequence to that of a cDNA clone LgACC 5' with an e-value of 3e-79, an identity of 170/177 (96%) with 0/177 (0%) gaps of the plus/plus strands.

After the identities of the genes were confirmed, QPCR was performed on cDNA from untreated plants and plants exposed to 1,2-dhATQ, Cu and their combination using the specific primers for actin, serine decarboxylase and acetyl CoA carboxylase under the same experiment conditions in order to use the Livak method to analyze the relative gene expression. This required the amplification efficiencies to be determined of the target genes, SDC and ACC, and the reference gene, ACT. The amplification at each cycle for a dilution range of 100x to 0.01x of the cDNA from target and references genes was measured and a quantification graph was generated (Figures 3.18A, C and E). The amplification efficiency for actin was calculated as 99.7% (Figure 3.18A). For serine decarboxylase, the amplification efficiency was calculated as 99% (Figure 3.18C). For acetyl coA carboxylase the amplification efficiency was calculated as 95% (Figure 3.18E). Since the amplification efficiencies were within 5% of each other and near 100% the relative difference in expression can be calculated using the Livak method. To ensure that nonspecific products were not formed during amplification after each cycle a melt curve was performed by increasing the temperature in small increments and measuring the fluorescent signal (Figure 3.18B, D and F). Only ACC formed primer dimers at some of the dilutions and this could lead to a skewing of the data (Figure 3.18F). In subsequent experiments the primers for ACC should be re-designed to prevent dimer formations.

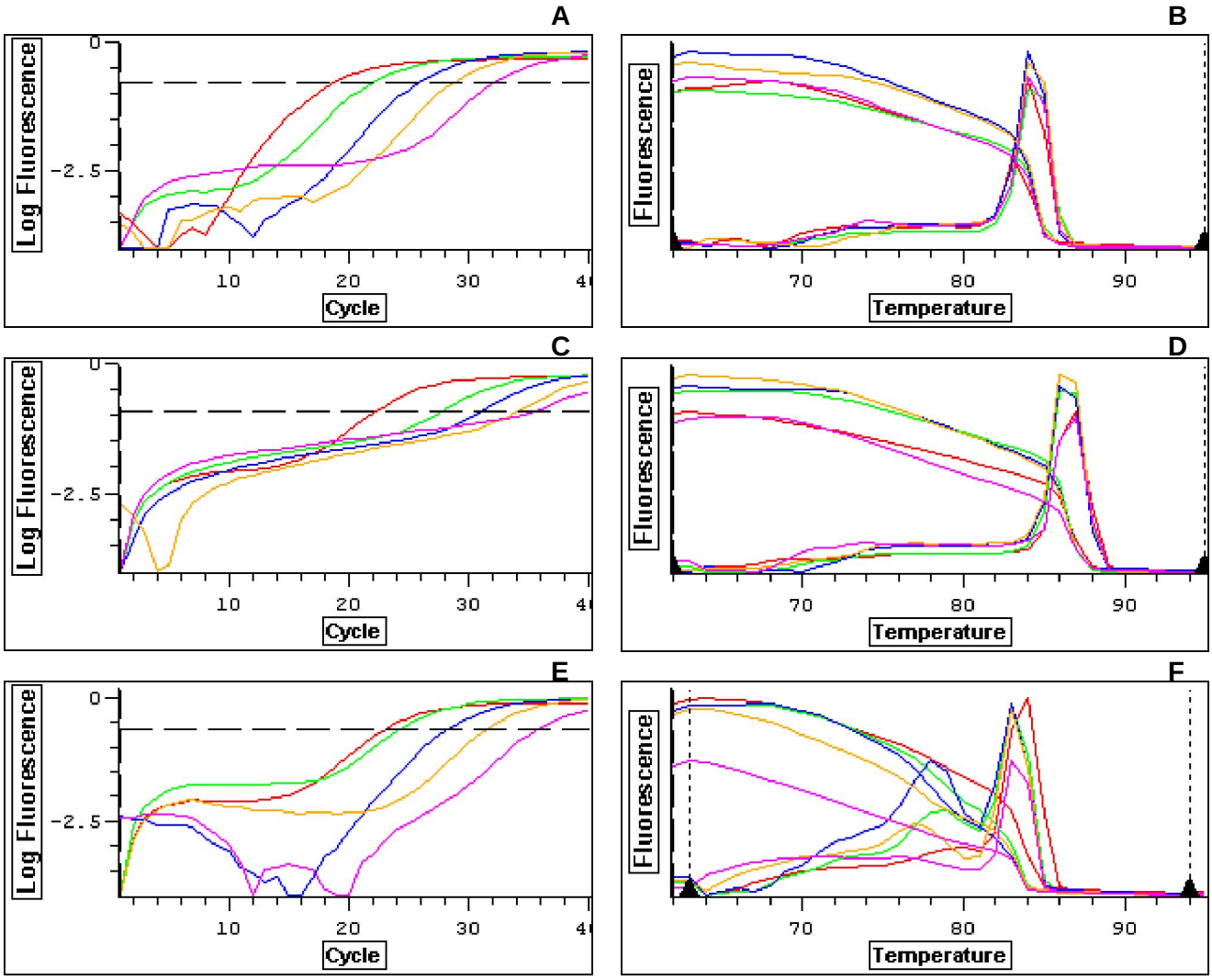

Figure 3.18 ACTquantification graph (A), ACT melt curve (B), SDC quantification graph (C), SDC melt curve (D) and ACC quantification graph (E) and ACC melt curve (F) obtained using QPCR.

The standard curves for actin (ACT), serine decarboxylase (SDC) and acetyl coA carboxylase (ACC) were constructed using a log dilution series. The lines represent SYBR green fluorescence of the cDNA of the dilution range from 0 to 40 cycles (A, C and D). After quantification was done, melt curves were performed where the temperature was increased until the fluorescent signal is lost. The peak represents the derivative and the lines the SYBR green fluorescence of the dilution series (B, D and F).

QPCR was performed for SDC, ACC and ACT using cDNA from untreated plants, plants exposed to 1,2-dhATQ, Cu and their combination at three independent times. The threshold cycle (C_T) for each of the target and references genes was normalized for untreated plants and plants exposed to 1,2-dhATQ, Cu and their combination. Normalization of the expression of the target gene to that of the reference gene compensates for difference in amount of sample tissue. The C_T value for actin was similar in all samples treated and untreated, making it an ideal reference gene in this study. The expression of serine decarboxylase was up-regulated when plants were exposed to 5 µM 1,2-dhATQ and a combination of 5 µM 1,2-dhATQ and 6 µM copper. SDC expression of plants exposed to only 6 µM copper was slightly down-regulated compared to the control, which could be an artifact of the experiment (Figure 3.19A). ACC expression was significantly up-regulated with exposure to 6 µM copper. Expression of ACC was down-regulated with exposure to 5 µM 1,2-dhATQ and the mixture compared to the control (Figure 3.19B). When plants were exposed to 1,2-dhATQ, Cu and their combination the expression of two genes involved in fatty acid synthesis namely, serine decarboxylase and acetyl CoA carboxylase was altered most likely as a result of ROS production or changes in the redox status of the cell.

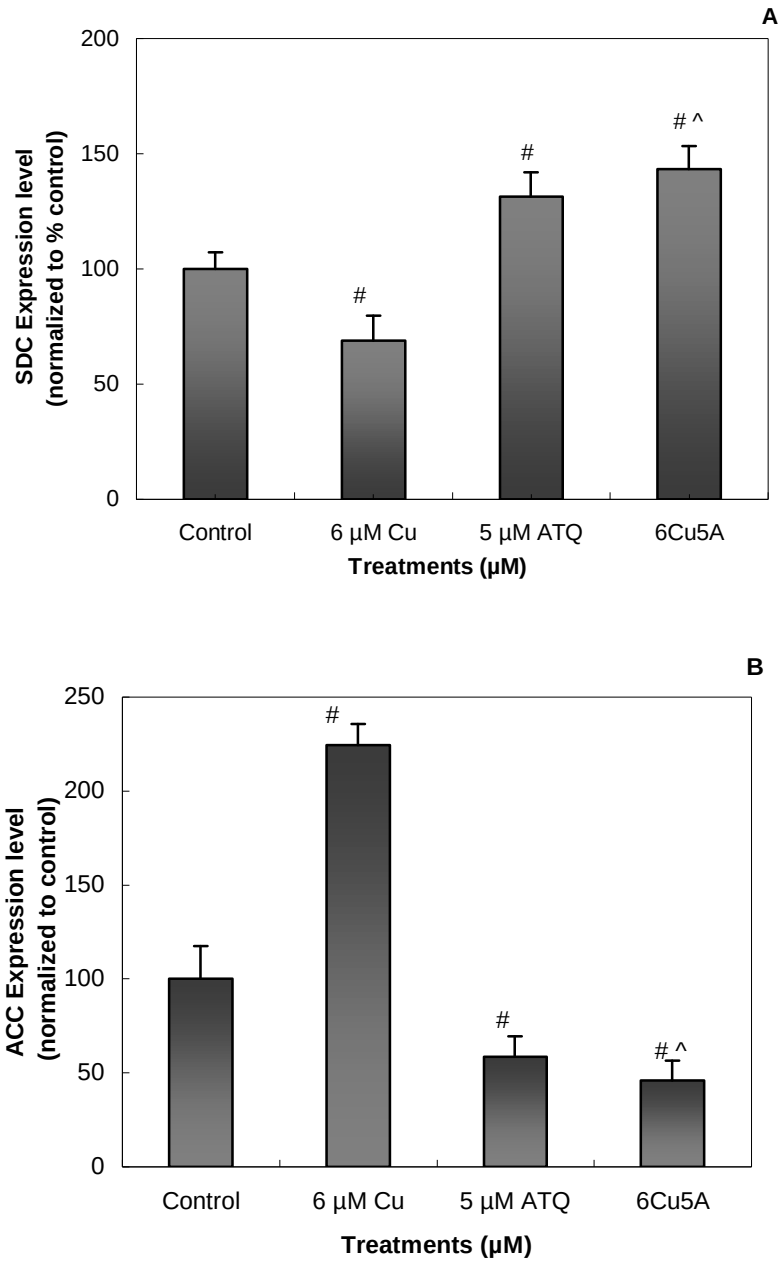

Figure 3.19 Expression of serine decarboxylase (A) and acetyl coA carboxylase (B) normalized to actin.

Plants were exposed to 6 µM copper and 5 µM 1,2-dhATQ and their combination for 4 hours after which the RNA was extracted, treated with DNase I and reverse transcribed to cDNA. Using specific primers, QPCR was performed. Bars represent average levels of SCD (A) and ACC (B) expression ± S.E. # indicates significant differences in regulation when comparing treatments to the control, * indicates differences of mixtures compared to 1,2-dhATQ alone and ^ indicates differences of mixtures compared to Cu alone (n=12).

Chapter 4
Discussion

This study looked at the effects of two ubiquitous environmental co-contaminants, 1,2-dihydroanthraquinone (1,2-dhATQ) and copper, on the physiology and gene expression of *L. gibba*. Growth assays using photosynthetic active radiation (PAR) or simulated solar radiation (SSR) with 4 µM and 6 µM copper (Cu), respectively, caused significant growth inhibition. Under both PAR and SSR, 1 µM 1,2-dihydroxyanthraquinone (1,2-dhATQ) caused significant growth inhibition. Synergistic growth inhibition was observed with several combinations of 1,2-dhATQ and Cu with an indirect catalytic mechanism. Glutathione ameliorated copper and mixture toxicity but increased 1,2-dhATQ toxicity. Plants exposed to 1,2-dhATQ, Cu and their combinations had increased reactive oxygen species (ROS) production after 4 days compared to untreated plants. 1,2-dhATQ impaired photosynthetic electron transport as seen using pulse amplitude modulated (PAM) fluorometry and fast repetition rate fluorometry (FRRF). The expression of two genes involved in fatty acid synthesis, serine decarboxylase (SDC) and acetyl CoA carboxylase (ACC) was altered by exposure to Cu and 1,2-dhATQ and their combination.

4.1 Growth Analysis of *L. gibba* exposed to Cu, 1,2-dhATQ and their combination

4.1.1 Growth of *L. gibba* exposed to copper under PAR and SSR

Copper toxicity manifested itself above 6 µM under PAR, however lower concentrations (<6 µM) were more toxic under SSR, reaffirming that under environmentally relevant conditions copper becomes more toxic (Akhtar 2004). The

decrease in growth rate with increasing copper concentrations was also accompanied by chlorosis and necrosis indicating cell death was occurring (Babu et al. 2003). Copper toxicity in this study is most likely due to high concentrations of copper redox-cycling with other cellular components forming ROS. Large ROS production could overwhelm the anti-oxidant defense system, leaving ROS that could destroy fatty acids, DNA and cellular organelles (Akhtar 2004; Frankart et al. 2002). The addition of 0.25 mM glutathione (GSH) to copper ameliorated the toxic effects of copper. GSH could lower ROS levels of plants exposed to copper to levels not significantly different from that of the untreated plants.

4.1.2 Growth of *L. gibba* exposed to 1,2-dhATQ under PAR and SSR

Unlike copper, 1 µM 1,2-dhATQ under both PAR and SSR caused significant growth inhibition (Babu et al. 2001; Lees 2005). 1,2-dhATQ most likely accumulates in the thylakoid membrane causing growth inhibition by affecting photosynthetic electron transport (Duxbury et al. 1997; Babu et al. 2001). The л-orbital system of 1,2-dhATQ strongly absorbs in the 200-300 nm range therefore under SSR it can undergo photomodification and photosensitization reactions causing an increase in the growth inhibition especially at concentrations greater than 4 µM (Huang et al. 1997). While GSH was able to lower the toxicity of copper, it increased the toxicity of 1,2-dhATQ. GSH is very efficient in the detoxification of xenobiotics by acting as a cofactor in conjugation reactions catalyzed by glutathione-S-transferase (GST) (Pompella et al. 2003). With conjugate formation, GSH levels could decline; therefore it was thought addition of GSH would allow more 1,2-dhATQ to be eliminated via the glutathione transferase pathway or other GSH conjugation reactions (Mullineaux and Rausch

2005; Hollòsy 2002; Edwards and Dixon 2004). The increase in growth inhibition when GSH was added to 1,2-dhATQ could be due to the formation of compounds more reactive than the parent compound or a change in the redox potential in the cell (Pompella et al. 2003; Edwards and Dixon 2004).

4.1.3 Growth of *L. gibba* exposed to 1,2-dhATQ and Cu combinations under PAR and SSR

As previously found by Babu et al. (2001) 3 µM 1,2-dhATQ and 4 µM copper showed, synergistic growth inhibition. Importantly in this study, synergistic toxicity was observed in several other combinations of 1,2-dhATQ and copper, under PAR and SSR, suggesting toxicity of mixtures could be underestimated in the natural environment. The mechanism behind this catalytic interaction will be discussed later. The toxicity of the mixture, at the highest concentrations of 1,2-dhATQ and copper, is additive indicating growth inhibition does reach a maximum. GSH lowered the growth inhibition of combinations of 1,2-dhATQ and Cu. Mixture toxicity involves a synergistic increase in ROS production and therefore it is thought that GSH could lower ROS levels thereby decreasing toxicity (Babu et al. 2001).

Unexpectedly, under SSR 0.25 mM GSH caused a significant increase in growth inhibition. Previous research by Karpinska et al. (2000) found photooxidative damage was accelerated with the addition of GSH in excess light. Excess GSH led to an overly reduced environment, which caused inhibition of ascorbate peroxidase gene expression and photosynthetic electron transport (Karpinska et al. 2000; Mullineaux and Rausch 2005). In this study excess GSH by redox-cycling could decrease the

trans-thylakoid pH gradient and the redox status of the Q_A-Q_B-PQ pools thereby inhibiting the plants ability to acclimate under SSR (Karpinska et al. 2000).

4.2 ROS production in *L. gibba* when exposed to Cu, 1,2-dhATQ and their combination

The mechanisms of toxicity cannot be derived from the growth data alone but must be examined with other physiological tests. Copper, being redox-active, through Fenton-like reactions causes formation of hydroxyl radicals and other ROS (Babu et al. 2001; Akhtar et al 2005). 1,2-dhATQ could also cause ROS production if it absorbs radiation and undergoes photosensitization or photomodification (Huang et al. 1997).

4.2.1 ROS production after 24 hour exposures to 1,2-dhATQ, Cu and their combination

In this study, 6 µM copper had significantly higher levels of ROS compared to untreated plants. These results are consistent with those of Akhtar (2004). In that study ROS production was concentration and time dependent and only significant above 6 µM copper. ROS levels were lowered with the addition 0.25 mM glutathione and this is most likely how GSH ameliorated copper toxicity as found by Babu et al. (2003).

With confocal microscopy it was possible to observe direct effects of copper on the mesophyll cells after 24 hours exposure to the contaminants. The major targets for copper-induced ROS production were the chloroplasts, where large increases in DCF fluorescence were observed within the organelle compared to plants only exposed to H_2DCFDA. Exposure to copper simultaneously lowered chlorophyll autofluorescence that could be due to membrane destruction. In some cases severe signs of stress

manifested as DCF-filled protrusions surrounding the chloroplasts (Data not shown). These protrusions were thought to be extensions of the chloroplast membrane or pockets of coagulated cytoplasm surrounding the chloroplast. More studies are needed to examine what is responsible for the protrusion as it could be linked to apoptosis.

DCF fluorescence was lowered in 1,2-dhATQ treated plants compared to untreated plants. There was no interference of 1,2-dhATQ with the dye itself however; the mechanism of ROS reduction by 1,2-dhATQ remains unclear. It appears as though 1,2-dhATQ acts as a sink for electrons therefore preventing ROS formation (Nykamp 2007).

4.2.2 ROS production after a 4 day exposure to 1,2-dhATQ, Cu and their combination

Previous work observed levels of ROS produced at day four and day eight were not different from each other; implying steady-state levels were reached by day four (Akhtar 2004; Lees 2005). This study as well as Lees (2005) found ROS production in 1,2-dhATQ exposures only increased after four day exposures compared to untreated plants. This implies that 1,2-dhATQ most likely does not directly cause ROS formation but that it does so potentially through redox imbalances. Increases in ROS were observed in plants exposed to 3 and 4 µM 1,2-dhATQ with and without Cu but not the 5 µM 1,2-dhATQ exposures. It is possible that cells are unable to produce ROS if they cannot photosynthesize due to the presence of 5 µM 1,2-dhATQ. After 4 days, s mixture of 3 and 4 µM 1,2-dhATQ with 4 µM Cu have higher ROS levels than plants exposed to only 3 and 4 µM 1,2-dhATQ. This suggests that after 4 days the anti-oxidant defense mechanisms are unable to lower ROS to acceptable levels, which

could lead to the synergistic increase in growth inhibition observed in combinations with 1,2-dhATQ and Cu.

4.3 Effects of 1,2-dhATQ, Cu and their combination on photosynthetic electron transport

Environmental stressors are known to inhibit photosynthesis. With the development of chlorophyll *a* fluorescent techniques these effects can be studied rapidly and non-invasively (Junea and Popovic 1999).

4.3.1 The effects of 1,2-dhATQ, Cu and their combination on F_v/F_m and qN obtained with PAM fluorometry

Pulse amplitude modulated (PAM) fluorometry can be used to analyze both instantaneous and steady-state photosynthesis. The former gives the maximal PSII activity and the latter gives sustained PSII activity (Junea and Popovic 1999). In this study at three exposure times, PAM fluorometry was used to examine the effects of 1,2-dhATQ, Cu and 1,2-dhATQ/Cu on photosynthesis.

F_v/F_m or the maximal quantum yield of PSII is widely used in research to assess photoinhibition in plants (Maxwell and Johnson 2000). In this study, exposure to 5 µM 1,2-dhATQ alone and with Cu and GSH diminished F_v/F_m slightly compared to untreated plants after 4 hours, 24 hours and 4 days. The decrease in F_v/F_m corresponds to damage to PSII, a known toxic effect of 1,2-dhATQ because it blocks electron transport at the Cytochrome b_6/f complex (Figure 1.2) (Babu et al. 2001). However, using this parameter alone to assess damage to the photosynthetic apparatus in this study would underestimate the impact of 3 µM 1,2-dhATQ exposures as seen from the PAM fluorometry traces. Therefore, F_v/F_m alone cannot

indicate the potential for photosynthesis as it cannot detect changes that occur further down the electron transport chain (Kromkamp and Forster 2003). It only measures the reduction from $P680^+$ to the electron carrier, Q_A, which involves the largest change in the redox status and could therefore result in the largest error (Oxborough 2004).

In this study, with non-photochemical quenching of fluorescence (qN), similar to F_v/F_m, little change was observed when plants were exposed to 1,2-dhATQ and Cu. qN is a measure of efficiency of heat dissipation relative to the dark-adapted state (Maxwell and Johnson 2000). Since it involves very complex non-radiative energy dissipation pathways linked to other regulatory systems using qN alone to assess the impacts of 1,2-dhATQ and Cu on plants is not recommended (Dewez et al. 2002).

4.3.2 The effects of 1,2-dhATQ, Cu and their combination on F_s obtained with PAM fluorometry

The effects of toxicants on photosynthetic electron transport can be studied from measuring the steady-state fluorescence (F_s). F_s was higher in plants exposed to 3 µM and 5 µM 1,2-dhATQ after 4 hours, 24 hours and 4 days, since 1,2-dhATQ prevents re-oxidation of the plastoquinol pool (Babu et al. 2001). For every two electrons that flow through Q_A to Q_B, one molecule of plastoquinone is reduced to plastoquinol (Koblizek et al. 2001). When plastoquinol cannot be re-oxidized to plastoquinone, fluorescence cannot be quenched (Maxwell and Johnson 2000). Interestingly, the presence of 4 and 6 µM copper allows plastoquinol re-oxidization to plastoquinone thereby quenching the fluorescence although not to the levels of untreated plants. It is speculated that the reduced plastoquinone pool serves as a source of electrons for

Cu^{+2}, after which Cu^{+} can interact with oxygen to produce ROS causing synergistic growth inhibition (Figure 1.2). After exposure to 5 µM 1,2-dhATQ the addition of glutathione slightly increased F_s perhaps due to GSH preventing re-oxidation of plastoquinol. The marginally lower F_s values at 4 days, relative to other exposure times, may correspond to the increased ROS production seen in the DCF experiments at day four.

4.3.3 The effects of 1,2-dhATQ, Cu and their combination on yield of photosynthesis and photochemistry obtained with PAM fluorometry

Photosynthetic yield is a measure of the overall quantum yield of photochemical energy conversion and therefore indicates the efficiency of steady-state photosynthesis (Lees 2005; Maxwell and Johnson 2000). This study revealed 3 and 5 µM 1,2-dhATQ within four hours inhibited photosynthesis as seen in the diminished yield parameter. Addition of 4 and 6 µM copper to 1,2-dhATQ, through re-oxidization of the PQ pool, quenched fluorescence and increased the yield compared to 1,2-dhATQ exposures alone. After 4 hours, the decrease in yield in the 5 µM 1,2-dhATQ exposure compared to 3 µM 1,2-dhATQ was greater, indicating this effect is concentration dependent. Lees (2005) speculated glutathione conjugation would diminish the effects of 1,2-dhATQ however; in this study GSH addition to 1,2-dhATQ caused a decrease in the yield of photosynthesis. GSH through redox-cycling could prevent the re-oxidation of plastoquinol decreasing the yield.

Photochemical quenching, qP, exhibited similar trends as to that of the yield of steady-state photosynthesis. qP indicates the proportion of open PSII reaction centres during steady-state photosynthesis (Maxwell and Johnson 2000). Changes in qP are

due to net closing or opening of reaction centres while photosynthesis is occurring (Maxwell and Johnson 2000). Exposure to 1,2-dhATQ decreased qP by blocking electron flow in a concentration-dependent manner. Addition of copper to 1,2-dhATQ increased qP because the re-oxidization of plastoquinol opened the reaction centres. GSH addition to 1,2-dhATQ-treated potentially diminished qP by inhibiting the opening of reaction centres thus keeping the plastoquinone pool reduced or somehow preventing electron transport further down-stream resulting in a back-up of electrons.

4.3.4 The effects of 1,2-dhATQ, Cu and their combination on F_v/F_m measured using FRRF

Single turnover techniques such as fast repetition rate fluorometry (FRRF) can be used to calculate the PSII functional cross-section (σ_{PSII}) and energy transfer between PSII reaction centres from kinetics of fluorescence transients with a single photochemical turn over of PSII (Kolber et al. 1998). Originally FRRF was designed for use with algal suspensions, therefore, a new protocol was developed for use with *L. gibba*. Gorbunov et al. (1999) used FRRF to find characteristic photosynthetic signatures for a variety of benthic organisms namely corals, sea grasses, macroalgae, and algal turf. They found that FRFF could be used to study differences in nutrient acquisition, photoinhibition, and molecular arrangement of the photosynthetic apparatus (Gorbunov et al. 1999).

F_v / F_m slightly increased in plants exposed to 6 µM Cu, 3 and 5 µM 1,2-dhATQ alone and in mixtures with Cu compared to untreated plants. This is potentially due to increased F_m when plants were exposed to 1,2-dhATQ or the instrument architecture.

As with PAM fluorometry this parameter cannot be used alone to assess the impacts of 1,2-dhATQ and Cu on photosynthesis.

4.3.5 The effects of 1,2-dhATQ, Cu and their combination on the cross-sectional absorption coefficient

During the saturation phase of FRRF, the PSII functional cross-section (σ_{PSII}) was measured. σ_{PSII} is the PSII light harvesting efficiency and therefore indicates the fraction of light absorbed by PSII to be used in photochemistry (Koblizek et al. 2001; Kromkamp and Forster 2003). Exposure to 3 and 5 µM 1,2-dhATQ had significantly lower σ_{PSII} compared to Cu treated and untreated plants. In high light, σ_{PSII} is decreased by photoprotective processes to reduce the light harvesting efficiency thus preventing damage (Gorbunov et al. 1999). Through inhibition of photosynthetic electron transport, 1,2-dhATQ could activate photoprotective processes since 1,2-dhATQ potentially decreased the amount of radiation that could be used in photochemistry. The addition of GSH to 1,2-dhATQ resulted in an increase in σ_{PSII} potentially due to its ability to change the redox status and perhaps inhibiting photoprotective processes.

4.3.6 The effects of 1,2-dhATQ, Cu and their combination on the time constant

During the relaxation phase of FRRF the time constant (τ) was obtained. This constant is defined as the time required for the re-oxidation of Q_A. When exposed to 3 and 5 µM 1,2-dhATQ τ increased, which could have been due to 1,2-dhATQ impairing Q_A re-oxidation resulting in effects on downstream electron flow. However, the addition of copper did not decrease the time required for Q_A re-

oxidation, possibly due to insufficient time allowed for the re-oxidation of Q_A through Cu redox cycling in the plastoquinone pool.

4.3.7 Proposed Mechanism of 1,2-dhATQ and Cu Mixture Toxicity

In this study, PAM fluorometry traces illustrated the overall effects of 1,2-dhATQ and 1,2-dhATQ in combination with Cu on photosynthetic electron transport. Similar to what Babu et al. (2001) found 4 and 6 µM copper does not affect photosynthesis. However, 3 and 5 µM 1,2-dhATQ, as early as 4 hours after exposure, caused a decrease in the steady-state efficiency of PSII. The above mentioned mixture effect first demonstrated by Babu et al. (2001) was replicated in this study, and was observed with 5 µM 1,2-dhATQ and 6 µM copper as well (Figure 4.1). The three different exposure times had very similar results indicating that the inhibitory effects of 1,2-dhATQ occurs rapidly and persists. Parameters only obtainable using a single turnover technique such as FRRF indicated 1,2-dhATQ decreased the size of light absorbing target and increased the time required for the re-oxidation of Q_A.

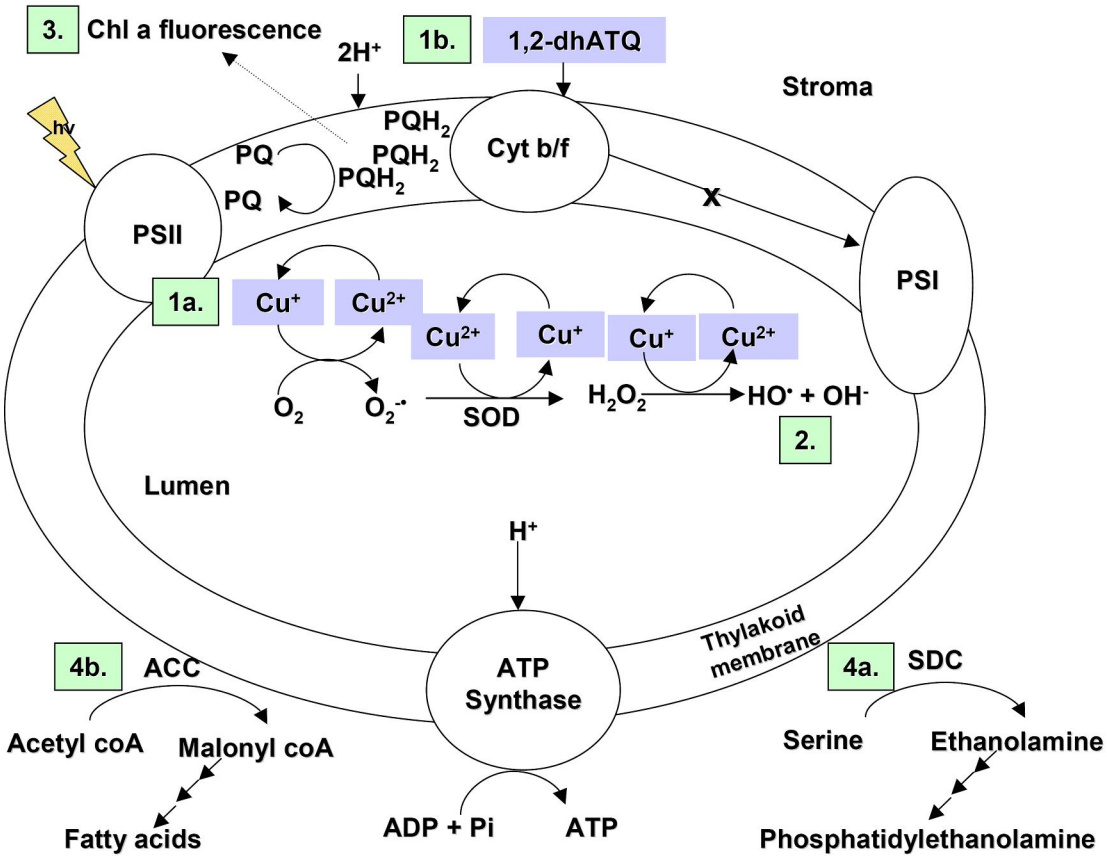

Figure 4.1 Effects of 1,2-dhATQ, Cu and their combination on ROS production, photosynthesis and gene expression.

Exposure to copper can lead to redox cycling thus forming ROS (1a). If 1,2-dhATQ is present the plastoquinone pool serves as a source for Cu cycling causing a large increase in ROS production that accounts for synergistic growth inhibition of mixtures (1b). ROS production occurs in copper exposure after 24-hour exposures and also in 1,2-dhATQ and mixture exposure after 4 days (2). The reduction of plastoquinone by 1,2-dhATQ caused an increase in chlorophyll *a* fluorescence that decreased photosynthetic electron transport (3). ACC expression can be up-regulated by copper exposures whereas SDC can be up-regulated by 1,2-dhATQ (4a and 4b) (Adapted from Babu et al. (2005).

4.4 Effects of 1,2-dhATQ and Cu on genes involved in fatty acid synthesis

Using QPCR the expression of genes involved in fatty acid synthesis were investigated by measuring the amplified PCR product at each cycle throughout the PCR reaction of plants exposed to 1,2-dhATQ and Cu and untreated plants (Gachon

et al. 2004). Previous work by Akhtar et al. (2005) identified several genes that were up-regulated when *Lemna gibba* was exposed to copper. In this study, serine decarboxylase (SDC) and acetyl Co-A carboxylase (ACC) were selected because they are involved in repair of the fatty acids and could be used as indicators of stress.

4.4.1 Effects of 1,2-dhATQ, Cu and their combination on the expression of serine decarboxylase

SDC has been implicated in biochemical processes related to environmental stress (Ho and Saito 2001). Work by Fujimore and Ohta (2003) and Akhtar et al. (2005) found SDC expression increased when exposed to Ni^{2}, Mn^{2+}, and copper, respectively. Serine decarboxylase provides ethanolamine used to make polar head groups of membrane phospholipids, namely phophatidyl ethanolamine and phosphatidylcholine (Ho and Saito 2001; Rontein et al. 2003; Akhtar et al. 2005).

In this study, exposure to 6 µM copper did not cause significant up-regulation of SDC. It is possible that a 4 hour exposure to copper was insufficient to cause SDC up-regulation compared to untreated plants. It is also possible that copper triggered antioxidant protection preventing damage to polar head groups making up-regulation of SDC unnecessary.

In this study exposure to 5 µM 1,2-dhATQ alone and with 6 µM copper significantly up-regulated the expression of SDC. It is possible that 1,2-dhATQ may have undergone photooxidation forming ROS that damaged the photosynthetic membrane. Perhaps the alteration of the redox status prevented the antioxidant defense system from protecting polar head groups, thus triggering the up-regulation of SDC. There appears to be no significant difference between the mixture and 1,2-

dhATQ exposures indicating SDC gene regulation may be linked to the redox status of the cell as well as ROS formation.

4.4.2 Effects of 1,2-dhATQ, Cu and their combination on the expression of acetyl CoA carboxylase

In this study, expression of ACC was also studied using the same exposure as those for SDC mentioned above. This enzyme catalyzes the carboxylation of acetyl CoA to malonyl CoA, which is used as a precursor to fatty acids in plastids, flavonoids, anthocyanins, membranes and storage lipids (Sasaki and Nagano 2004; Zhang and Powles 2006). The *de novo* fatty acids synthesis occurs in the plastids where the fatty acids are modified or exported to the cytosol for further modification (Sasaki and Nagano 2004).

ACC has been found to be up-regulated in response to hydrogen peroxide and copper exposure (Figueroa-Balderas 2006; Akhtar et al 2005). In this study, copper exposure up-regulated ACC expression. Since copper toxicity has been linked to increased ROS, up-regulation of ACC could be used to replace damaged fatty acids. Also it is possible that ACC could provide precursors for flavonoid production since these compounds can act as ROS scavengers (Akhtar 2004; Figueroa-Balderas et al. 2006).

Photosynthesis and metabolism are controlled by diverse redox reactions and deviation from normality can trigger responses (Dietz and Scheibe 2004). Light, stromal pH, Mg^{+} ion concentration and redox status also determine the regulation of ACC (Sasaki and Nagano 2004). During photosynthesis, the stoma pH increases from 7 to 8 and the Mg ion concentration increases from 1 to 3 mM, thus activating

plastidic ACC (Sasaki and Nagano 2004). In this study, exposure to 1,2-dhATQ alone and in combination with Cu down-regulated ACC expression. It is possible that 1,2-dhATQ blocks electron flow preventing photosynthesis, thus preventing changes in pH and Mg ion concentrations, redox status of the cell and lastly production of ATP. In doing so this could down-regulate ACCase found in the chloroplasts as it requires specific conditions for activity and is ATP dependant.

4.5 Study Conclusions

Using 8 day growth assays the effects of copper, 1,2-dhATQ and their combinations on *L. gibba*, with and without a ROS scavenger under photosynthetic active radiation (PAR) and simulated solar radiation (SSR) on plant growth were studied. The growth assays confirmed that both toxicants were taken up into the plants and caused growth inhibition at environmentally relevant concentrations. Copper toxicity was apparent after 6 µM while 1,2-dhATQ was toxic at concentrations as low as 1 µM. Synergistic toxicity was seen at several combinations of 1,2-dhATQ and copper (Figure 4.1). Unexpectedly, GSH and 1,2-dhATQ and GSH alone under SSR together were more toxic to the plants. It is possible that the GSH with 1,2-dhATQ or under SSR caused a more reduced environment preventing up-regulation of antioxidant defenses.

ROS production in whole plants was quantified and located within the cell using CLSM. ROS production in *Lemna* treated with copper or copper and 1,2-dhATQ showed differences indicating separate mechanisms of toxicity. It was found that exposure to copper increased ROS production in the chloroplasts causing damage to the chloroplast membrane, while 1,2-dhATQ suppressed ROS production after 24

hour exposures. However 1,2-dhATQ and mixture caused increases in ROS production after 4 day exposures suggesting their toxicity does not directly involve ROS production through redox cycling as Cu. GSH addition to Cu, 12-dhATQ and mixture was able to lower the ROS levels most likely via the glutathione-ascorbate cycle.

Photosynthetic electron transport was studied with PAM and FRR fluorometry. Copper at concentrations used in this study did not affect photosynthesis while 1,2-dhATQ caused an increase in the steady-state fluorescence (Figure 4.1 – 3). This is due to the inability of plastoquinol to be re-oxidized to plastoquinone, in the presence of 1,2-dhATQ, which quenches fluorescence. The effect on photosynthesis is seen by a decrease in the F_v/F_m, qP, yield of photosynthesis and σ_{PSII} while F_s and τ increased as re-oxidation of Q_A does not occur rapidly. Cu addition to 1,2-dhATQ improved fluorescent parameters by re-oxidizing plastoquinol likely causing ROS production that accounts for the synergistic increase in growth inhibition. Addition of GSH to 1,2-dhATQ also impacted photosynthesis negatively making it unlikely that 1,2-dhATQ toxicity can be relieved by conjugate formation with GSH. It appeared as though GSH with 1,2-dhATQ created a very reduced environment either by preventing PQ re-oxidation or other redox reactions in the electron transport chain thus preventing gene expression of antioxidant defense enzymes causing stress that could lead to cell death.

Exposure to copper down-regulated SDC but up-regulated ACC while 1,2-dhATQ and mixture exposures had the opposite effects. The down-regulation of SDC in copper exposure was very slight and could be an artifact from the reverse

transcription or Livak calculations. The up-regulation of SDC caused by 1,2-dhATQ could be due to the production of ROS in the membrane by 1,2-dhATQ undergoing photosensitization reactions or changes in redox status of the cell. ACC up-regulation Cu exposure could be to replace damaged fatty acids. 1,2-dhATQ by altering the pH could have prevented ACC expression. It should be noted that QPCR only measures the expression at a certain time point and since gene expression is very transient different exposure concentration and periods could alter results.

4.6 Future work

It might be interesting to perform PAM fluorometry on SSR treated plants as it is known that SSR light would cause a down-regulation of photosynthesis. Research by He and Häder (2002) showed that compared to control plants UV-B/UV-A light lowered the F_v/F_m and qP while increasing the qN parameters. To further evaluate the differences between PAM and FRR fluorometry, another chemical such as DCMU, which prevents re-oxidation of Q_A, could be used. In order to use *Lemna gibba* as a model organism in molecular ecotoxicology, more genes that change in response to toxicants need to be identified and characterized. If cDNA microarrays with QPCR are used, one could then identify what type of toxicant exposure has occurred once exposure studies have been done. Overall, this study clearly shows mixtures of metals and polycyclic aromatic hydrocarbons can cause severe growth inhibition at environmentally relevant levels.

References

Akhtar, T.A. 2004. Identification of similar stress responses elicited by copper and ultraviolet radiation on the aquatic plant *Lemna gibba*. University of Waterloo: Waterloo.

Akhtar T.A., M.A. Lampi, and B.M. Greenberg. 2005. Identification of six differentially expressed genes in response to copper exposure in the aquatic plant *Lemna gibba* (Duckweed).Environ Toxicol Chem. 24:1705-15.

Alkio, M. T.M. Tabuchi, X. Wang and A. Colon-Carmona. 2005. Stress responses to polycyclic aromatic hydrocarbons in *Arabidopsis* include growth inhibition and hypersensitive response-like symptoms. Journal of Experimental Botany. 56:2983-2994.

Altschul, S.F., Madden, T.L., Schäffer, A.A., Zhang, J., Zhang, Z., Miller, W. & Lipman, D.J. 1997. Gapped BLAST and PSI-BLAST: a new generation of protein database search programs. Nucleic Acids Res. 25:3389-3402.

Anderson, S., W. Sadinski, L. Shugart, P. Brussard, M. Depledge, T. Ford, J. Hose, J. Stegeman, W. Suk, I. Wirgin, G. Wogan. 1994. Genetic and Molecular Ecotoxicology: A Research Framework. Environmental Health Perspectives. 12:3-8.

Andrés-Colas N., V. Sancenón, S. Rodrguez-Narvarro, S. Mayo, D.J. Thiele, J.R. Ecker, S. Puig, and L. Penarrubia. 2006. The Arabidopsis heavy metal P-type ATPase HMA5 interacts with metallochaperones and functions in copper detoxification of roots. The Plant Cell Journal.45:225-236.

Arfsten, D.P., D.J. Schaeffer and D.C. Mulveny. 1996. The effects of near ultraviolet radiation on the toxic effects of polycyclic aromatic hydrocarbons in animals and plants: a review. Ecotoxicology and Environmental Safety. 33: 1-24.

Babu, T.S., J.B. Marder, S. Tripuranthakam, D.G. Dixon and B.M. Greenberg. 2001. Synergistic effects of a photooxidized polycyclic aromatic hydrocarbon and copper on photosynthesis and plant growth: evidence that in vivo formation of reactive oxygen species is a mechanism of copper toxicity. Environmental Toxicology and Chemistry. 20:1351-1358.

Babu, T.S., T.A. Akhtar, M.A. Lampi, S. Tripuranthakam, D.G. Dixon, and B.M. Greenberg. 2003. Similar stress responses are elicited by copper and ultraviolet radiation in the aquatic plant *Lemna gibba*: Implication of reactive oxygen species as common signals. Plant Cell Physiol. 44:1320-1329.

Babu, T.S., S. Tripuranthakam, and B.M. Greenberg. 2005. Biochemical responses of the aquatic higher plant *Lemna gibba* to a mixture of copper and 1,2-dihydroxyanthraquinone: synergistic toxicity via reactive oxygen species. Environmental Toxicology and Chemistry. 24:3030-3036.

Belfiore, N.M. and S.L. Anderson. 2001. Effects of contaminants on genetic patterns in aquatic organisms: a review. Mutation Research. 489:97-122.

Bio-rad Laboratories Inc. 2004. Real-Time PCR Application Guide. Life Sciences Group.

Boudou, A. and F. Ribeyre. 1997. Aquatic Ecotoxicology: From the Ecosystem to the Cellular and Molecular levels. Environmental Health Perspectives. 105:21-35.

Bradley, B., F.A Shrader, D.G. Kimmel, J.C. Meiller. 2002. Protein expression signatures: an application of proteomics. Mar Env. Res. 54:373-377.

Briat, J.F. and M. Lebrun. 1999. Plant responses to metal toxicity. Life Sciences. 322:43-54.

BrØnstad, A., B.K. Larsen, A. Skadsheim, M.B. Jones, and O.K. Andersen. 2006. The potential of ecotoxcoproteomics in environmental monitoring: biomarker profiling in mussel plasma using proteinchip array technology. Journal of Toxicology and Environmental Health. 69:77-96.

Calace, N., B.M. Petronio and M. Pietroletti. 2006. Metal bioavailability: How does it significance change in time? Annali di chimica. 96:1-6.

Canadian Environmental Protection Act (CEPA). 1994. Priority substances list assessment report – Polycyclic Aromatic Hydrocarbons. Government of Canada Health Canada, Canada.

Canadian Environmental Protection Act (CEPA). 1999. Priority substances list assessment report – Releases from Primary and Secondary Copper Smelters and Copper Refineries. Government of Canada , Health Canada, Canada.

Dietz, A.C. and J.L. Schnoor. 2001. Advances in Phytoremediation. Environmental Health Perspectives. 109:162-169.

Dietz, K.J. and R. Scheibe. 2004. Redox regulation: an introduction. Physiolgia Plantarum. 120:1-3.

Deprez, R.H.L., A.C. Fijnvandraat, J.M. Ruiter, and A.F.M. Moorman. 2002. Sensitivity and accuracy of qualitative real-time polymerase chain reaction using SYBR green I depend on cDNA synthesis conditions. Analytical Biochemistry. 307:63-69.

Dewez , D., M. Marchland, P. Eullaffroy, and R. Popovic. 2002. Evaluation of the Effects of Diuron and Its Derivatives on *Lemna gibba* Using a Fluorescence Toxicity Index. Wiley Periodicals.

Duxbury, C.L., D.G. Dixon, and B.M. Greenberg. 1997. Effects of Simulated Solar Radiation on the bioaccumulation of Polycyclic Aromatic Hydrocarbons by the duckweed *Lemna gibba*. Environmental Toxicology and Chemistry. 16:1739-1748.

Edwards, R. and D.P. Dixon. 2004. Metabolism of Natural and Xenobiotic Substrates by the Plant Glutathione S-Transferase Superfamily In. Molecular Ecotoxicology of Plants. Springer: Germany.

Fairchild J.F., D.S. Ruessler, P.S. Haverland and A.R. Carlson. 1997. Comparative sensitivity of *Selenastrum capricornutum* and *Lemna minor* to sixteen herbicides. Arch. Environ. Contam. Toxicol. 32:352-357.

Farooq, M., G.S. Babu, R.S. Ray, R.B. Misra, U. Shankar and R.K. Hans. 2000. Sensitivity of Duckweed (*Lemna major*) to Ultraviolet-B Radiation. Biochemical and Biophysical Research Communications. 276:970-973.

Ferrat, L, C. Pergent-Martini, and M. Romeo. 2003. Assessment of the use of biomarkers in aquatic plants for the evaluation of environmental quality: application to seagrasses. Aquatic Toxicology. 65:187-204.

Fox, T.C. and M.L. Guerinot. 1998. Molecular biology of cation transport in plants. Annual Review of Plant Physiology and Plant Molecular Biology. 49:669-696.

Frankart, C., P. Eullaffroy, and G. Vernet. 2002. Photosynthetic responses of *Lemna minor* exposed to xenobiotics, copper, and their combinations. Ecotoxicology and Environmental Safety. 53:439-445.

Fujimore, K. and Daisaku Ohta, 2003. Heavy metal induction of *Arabidopsis* serine decarboxylase. Biosci. Biotechnol. Biochem. 67:896-898.

Gachon, C., Mingam, A. and B. Charrier. 2004. Real-time PCR: what relevance to plant studies? Journal of Experimental Botany. 55:1445-1454.

Greenberg, B.M., X.D. Huang and D.G. Dixon. 1992. Application of the aquatic higher plant *Lemna gibba* for ecotoxicological assessment. Journal of Aquatic Ecosystem health. 1:147-155.

Gorbunov, M.Y., P.G. Falkowski, and Z.S. Kolber. 2000. Measurement of photosynthetic parameters in benthic organism in situ using a SCUBA-based fast repetition rate fluorometry. Limnol. Oceanogr. 45:242-245.

He, Y. and D.P. Häder. 2002. UV-B-induced formation of reactive oxygen species and oxidative damage of the cyanobacterium Anabaena sp.: protective effects of ascorbic acid and N-acetyl-L-cysteine. Journal of Photochemistry and Photobiology: biology. 66:115-124.

Ho, C.L. and K. Saito. 2001. Molecular biology of the plastidic phosphorylated serine biosynthetic pathway in *Arabidopsis thaliana*. Amino Acids. 20:243-259.

Huang, X.D., D.G. Dixon, B.M. Greenberg. 1993. Impact of UV Radiation and Photomodification on the toxicity of PAHs to the higher plant *Lemna gibba* (Duckweed). Environmental Toxicology and Chemistry. 12:1067-1077.

Huang, X.D., B.J. McConkey, T.S. Babu, and B.M. Greenberg. 1997. Mechanisms of photoinduced toxicity of photomodified anthracene to plants: inhibition of photosynthesis in the aquatic higher plant *Lemna gibba* (duckweed). Environmental Toxicology and Chemistry. 16:1707-1715.

Hutner, S.H. 1953. Comparative physiology of heterotrophic growth. In: W.E. Loomis (ed.). Growth and differentiation of plants. Iowa State College Press. Pp. 417-446.

Juneau, P. and R. Popovic. 1999. Evidence for the Rapid Phytotoxicity and Environmental Stress Evaluation using the PAM fluorometric Method: Importance and Future Application. Ecotoxicology. 8:449-455.

Juneau, P., A. El Berdey, and R. Popovic. 2002. PAM Fluorometry in the determination of the sensitivity of *Chlorella vulgaris*, *Selenastrum capricornutum*, and *Chlamydomonas reinhardtii* to Copper. Arch. Environ. Contam. Toxicol. 42:155-164.

Karpinska, B., G. Wingsle, and S. Karpinski. 2000. Antagonistic effects of hydrogen peroxide and glutathione on acclimation to excess excitation energy in *Arabidopsis*. Life. 50:21-26.

Kim, Y.S., J. Min, H.N. Hong, J.H. Park, K.S. Park and M.B. Gu. 2007. Gene expression analysis and classification of mode of toxicity of polycyclic aromatic hydrocarbons (PAHs) in *Escherichia coli*. Chemosphere. 66:1243-1248.

Koblizek, M., D. Kaftan, D. and L. Nedbal. 2001. On the relationship between the non-photochemical quenching of the chlorophyll fluorescence and the Photosystem II light harvesting efficiency. A repetitive flash fluorescence induction study. Photosynthesis Research. 68:141-152.

Kolber, Z.S., O. Prasil and P.G. Falkowski. 1998. Measurements of variable chlorophyll fluorescence using fast repetition rate techniques: defining methodology and experimental protocols. Biochimica et Biophysica Acta. 1367:88-106.

Korte, F., G. Kvesitadze, D. Ugrekhelidze, M. Gordeziani, G. Khatisashvili, O. Buadze, G. Zaalishvili, and F. Coulston. 2000. Organic Toxicants and Plants. Ecotoxicology and Environmental Safety. 47:1-26.

Kromkamp, J.C. and R.M. Forster. 2003. The use of variable fluorescence measurements in aquatic ecosystems: differences between multiple and single turnover measuring protocols and suggested terminology. Eur. J. Phycol. 38:103-112.

Kubista, M., J.M. Andrade, M. Bengtsson, A. Forootan, J. Jonak, K. Lind, R. Sindelka, R. Sjoback, B. Sjogreen, L. Strombom, A. Stahberg, and N. Zoric. 2006. The real-time polymerase chain reaction. Molecular Aspects of Medicine. 27:95-125.

Laney, S.R. 2003. Assessing the error in photosynthetic properties determined by fast repetition rate fluorometry. Limnol Oceanogr. 48:2234-2242.

Laney, S.R. and R.M. Letelier. 2008. Artifacts in measurements of chlorophyll fluorescence transients, with specific application to fast repetition rate fluorometry. Limnol. Oceanogr. Methods. 6: 40-50.

Lees, H. 2005. The Effects of Cadmium and 1,2-dhATQ on Reactive Oxygen Species (ROS) Production, Photosynthesis and Gene Expression in *Lemna gibba* (Duckweed). Waterloo: University of Waterloo.

Lettieri, T. 2006. Recent Applications of DNA Microarray Technology to Toxicology and Ecotoxicology. Environmental Health Perspectives. 114:4-8.

Lombardi, M.R., M.P. Lesser and M.Y. Gorbunov. 2000. Fast repetition rate (FRR) Fluorometry: variability of chlorophyll *a* fluorescence yields in colonies of the corals, *Montastaea faveolata* (*w.*) and *Diploria labyrinthiformes* (*h.*) recovering from bleaching. Journal of experimental marine biology and ecology. 252:75-84.

Mallakin, A., B.J. McConkey, G. Miao, B. McKibben, V. Snieckus, D.G. Dixon, and B.M. Greenberg. 1999. Impacts of structural photomodification on the toxicity of environmental contaminants: anthracene photooxidation products. Ecotoxicology and Environmental Safety. 43:204-212.

Mallakin, A., D.G. Dixon, and B.M. Greenberg. 2000. Pathway of anthracene modification under simulated solar radiation. Chemosphere. 40:1435-1441.

Mallakin, A., T.S. Babu., D.G. Dixon, and B.M. Greenberg. 2002. Sites of Toxicity of Specific Photooxidation Products of Anthracene to Higher Plants: Inhibition of Photosynthetic Activity and Electron Transport in *Lemna gibba* L. G-3 (Duckweed). Inc. Environ Toxicol. 17:462-471.

Mallakin, A., T.S. Babu, D.G. Dixon, and B.M. Greenberg. 2002. Sites of toxicity of specific products of Anthracene to higher plants: inhibition of photosynthetic activity and electron transport in *Lemna gibba* L. G-3 (Duckweed). Wiley Periodicals:462-471.

Maxwell, K. and G.N. Johnson. 2000. Chlorophyll fluorescence - A practical guide. Journal of Experimental Botany. 51:659-668.

McConkey B.J., P.G. Mezey, D.G. Dixon, and B.M. Greenberg. 2000. Fractional Simplex Designs for Interaction Screening in Complex Mixtures. Biometrics. 56: 824-832.

Mkandawire, M. and E.G. Dudel. 2005. Assignment of *Lemna gibba* L. (duckweed) bioassay for *in situ* ecotoxicity assessment. Aquatic Ecology. 39: 151-165.

Mullineaux, P.M. and T. Rausch. 2005. Glutathione, photosynthesis and the redox regulation of stress-responsive gene expression. Photosynthesis Research. 86:459-474.

Nykamp, J.A. 2007. Effects of Polycyclic Aromatic Hydrocarbons, Metals and Polycyclic Aromatic Hydrocarbon / Metal Mixtures on Rat Corpus Luteal Cells and Placental Cell Line, JEG-3. University of Waterloo.

Oberemm, A. L. Onyon., and U. Gundert-Remu. 2005. How can toxicogenomics inform risk assessment? Toxicology and Applied Pharmacology. 207:S592-S598.

OECD. 2002. *Lemna* sp. Growth Inhibition Test, Guideline 221. Organization for Economic Corporation and Development, Berlin.

Ohe, T., T. Watanabe and K. Wakabayashi. 2004. Mutagens in surface waters: a review. Mutation Research. 567:109-149.

Oxborough, K. 2004. Imaging of chlorophyll *a* fluorescence: theoretical and practical aspects of an emerging technique for the monitoring of photosynthetic performance. Journal of Experimental Botany. 55:1195-1205.

Pätsikkä, E. E.M Aro, and E. Tyystjärvi. 1998. Increase in Quantum Yield of Photoinhibition contributes to copper toxicity *in vivo*. Plant Physiol. 117:619-627.

Pemberton, K., R.E.H. Smith, G.M. Silsbe, T. Howell and S.B. Watson 2007. Controls on phytoplankton physiology in Lake Ontario during the late summer: evidence from new fluorescence methods. Can. J. Fish. Aquat. Sci. 64:58-73.

Pompella, A., A. Visvikis, A. Paolicchi, V. De Tata, and A.F. Casini. 2003. The changing faces of glutathione, a cellular protagonist. Biochemical Pharmacology.l 66:1499-1503.

Prasad, M.N.V., P. Malec, A. Waloszek, M. Bojko, and K. Strzalka. 2001. Physiological responses of *Lemna trisulca* L. (duckweed) to cadmium and copper bioaccumulation. Plant Science. 161:881-889.

Puig, S. N. Andrés-Colas, A. Garcia-Molina and L. Penarrubia. 2007. Copper and iron homeostasis in *Arabidopsis*: responses to metal deficiencies, interaction and biotechnological applications. Plant, Cell and Environment. 30:271-290.

Ramesh, A., S.A. Walker, D.B. Hood, M.D. Guillen, K. Schneider, and E.H. Weyand. 2004. Bioavailability and Risk Assessment of Orally Ingested Polycyclic Aromatic Hydrocarbons. International Journal or Toxicology. 23:301-333.

Raven, P.H., R.F. Evert, and S.E. Eichhorn. 2003. Biology of Plants. New York: W.H. Freeman and Company.

Ren, L., X.D. Huang, B.J. McConkey, D.G. Dixon, and B.M. Greenberg. 1994. Photoinduced Toxicity of Three Polycyclic Aromatic Hydrocarbons (Fluoranthene, Pyrene, and Naphtalene) to the Duckweed *Lemna gibba* L. G-3. Ecotoxicology and Environmental Safety. 28:160-171.

Rontein, D., D. Rhodes, and A.D. Hanson. 2003. Evidence from Engineering that Decarboxylation of Free Serine is the Major Source of Ethanolamine Moieties in Plants. Plant Cell Physiol. 44:1185-1191.

Sanderman, H. (Ed.). 2004. Molecular Ecotoxicology of Plants. Springer: Germany.

Sasaki, Y. and Y. Nagano. 2004. Plant Acetyl-CoA Carboxylase: Structure, Biosynthesis, Regulation and Gene Manipulation for Plant Breeding. Biosci. Biotechnol. Biochem. 68:1175-1184.

Schützendübel, A. and A. Polle. 2002. Plant responses to abiotic stresses: heavy metal-induced oxidative stress and protection by mycorrhization. Journal of Experimental botany. 53:1351-1365.

Shank, R.C. General Toxicology. 2004. In. Toxicogenomics – Principles and Applications. John Wiley & Sons, Inc.: U.S.A.

Sherry, J.P. 2003. The role of biomarkers in the health assessment of aquatic ecosystem. Aquatic Ecosystem Health and Management. 6:423-440.

Shugart, L. and C. Theodorakis. 1998. New trends in biological monitoring: applications of biomarkers to genetic ecotoxicology. Biotherapy. 11:119-127.

Snape, J.R., S.J. Maund, D.B. Pickford, and T.H. Hutchinson. 2004. Ecotoxicogenomics: the challenge of integrating genomics into aquatic and terrestrial ecotoxicology. Aquatic Toxicology. 67:143-154.

Sternberg, E.D. and D. Dolphin. Porphyrin-based photosensitizers for use in photodynamic therapy. Tetrahedron. 54:4151-4202.

Suggett, D.J., M. Moore, K. Oxborough and R.J. Geider. 2000. Fast Repetition Rate (FRR) Chlorophyll *a* Fluorescence Induction Measurements. CTG: http://www.chelsea.co.uk/Technical%20Papers/FRRFmethodsManual.pdf

Suggett, D.J., K. Oxborough, N.R. Baker, H.L. Macintyre, T.M. Kana, and R.J. Geider. 2003. Fast repetition rate and pulse amplitude modulation chlorophyll a fluorescence measurements for assessment of photosynthetic electron transport in marine phytoplankton. Eur. J. Phycol. 38:371-384.

Suresh, B. and G.A. Ravishankar. 2004. Phytoremediation – A Novel and Promising Approach for Environmental Clean-up. Critical Reviews in Biotechnology. 24:97-124.

Teisseire, H. and V. Guy. 2000. Copper-induced changes in antioxidant enzymes activities in fronds of duckweed (*Lemna Minor*). Plant Science. 153:65-72.

Tront, J.M. 2004. Plant activity and organic contaminant processing by aquatic plants. Georgia Institute of Technology.

Waring, J.F., X. Dai, Y. He, P.Y. Lum, C.J. Roberts, and R. Ulrich. A short introduction to the expression profile toolbox. 2004. In. Toxicogenomics – Principles and Applications. John Wiley & Sons, Inc.: U.S.A.

Xie F., S.A. Kozair, M.A. Lampi, D.G. Dixon, W.P. Norwood, U. Borgmann, X.D. Huang, and B.M. Greenberg. 2006. "Assessment of the toxicity of mixtures of copper, 9,10-phenanthrenequinone, and phenanthrene to *Daphnia magna*: Evidence for a reactive oxygen mechanism." Environmental Toxicology and Chemistry. 25:613-622.

Zenk, M.H. 1996. Heavy metal detoxification in higher plants – a review. Gene. 179:21-30.